Novel Decontamination Materials for use in the Civil Nuclear Industry

A thesis submitted to the University of Manchester for the degree of Doctor of Philosophy in the Faculty of Science and Engineering.

2018

Joshua J. Moore

School of Chemistry

University of Manchester

Table of Contents

Word count: 41,716

List of Figures

List of Tables

List of Equations

Glossary of Abbreviations

2D	Two dimensional
AGR	Advanced gas cooled reactor
AIBN	Azobisisobutyronitrile
AMU	Atomic mass units
CBRN	Chemical, biological and/or radionuclide
CMC	Critical micelle concentration
CORD	Chemical oxidising/reducing decontamination
DEG	Diethylene glycol
DF	Decontamination factor
DI	Deionised
DLS	Dynamic light scattering
DTPA	Diethylenetriaminepentaacetic acid
EDTA	Ethylenediaminetetraacetic acid
EGmBE	Ethylene glycol monobutyl ether
EWC	Equilibrium water content
FEG-SEM	Field emission gun scanning electron microscopy
FT-IR	Fourier transform infrared spectroscopy
GC	Gel content
Gc	Crossover point (in cases of rheology)
GDF	Geological disposal facility
GD-OES	Glow discharge optical emission spectroscopy
h-BN	Hexagonal boron nitride
HEDPA	1-hydroxyethane-1,1-diphosphonic acid
HEMA	2-hydroxyethyl methacrylate
HLW	High level waste
ILW	Intermediate level waste
INES	International nuclear event scale
IPA	Isopropyl alcohol
IPN	Interpenetrating network
IR	Infrared

LLW	Low level waste
LOMI	Low oxidation state of metal ions
LVE	Linear viscoelastic region
MBAM	N,N'-Methylenebisacrylamide
MEDOC	Metal decontamination by oxidation with cerium
NIPAM	N-isopropylacrylamide
PdI	Polydispersity index
PDMS	Dimethylpolysiloxanes
PEO	Polyethylene oxide
pHEMA	Poly(2-hydroxyethyl methacrylate)
pNIPAM	Poly(N-isopropylacrylamide)
PUREX	Plutonium uranium redox extraction
PVA	Polyvinyl alcohol
PVP	Polyvinylpyrrolidone
RPM	Revolutions per minute
SDBS	Sodium dodecylbenzenesulphonate
SDS	Sodium dodecyl sulphate
SEM	Scanning electron microscopy
SE-SEM	Secondary electron scanning electron microscopy
T ½	Half life
VLLW	Very low level waste
ZP	Zeta potential

Abstract

Nuclear power is a low carbon, high output energy source which is employed on a global scale. However, it is not without drawbacks; the generation of long lived radioactive waste has presented a problem since the operation of the first nuclear reactors in the 1940s. The treatment of radioactive waste materials is therefore of considerable importance to prevent further spread of radionuclides, deterioration of storage conditions and the potential for accidents.

With these considerations in mind projects were undertaken investigating the use of new hydrogels for the decontamination of radionuclides and the use of foams for neutron poisoning applications.

The development of a new hydrogel decontamination method for the removal of ^{137}Cs and ^{90}Sr radionuclides from stainless steel surfaces was explored and the significant number of synthesised gels characterised with full rheological profiles. Many targeted gel loadings were examined for the delivery of effective decontamination treatments; with solid encapsulation of radionuclides, high DFs (up to 95 for ^{137}Cs and 24 for ^{90}Sr on stainless steel substrates, exceeding literature precedents), no lateral spread of radionuclide contamination and a minimal volume of liquid waste reported. This shows excellent potential for industrial and research lab applications for the safe treatment and disposal of localised, highly contaminated surfaces with the need for minimal human interaction; thus greatly reducing potential dose. The ease of transport, storage and stability of these materials shows great promise for emergency implementation in the case of a "dirty bomb" chemical, biological or radionuclide (CBRN) attack scenario, where deployment would be of minimal difficulty and high effectiveness without the risk of property destruction.

The concept of neutron poisoning foams for accident remediation or emergency scenarios was investigated, with potential loading materials examined; building up to experimental studies of the feasibility of this technology. The experimental configurations and investigations into this concept have no prior literature precedent and address a key contingency need with full detailed assessment of the plausibility and potential materials which may be applied to this problem. This work concluded that a neutron poisoning foam is not a feasible delivery method.

Declaration

A small portion of the gel synthesis and rheology work described herein was also included in the MSci report (University of Manchester) of supervised student Dingding Yan.

No other portion of the work referred to in the thesis has been submitted in support of an application for another degree or qualification of this or any other university or other institute of learning.

Copyright Statement

The author of this thesis (including any appendices and/or schedules to this thesis) owns certain copyright or related rights in it (the "Copyright") and s/he has given The University of Manchester certain rights to use such Copyright, including for administrative purposes.

Copies of this thesis, either in full or in extracts and whether in hard or electronic copy, may be made **only** in accordance with the Copyright, Designs and Patents Act 1988 (as amended) and regulations issued under it or, where appropriate, in accordance with licensing agreements which the University has from time to time. This page must form part of any such copies made.

The ownership of certain Copyright, patents, designs, trademarks and other intellectual property (the "Intellectual Property") and any reproductions of copyright works in the thesis, for example graphs and tables ("Reproductions"), which may be described in this thesis, may not be owned by the author and may be owned by third parties. Such Intellectual Property and Reproductions cannot and must not be made available for use without the prior written permission of the owner(s) of the relevant Intellectual Property and/or Reproductions.

Further information on the conditions under which disclosure, publication and commercialisation of this thesis, the Copyright and any Intellectual Property and/or Reproductions described in it may take place is available in the University IP Policy (see http://documents.manchester.ac.uk/DocuInfo.aspx?DocID=24420), in any relevant Thesis restriction declarations deposited in the University Library, The University Library's regulations (see http://www.library.manchester.ac.uk/about/regulations/) and in The University's policy on Presentation of Theses.

Rationale for presentation in the journal format

The presentation of this thesis in the alternative, journal format aims to present the work undertaken in the form of two papers with additional results chapters in the form of the relevant supporting information. The rationale behind this decision was to allow a set of work around a central theme of new materials in decontamination and decommissioning in the civil nuclear industry to be best presented for eventual publication.

The gels work undertaken is substantial, new and presents results with clear advantages over current state of the art; this is a prime candidate for a high impact publication, with further work possible for a follow up publication. This paper iteration is due to be submitted to the Royal Society of Chemistry Journal of Materials Chemistry A. For inclusion in this thesis the paper has been re-formatted in a manner which does not disrupt the flow of the thesis and presents consistency of figures and references with the other paper and chapters.

The body of work centred upon the incorporation of neutron poisoning substances into foams for emergency or accident remediation contingency planning, however, returned negative results as the concept could not be realised. Whilst this is not suitable for a high impact publication the research is scientifically valid and the previously uninvestigated concept warrants dissemination. This will allow alternative contingencies to be considered for potentially hazardous events. This body of work has been prepared according to submission guidelines for the Nature Publishing Group's Scientific Reports journal. Formatting has, as detailed above, been adjusted to assimilate into an overall coherent style.

Overall this thesis documents investigations into new materials to combat the challenges present in both modern and legacy nuclear materials at one of the most complex civil nuclear sites in the world, Sellafield, the impacts of which are applicable to many other scenarios outside of this site. Much of the work involved has revolved around potential impact assessments, various radioanalytical techniques, formulation development, materials characterisation and small scale implementations of the materials investigated in these scenarios. It is hoped that

journal format publication will disseminate this information to the fields in which it will be most useful.

Joshua J Moore, the main author of the paper entitled "Foams for neutron poisoning applications", was responsible for the entirety of the practical work and paper preparation carried out. Stephen Yeates provided academic supervision and project direction, Francis Livens provided academic direction and valuable discussions, Alex Jenkins provided industrial supervision and contact via Sellafield Ltd. for scenario discussions.

Of the authors listed on the "Decontamination of Caesium and Strontium from stainless steel surfaces using hydrogels" paper and supporting information, the main author; Joshua J Moore, was responsible for paper preparation and all experimental work; with the exception of SEM which was carried out by Thomas Raine and EPM which was carried out by technical services. Principal academic supervision and paper revisions were carried out by Stephen Yeates. Katherine Morris and Gareth Law provided valuable discussions and characterisation expertise whilst Katie Law provided radiochemistry working and techniques guidance. Francis Livens provided additional academic supervision and industrial supervision was carried out by Alex Jenkins.

Acknowledgements

I must first express my sincere gratitude to my supervisor; Professor Steve Yeates for giving me the freedom to develop into an independent researcher and providing exceptional guidance and direction in the more difficult stages of my PhD. My co-supervisor, Professor Francis Livens, must also be thanked for guidance and incredibly helpful discussions. Thanks are also warmly extended to Sellafield Ltd. for industrial sponsorship.

My thanks are also extended to those who have helped me in a professional capacity with their years of accumulated knowledge, insight and patience in instruments training: Professor Kath Morris, Dr Gareth Law, Mrs Katie Law, Professor Jonathan Billowes, Dr Jon Fellowes, Dr Ben Spencer, Dr Adam Lang and Dr Becky Dey.

I also wish to thank those who have helped and encouraged me along the way; particularly Rose Oliver for her constant encouragement, care and understanding during this process. Thanks to my Parents and my Grandmother; who have shown an enduring belief in me and also to my late Grandfather; who always offered sage advice and was delighted at the prospect of me undertaking a PhD.

This thesis would not be possible were it not for the support of my friends and colleagues in OMIC, be it with project guidance or the sacred ritual of Friday beers: Barney Haire, Tom Raine, Raymundo "Big Ray" Marcial Hernandez, Glenn Sunley Saez, Vanessa Tischler, Daryl McManus, Fiona Porter, Junru Zhang, Vaiva Nagyte, Robyn Worsley, Matt Boyes, Seb Bro22, Ben Lidster, Dan Tate, James Crossland, Becky Dey, YuYoung Shin, Bahare Tamaddondar, Joe Wheeler, Kane Heard, Rick Sanchez, Jair Guzman, Adam Parry, Andrew Foster and Wayne Harrison.

Thank you to Frank Mair, John Agger and Tom Smith, for teaching me the joys of outreach and controlled explosions.

Thanks are also extended to the members of the Vikings, particularly Hrafnsdale, who were always on hand to relieve the stresses and strains of life through the liberal application of sword fighting.

The chemists are a strange class of mortals, impelled by an almost insane impulse to seek their pleasures amid smoke and vapour, soot and flame, poisons and poverty
Johann Joachim Becher (Gaither, C. C. *Gaither's Dictionary of Scientific Quotations*. (Springer New York, 2008).)

Chapter 1 - Introduction

1.1 - A brief summary of the UK nuclear industry

The nuclear industry in the UK began to build rapidly after the end of the second world war as research into primarily military and later, civil applications gained momentum. Initially the principal use of UK reactors was to produce plutonium for weaponry applications (the most famous example being the Windscale piles) but in 1956 Britain was able to boast the world's first commercially active nuclear power station.[1]

As of 2014 several different designs of reactor had operated and continued to operate in the UK; with a progression from the earlier Magnox reactors (of which only one remained in operation as of 2014), through advanced gas cooled reactors (of which 14 were in operation) and on to the solitary pressurised water reactor. These 16 reactors were together responsible for approximately 19% of the UK's electricity generation.[2]

In the UK in 1957 an early generation reactor; one of the Windscale piles, experienced a reactor fire which resulted in a release of radionuclides. Since the development of successive generations of reactors with enhanced safety features the risk of further major incidents is considered to be low. Plans are therefore in place to build additional nuclear power stations at several sites across the UK, with the exception of Scotland.

1.2 - Radioactivity and decay

Radioactivity can be best defined as "the process of the spontaneous decay and transformation of unstable atomic nuclei accompanied with the emission of nuclear particles and/or electromagnetic radiation".[3] The form of radiation emitted by radioactive materials is known as ionising radiation due to its ability to ionise atoms with which it comes into contact and is capable of directly damaging living cells.[4]

There are 3 methods of radioactive decay with which we must principally be concerned during the handling and decontamination of radioactive material: α (alpha), β (beta) and γ (gamma).

An α particle consists of a nucleus of a helium atom, $^{4}_{2}\text{He}^{2+}$, which is emitted from a radionuclide with an increase in energy via a mechanism known as α-decay:

$$^{238}_{92}\text{U} \longrightarrow \, ^{234}_{90}\text{Th} + \, ^{4}_{2}\text{He}$$
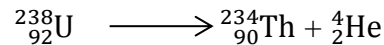
Figure 1 - α decay of ^{238}U

The relatively high mass and charge of the α particle when compared to other decay products results in strong ionisation of matter when contacted but imparts upon the particle weak penetrating power.[4] Hence α radiation travels only a short distance in air and is blocked by thin barriers such as skin but has the potential to cause serious harm if exposed to internal areas of the body. α sources find everyday use as the detector components of smoke alarms.

Emission of a β particle occurs during radioactive decay of a radionuclide with a neutron/proton imbalance; where a neutron is converted to a proton via the emission of a negatively charged β particle (negatron) and a charge less antineutrino (ῡ).[3]

$$^{14}_{6}C \longrightarrow \, ^{14}_{7}N + \, \beta^{-} + \, \bar{\text{υ}}$$
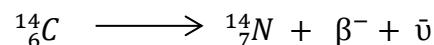
Figure 2 - β decay of ^{14}C

Emission of a positively charged β particle (positron) is also possible, resulting in the emission of a neutrino (υ) and conversion of a proton to a neutron.

γ decay most commonly occurs after the α or β decay of a radionuclide leaves a product in the excited state (nuclear isomer); the dissipation of this excess energy as γ radiation allows the product to return closer to the ground state. The energy of a γ decay can be quantified using:

$$E_\gamma = h\upsilon = E_1 - E_2$$

Equation 1 - Energy of a γ emission

Where E_1 and E_2 are the different energy levels of the nuclear isomer.[3] Whilst the emitted γ radiation possesses lesser ionising abilities when compared to α or β particles it is of particularly high energy and thus is highly penetrative, requiring high levels of shielding with materials such as lead (due to its high density) to enable safe working conditions.[4]

1.2.1 - Neutrons

When compared with other forms of radioactivity, the neutron was discovered relatively late (by James Chadwick in 1932). By targeting beryllium with an α emitter he was able to detect an emitted particle with an extremely high penetrating power; requiring a material with a large number of nuclei per unit area, such as paraffin wax, to shield against.[3]

A neutron possesses no charge, a mass of 1 atomic mass unit (amu), a limited stability of around 15 minutes when outside a nucleus and does not directly ionise matter. Most common commercially available neutron sources are formed by the combination of an α emitter (often ^{241}Am) with beryllium metal, whereby the collision of an α particle with beryllium results in the formation of ^{12}C accompanied by the ejection of a neutron.[3] Spontaneous neutron emitters, such as ^{252}Cf, are also available.

Neutrons are usually classified by their energies, velocities or wavelengths which can be easily converted if one is known via:

$$E = \frac{1}{2}mv^2$$

Equation 2 - Relationship between energy and velocity where E=energy (J), v=velocity (m/s) and m=mass of neutron (1.67x10^{-27}kg)

And:

$$\lambda = \frac{h}{mv}$$

Equation 3 - Calculation of wavelength (λ, m) where h=Planck's constant ($6.63x10^{-34}$ J/s)

Defining neutrons by the energy they possess results in the following classifications:

Neutron classification	Energy (eV)
Cold	<0.003
Thermal	0.003-0.4
Epithermal	0.4-100
Intermediate	100-200,000
Fast	200,000-10,000,000
High energy	>10,000,000

Table 1 - Classification of neutrons by energy[3]

Although it must be noted that different literature sources frequently give differing classifications along broadly similar lines. Neutrons are of particular importance in nuclear power generation as the initiators of fission reactions.

In order to reduce the neutron flux in a reactor environment substances termed "neutron poisons" are commonly employed. These are substances with a high neutron absorption cross section (such as ^{10}B, ^{155}Gd and ^{157}Gd) which can eliminate neutrons from the fission chain reaction and thus "poison" the reaction.[5] Further discussion of neutron poisons can be found in chapter 6.2.

1.2.2 - Nuclear fission

Current reactors operate using nuclear fission as a means to release the nuclear potential energy of fissile nuclei and convert them into smaller nuclides with a greater binding energy per nucleon.[6] The heat generated from such reactions is used to heat a secondary circuit in order to drive electricity generating turbines, producing

significantly larger power outputs per unit volume of fuel than older methods such as coal or gas power stations.[4]

Fissile nuclei are those in which a zero energy neutron is capable of inducing fission and feature odd-A nuclei (odd mass number nuclei). Common examples include: $^{233}_{92}U$, $^{235}_{92}U$, $^{239}_{94}Pu$ and $^{241}_{94}Pu$.[6]

Of paramount importance to nuclear fission reactors is the nuclide $^{235}_{92}U$ which, despite only having a mere 0.72% natural abundance, is the key isotope of uranium required for the majority of power generating fission reactions. When a neutron is absorbed by $^{235}_{92}U$ it mostly (in over 80% of cases) becomes the unstable isotope $^{236}_{92}U$:

$$^{235}_{92}U + {}^{1}_{0}\text{n} \longrightarrow {}^{236}_{92}U + \gamma$$
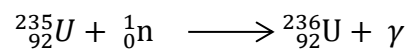
Figure 3- Neutron capture in $^{235}_{92}U$; note γ emission.

This unstable isotope then rapidly splits into two fragments (fission products of which there are 60 producible species, ordinarily with a mass difference ratio[7] of 3:2 accompanied by the emission of approximately 2.5 fast neutrons and 200 MeV of energy as average yields.[3,6]

The release of multiple neutrons allows a reactor to sustain itself in a chain reaction, although a moderator (often graphite or D_2O) is also required in order to ensure the neutrons are reduced to the energy levels of thermal neutrons to facilitate fission.[3]

Since each fission event of uranium results in the ejection of more than 1 neutron it is possible for the reaction rate to increase exponentially, leading to an excess build-up of heat above that which the cooling system is able to remove. It is therefore necessary to build safeguards into the reactor to ensure any reaction can be halted by absorbing (or capturing) excess neutrons.

1.3 - Current UK reactor designs

The Magnox reactor design involves the use of graphite moderators surrounding natural uranium fuel contained within vessels constructed from a magnesium alloy (resulting in the Magnox name). Pressurised CO_2 gas is circulated as the primary coolant with a second heat transfer circuit containing water used to power steam turbines for electricity production.[8] This reactor design is also capable of producing weapons grade plutonium.

Advanced gas cooled reactors (AGR) are currently the most common in the UK with the first commercial power generating station opening in 1976. The design uses the same primary coolant (pressurised gaseous CO_2) and moderator (graphite) as Magnox but differs in using an enriched uranium oxide fuel within a stainless steel can.[2]

Pressurised water reactors are a more modern concept than the Magnox and AGR and the current example at Sizewell B is the UK's newest (1995), featuring a move towards a pressurised water coolant with a zirconium alloy cladding for the uranium oxide fuel.[2]

1.4 - Major nuclear reactor incidents

As mentioned earlier, the probability of UK reactor accidents is considered to be low but the last 30 years have seen significant failures and release of radioactive material from the high profile events at Chernobyl and Fukushima. Whilst Fukushima was rated as a level 7 accident on the International Nuclear Event Scale (INES) the atmospheric release and contaminated land was significantly less than Chernobyl; estimated at approximately $1/10^{th}$ of the scale of the Chernobyl accident.[9] The Fukushima accident occurred due to the effects of a highly damaging earthquake and tsunami upon the plant, leading to a loss of reactor coolant circulation which caused the zirconium-coated control rods to react with the coolant to produce large volumes of hydrogen gas. As the hydrogen gas leaked out of the cooling circuits and mixed with atmospheric oxygen a series of explosions occurred, resulting in the release of radioactive material.[9]

In the case of the Chernobyl accident no natural occurrences were at the root cause; merely significant human error, stupidity and dangerously poor design. An experiment being conducted upon the cooling system began the cascade of factors leading to the accident; as the cooling system was slowed more steam began to build in the reactor, increasing the reaction rate. As the temperature of the core increased more steam was generated leading to a further acceleration of the reaction to unstable levels.[10] Ordinarily the presence of control rods would have provided a factor of mitigation but these were almost fully withdrawn in defiance of all protocols to the extent that the overheating of the core caused deformations in the graphite moderator, preventing reinsertion and leading to an explosive release of steam. This was followed by a second explosion due to air ingress, destroying the containment building and setting the graphite moderator aflame.[10] In addition to the radioactive material released by the explosion the fire meant the release continued for several days, spreading high levels of radioactive material in a plume across Russia and Europe.

In attempts to mitigate the fire and breached core a blanketing method was undertaken with delivery by helicopter. Dropped into the remnants of the core were 2400 tonnes of lead shot, 1800 tonnes of clay, 800 tonnes of dolomite and 40 tonnes of boron carbide.[10] The deposition of boron carbide is of particular note here as this was used to halt the continuing fission reaction in the exposed fuel. Halting the fission reaction was a key requirement to stopping the continuation of the fire and reducing the temperature of the core fuel.

1.5 - Decontamination literature review

1.5.1 - Classification and disposal

The UK system of radioactive waste classification consists of a four tier system based on the activity levels of the waste: very low level waste (VLLW) exhibits activities of around 10 Becquerels per gram[11] and generally consists of rubble from demolition activities which can be safely disposed of by landfill. Low level waste (LLW) exhibits activities of around 1000 Becquerels per gram and consists of material such as protective clothing (in many cases originating from medical applications of active material). LLW must be disposed of in the national LLW repository.[12] Intermediate level waste (ILW) exhibits activities of around 100,000 Becquerels per gram, tends to exhibit a longer half-life, consists of materials such as spent fuel cladding and used filters (usually embedded in concrete for safety and ease of transportation) and in the UK is currently held in temporary storage at several sites with the eventual intention of storage in a geological disposal facility (GDF). High level waste (HLW) exhibits the highest levels of activity in the billions of Becquerels per gram and is usually composed of vitrified fission products with very long half-lives and heat-generating abilities. HLW must be stored with cooling facilities (such as the cooling ponds at Sellafield)[13] and is held in interim storage awaiting deep geological disposal.

The storage and disposal of radioactive waste becomes both increasingly hazardous and expensive with increasing classifications of activity; hence if decontamination of products such as ILW can reduce the majority of the volume down to LLW or VLLW then the need for expensive safety measures and disposal techniques is eliminated.

1.5.2 - Radionuclide contamination

During the standard operation of a nuclear plant the production of radionuclides is inevitable and many of these species are highly mobile (^{137}Cs, for example). Such species are produced during fission; neutron capture occurring in uranium and

transuranic elements and the ability of many materials used around the reactor (including corrosion products of these materials and material mobile in the coolant) to undergo neutron capture.[14] Figure 4 illustrates the distribution of daughter radionuclides produced,[15] of note are the highest yields of fission products around mass numbers 90 and 140. These contaminants are found in particularly high concentrations on any material which is incorporated within the primary core but are also routinely spread across plant sites in the coolant, during maintenance or in the extreme event of an accident.
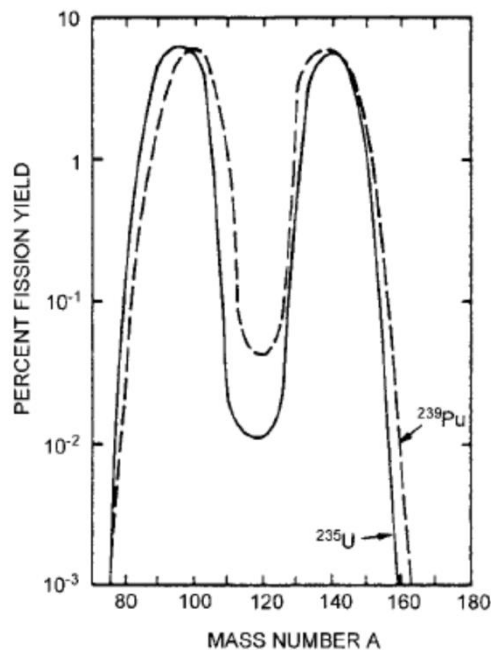
Figure 4– Thermal neutron fission yields for ^{235}U and ^{239}Pu (taken from Nuclear Reactor Physics).[15]

Key radionuclides of concern include: ^{137}Cs- a highly mobile β and γ emitter produced in high yield as a uranium fission product with a half-life ($t_{1/2}$) of approximately 30 years,[16] the ease with which it forms highly water soluble salts combines with these properties to make it of particular concern, especially in the aftermath of the Fukushima disaster.[17] The negative sorption sites present in building materials often lead to caesium bonding with these materials.[18]

^{90}Sr- a β emitter also produced in high yield as a uranium fission product with a half-life of approximately 28 years, the ease of which any ^{90}Sr can be incorporated into bone provides sufficient justification for decontamination targeting.[19] The β emitter

28

[60]Co is produced as a corrosion product with a shorter half-life of approximately 5 years[14] and is of particular concern as it possesses a longer half-life that most other corrosion products and is often incorporated as a component of materials in the reactor circuits or as oxides and "sludge" in coolant circuits.[14]

1.5.3 - Why decontaminate?

The overlying objective of the whole decontamination process is to ensure the maximum protection to the health and safety of workers, the public and the environment.[20]

The choice to decontaminate in civil nuclear applications is typically based upon a variety of factors and practicalities,[21,22] namely:

- Potential for release/transport- The higher the potential for environmental release the more prudent decontamination operations are.
- Level of hazard- Will the activity present cause issues to workers/storage conditions?
- Cost- Will decontamination make disposal cheaper or will the decontamination technique be more expensive?
- Reuse- Does the equipment/land need to be reused or could it be reused?
- Volume of waste- Can decontamination reduce the volume of waste to be treated?
- Production of secondary waste- Is secondary waste produced and is this treatable?
- State of waste- Solid waste is easier to handle than liquid, gaseous waste is to be avoided wherever possible due to ease of transport/inhalation.
- Contaminant half lives- Could the contaminated material be stored until it is no longer active?
- Public acceptance- Would this action be considered responsible handling of radioactive material and would the public perceive it as such?

Once the decision to decontaminate has been made the most suitable method of decontamination must be identified. Many different methods exist, varying from

mechanical/physical to chemical and even biological mechanisms of action. Detailed below are the major decontamination methods reportedly used in nuclear facilities worldwide, typical scenarios of use and efficacy evaluations.

1.5.4 - Decontamination methods

Decontamination, in terms of radionuclides, is the transfer of contaminants from any site where they are problematic to a controlled, safer destination.[14] The effectiveness of a method of decontamination is conventionally measured by calculation of the decontamination factor:

$$DF = \frac{Initial\ contamination\ level}{Contamination\ level\ after\ decontamination\ process}$$

Equation 4 - Calculation of the decontamination factor[23]

The process of decontamination can occur in several forms depending on the contaminant, contaminated surface/substance and practicality considerations.

1.5.5 - Mechanical/physical

Mechanical decontamination encapsulates any form of decontamination method where mechanical action is used and can be applied to any surface; common methods in use involve water jetting, scarification and basic scrubbing and result in either the cleaning of the surface or the more aggressive removal of surface and contaminant.[20] These methods are most commonly used when contamination is near to the surface, although techniques like scarification may be employed to deeper levels (albeit with increased complications).

The water/abrasive (e.g. sand, aluminium oxide, plastic or glass beads) jetting techniques have been used to great effect in the nuclear industry and with reasonable

ease, achieving high decontamination factors.[24] This technique does, however, come with several disadvantages: damage to fragile surfaces by abrasives, exposure of workers operating the machinery and the generation of large volumes of secondary waste.[25] Scarification (physical ablation of the surface) of concrete also results in similar potential hazards and as such scabbling machines are often fitted with extractor systems.[20]

Techniques such as steam vacuum cleaning, CO_2 pellet blasting, liquid N_2 blasting, Freon blasting and wet ice blasting are all variations of abrasive blasting or water jetting with a differing medium.[21] The added heat of steam vacuum cleaning improves contaminant dissolution and results in a small volume of liquid waste but care must be taken to avoid mobilisation of radionuclides,[26] CO_2 blasting has proven effective due to the combination of vaporisation, thermal shock and abrasion but can damage less robust surfaces, liquid N_2 likewise may result in surface embrittlement, Freon blasting results in a release of halocarbons[21] (now considered unacceptable) and wet ice blasting combines the benefits of water jetting and abrasive blasting without solid waste.[27] Another variant on water/abrasive blasting is sponge blasting; a technique whereby urethane sponges in water scrub a surface through a repetitive cycle of expansion and contraction.[28]

The most aggressive mechanical techniques are those where a significant portion of the contaminated surface is forcibly removed with the aim of taking radioisotopes with it for disposal. These techniques include scarification, milling, cutting away surfaces, shaving and grinding etc. Most of these techniques either require human operators (increasing exposure risks/levels) or expensive remote operating systems but result in a high success rate for deep seated radioisotope contaminants.[24] As detailed previously; the appropriate controls must be put in place to prevent highly hazardous airbourne dust particles transporting radionuclides.[29]

Microwave scabbling has also found use on the UK Sellafield site; either vaporising water within concrete to create internal pressure[30] or making use of thermal differentials to blast away the surface layer(s) by explosive structural failure, the exact mechanism is somewhat debated.[31] This technique, however, requires adequate moisture present within the concrete.[25] Laser ablation has also been applied to

contamination at surface level or within surface coatings; allowing remote operation and minimal volumes of secondary waste.

Strippable polymer coatings have also been used to good effectiveness on loosely contaminated non-porous surfaces, with surface radionuclide contaminants being removed with the coating.[26,32–34] Typically a solution is sprayed or painted onto a surface and removed by a peeling action once the solution has dried and a coating has formed (see figure 5) with or without additional radiation detection functionality. They may also be left in place to prevent the mobilisation of surface contamination.
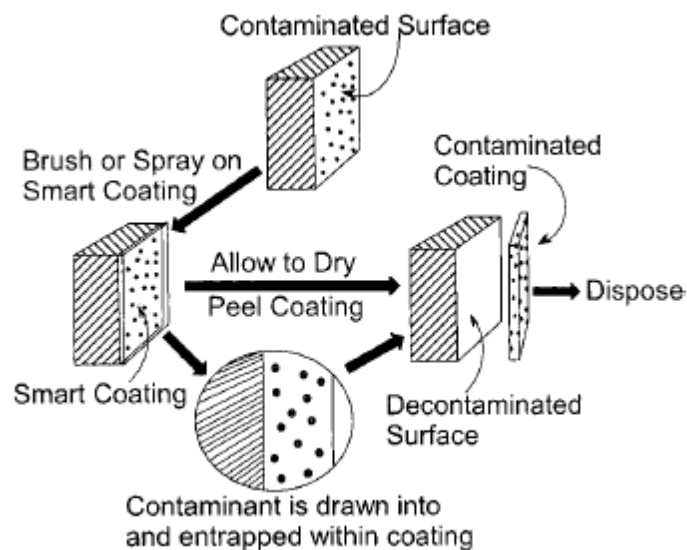
Figure 5– Mechanism of strippable polymer coating decontamination (taken from Gray et al)[29]

Reported uses range from a very basic solution of PVA dissolved in methanol exhibiting limited removal of ^{60}Co and ^{137}Cs radionuclides from steel[35] to compositions including PVA, PEO and PVP with indicators such as 2-(5-Bromo-2-pyridylazo)-5-(diethylamino)phenol to change colour in the presence of uranium and plutonium.[29] Evaluations of these coatings often recount DFs between 4-20.[36] This technique has often proved largely unsuccessful in application on porous surfaces.[24,36] Strippable polymer coatings often overlap somewhat with gel decontaminating agents (detailed in section 2.5.4) in terms of deployment techniques and actions.

In the case of contaminated buildings mechanical decontamination is often the most viable option as full immersion in reagents would be extremely impractical, although the use of small volumes of chemical decontaminants in combination with mechanical processes often yields extremely effective results.

1.5.6 - Electrochemical

Electrochemical decontamination involves the use of chemicals in association with a magnetic field and results in the anodic removal of contaminants from a surface.[25] In order to implement this method the materials are commonly submerged in a heated and agitated reagent tank with a secondary water rinse. The most commonly used reagent for this form of electropolishing (effectively the inverse of electroplating) is phosphoric acid as it is considered stable, minimises recontamination, possesses good complexing properties and results in minimum airborne contamination.[37]

Whilst high decontamination factors are achievable this technique is limited by the restriction to conductive materials only, complex geometries, requirement for cleaning of the surface beforehand (grease, oxides or other adhering materials prove disruptive) and the need to immerse the contaminated materials in electrolyte tanks.

1.5.7 - Chemical

Chemical decontamination techniques involve the application of any form of chemical reagent or solvent and are, generally, the most widely used decontamination method[14] with applications ranging from immersion in a tank to direct application in small quantities on a surface.[21] This technique is particularly suited for metal decontamination.[20] The components of such mixtures often include one or a combination of: acids, alkalis, detergents or complexing agents with the potential to either be aggressive or mild depending on the formulation and application, allowing precise control of factors such as surface damage and removal.[25] Decon 90 would stand out as a particularly well adopted example. The general method of chemical based decontamination processes is the dissolution of

the contaminated surface layer or the bulk metal depending on whether the metal is planned for continued use or recycling. Many chemical decontamination techniques require multiple steps; for example oxidation, dissolution and complexation steps featuring the use of a range of concentrated to dilute active components depending on the degree of corrosion acceptable and decontamination required.[20]

Mineral acids such as sulphuric, phosphoric, nitric and fluoroboric (or their acid salts) are commonly employed in order to dissolve metal oxide films and increase metal ion solubility at low pH.[28] Each acid has a particular preferred use; sulphuric is generally used to remove non-calcium containing deposits, phosphoric is employed to decontaminate carbon steel surfaces, nitric is preferred for the removal of metal oxide layers and fluoroboric can be applied to any metallic surface with a minimal depth of dissolution.[24]

Commonly used organic acids include citric acid, oxalic acid, oxalic peroxide and formic acid[28] which are typically used for the second step of two-part stainless steel decontamination procedures, iron rust and fission product removal, dissolution of UO_2 with film removal and in conjunction with a complexant in an ultrasound bath respectively. Oxalic acid treatment must be monitored to prevent redeposition of active material encapsulated in ferric oxalate.[24]

Inversely basic reagents are used in a similar way to common cleaning applications for the removal of surface adherants, as a solubility aid, de-corroder and surface passivator. Many uses of basic reagents form part of a multi-step treatment process, with the basic solution commonly used as a preparatory step.[28]

DFs of greater than 10,000 have been reported[24] in the decontamination of steels by use of the MEDOC process consisting of cerium (IV) as a strong oxidant in sulphuric acid with continuous regeneration using ozone to dissolve metal oxide and base metal layers.[38]

Other forms of chemical decontamination processes make use of ligands which have a high affinity for the complexation of metal ions (such as EDTA-ethylenediaminetetraacetic acid) to solubilise them, prevent unintentional redeposition and allow for later recovery when necessary.[20] May other chemical methods used are those commonly encountered in various cleaning applications

outside of radioisotope applications: detergents or surfactants are used to remove surface contamination on non-corroded surfaces[28] (commonly trapping contaminants within micelles for removal[39]), bleaching aides the removal by breakdown of chemical-based contaminants and solvents are used to solubilise organic material which is carrying radioisotopes.[20]

Many two-step decontamination procedures use either reducing or oxidising agents as an initial step to increase the solubility of contaminants or contaminated materials prior to dissolution. Examples include alkaline permanganate to oxidise Cr(III) oxides in stainless steels to to Cr(VI) followed by either citric acid, sulphamic acid or oxalic acid to remove oxide layers or surface films.[24] Techniques such as the LOMI (Low oxidation state of metal ions) process using dilute solutions of vanadium formate and picolinic acid[40] and CORD (Chemical oxidising/reducing decontamination) process rely upon this principle.[24]

A significant number of proprietary chemical decontamination processes exist, many tailored to specific substrates. It is often difficult to provide a full overview of many of these processes due to their proprietary nature. The TechXtract chemical decontamination process utilises a combination of emulsifiers, electrolytes, wetting agents, flotation reagents, buffered acids and chelating ligands.[41] This process aims to treat porous surfaces by penetrating pores, break the bonds holding contaminants in place and fix them in solution. Enhancement of the process requires the application of physical techniques such as sonication or scrubbing, with up to 90% contaminant removal reported, including leach back.[41] The DECONCRETE decontamination process works in a similar manner but is reportedly is based upon phosphoric acid.[37]

Multiple different compositions of chemical decontamination agents have been formulated and used worldwide, such as chemical foams, gels and pastes.[20] Foams are commonly used as carriers for the reagents detailed above with reduced volumes of liquid required and waste produced or simply in the same method as a detergent due to the presence of high surfactant concentrations. Gels and pastes are applied to a surface as a reagent carrier in much the same way as foams but result in a lengthier contact time prior to mechanical removal from the surface, in the case of pastes the mechanical action may be an active part of the decontamination process.[37] Many gel

based decontamination methods rely on a similar method of application and action to peelable polymer coating: spray application followed by contaminant absorption and gel removal.

1.5.8 - Gel decontamination processes

Many gel decontamination processes have been reported in the literature, with operational removal in the form of peelable coatings. A general distinguishing feature between the previously detailed peelable coatings and gel based decontamination is the mechanism of removal: peelable coatings will rely upon physical encapsulation whilst gels will also incorporate chemical reagents.

Castellani *et al*, for example, report aqueous carrageenan (a polysaccharide derived from seaweed) and precipitated silica gels applied by immersion.[42] This formulation is designed to be combined with traditional decontamination reagents such as HNO_3 and NaOH to form a coating which solidifies for mechanical removal (see Figure 6). Benefits include increased contact time with a lower volume of reagents and no liquid waste. The decontamination of ^{60}Co from black steel was reported with a mean DF of 12.[42]

Figure 6- Decontamination by gel immersion followed by mechanical removal (taken from Castellani et al)[42]

Further work by Castellani *et al* in a later publication evaluates the addition of sodium polyacrylate to these gel formulations; resulting in more rapid substrate wetting with greater efficiency reported. [43] A similar claim is made by Faure *et al* in US patent US 8,636,848 B2; broadly claiming an aqueous formulation containing

inorganic viscosity modifier (silica is detailed) with surfactant, oxidising agents (typically Ce(IV)), acid/base and gelling agents.[44] The gel is claimed to dry and form a vacuumable coating.

Gurau and Deju compared the commercially available Decongel 1101 in the removal of ^{60}Co and ^{137}Cs from common plant substrates.[45] The Decongel was applied using a trowel, palette knife and paintbrush before a 24 hour drying period followed by removal by peeling. Reported DFs range from 10 to 110 with typical DFs between 90-100 for non-porous materials. The authors conclude multiple applications are typically necessary.

Jung *et al* report an aqueous polyvinyl alcohol (PVA), sodium dodecyl sulphate (SDS) and diethylenetriaminepentaacetic acid (DTPA) decontamination gel boasting over 99% inactive CsCl removal from 304 grade stainless steel with removal by drying and peeling.[46] US patent 7,166,758 B2 details a 1-hydroxyethane-1,1-diphosphonic acid (HEDPA) decontamination gel using variations of glycerol, polyethylene glycols, silica gels and a polyacrylamide/polyacrylate crosslinked gel for the decontamination of steel substrates.[47]

Several reported gel-based decontamination reagents are comprised of crosslinked polymer networks with water as a swelling agent. These forms of gel fall under the category of hydrogels; a subset of interpenetrating polymer networks upon which this body of work is based and which is discussed and examined in detail in chapters 2-4.

Also reported are gas phase techniques such as the injection of chlorine trifluoride into cells containing diffusion cascade equipment for reaction with uranium deposits.[24] Gas-dispersed "chemical fog" has also been deployed in Germany with methods such as electrostatic deposition after ultrasonic generation. Russian methods have involved fogs composed of water or acid to remove contamination from liquid metal cooled reactor plant.[24]

Whilst there are numerous advantages to chemical decontamination techniques such as high decontamination factors, tailoring to individual radionuclides and limited airborne contamination; disadvantages such as safe handling difficulties, limited effectiveness on porous mediums and the major issue of the generation of high

volumes of liquid waste requiring treatment must be addressed.[25] In terms of use on porous substrates there is often the risk of causing further penetration of the contaminants into the substrate, increasing the difficulty of removal.[32]

1.5.9 - Other decontamination methods

Several other decontamination technologies exist which either complement or act in a similar way to the techniques described previously. Ultrasonic decontamination, for example, uses ultrasonic waves to form cavitation bubbles which collapse into high energy jets, removing surface of adhered contaminants when submerged in either water or chemical decontaminating agents.[48] The melting of steels may be considered somewhat of a decontamination technique as the radionuclides present in the steel often separate in the liquid state; collecting in the slag or dust for disposal while the metal may be recycled.[49]

Thermal degradation is, as the name suggests, use of a high temperature incendiary device upon a non-combustible surface (e.g. stainless steel) to destroy any degradable organic matter on the surface. A second step may be employed to remove radionuclides which were trapped within these materials.

A decontamination method of note for contaminated effluent waste is the use of radiation resistant algae for the uptake of radionuclides from aqueous solutions; a process termed biodecontamination.[50,51] The intention of this method is to introduce a colony of algae to an aqueous environment and allow multiplication (as the presence of CO_2, light and several dissolved minerals in an aqueous solution is sufficient for multiplication, as evidenced by the algal blooms present in the storage ponds of Sellafield Ltd.[52]). The algae then uptake and concentrate radionuclides for removal by filtration and a drying step to reduce the volume of waste. The use of *Coccomyxa actinabiotis* has been reported with use in a 360 m^3 radioactive waste storage pond at a concentration of 10^7 cells mL^{-1} with high levels of decontamination observed.[50] Investigations into the filtration system were carried out by de Gouvion *et al*, suggesting the feasibility of recovering 85% of initial algae by mass for later reuse.[51]

1.5.10 - Choice of method

Choice of decontamination method requires consideration of multiple factors: the accessibility of the surface, the composition of the contaminated substrate, nature of the contamination, history of the substrate (e.g. previous treatments or potential structural damage), substrate porosity, generation/treatment of secondary waste, mobility of generated waste, level of decontamination required, cost, human dose levels, time required and capability to ensure required temperatures, agitation, and removal of waste products.[20]

Since the majority of substrates requiring decontamination in nuclear sites are concrete and metal[37] many techniques can be considered for one substrate yet not the other. For example porous substrates like concrete allow contaminant penetration to a greater depth, necessitating either removal of material to this depth by physical means (scabbling, milling etc.) or the application of a chemical treatment capable of desorbing and drawing out these contaminants (such as certain gels or peelable coatings). Liquid techniques which do not control the volume of liquid deposited are likely to increase contaminant penetration depth.[21]

In the case of painted substrates the contamination can typically be assumed to reside at or near the surface. In these cases techniques such as vacuuming, detergent wiping or physical strippable coatings can be employed to remove contamination sitting at the surface, as employed on the Sellafield site during an event documented recently by Cavaghan.[32] Water jetting could also be applied to this scenario but would result in a large volume of liquid waste.

Where contaminated steels are encountered the depth of the contamination must again be considered. Contamination sitting at the surface may employ the same methods may as described for painted substrates. If the contamination sits in the oxide layer then more aggressive chemical decontamination should be considered depending on the form of the contaminant (refer to section 1.5.7). Complex geometries would suit foam or gel application methods.[20]

In this body of work the use of hydrogels for the decontamination of stainless steel substrates will be investigated and the concept and implementation of a foam based reagent delivery system for neutron poisoning applications will be evaluated.

1.6 - Aims and Objectives

This project aimed to investigate new materials approaches applied to scenarios in the civil nuclear industry. The incorporation of new active components to existing base technologies and the further development of these base technologies were to be investigated.

Overall there were two main objectives:

1- To develop a new gel-based decontamination technique for the removal of radionuclides from stainless steel substrates.

2- To investigate the feasibility of incorporating neutron poisoning substances into fire-fighting foams for potential application in emergency or accident remediation scenarios.

The rationale behind these objectives is the improvement of existing technologies with a focus on safe and responsible handling of radioactive materials, with particular regard to legacy materials from historical plant operations.

This particular type of hydrogels was chosen for investigation due to prior art in both fine art restoration and radionuclide decontamination but without overlap between the art restoration class of gels and radionuclide applications. It was hypothesised that such materials would provide effective uptake, a stable medium for the transport of decontaminating reagents and a tough, robust and encapsulating containment solution once radionuclides are removed from the surface. The localised nature of the application of these gels was expected to provide a tool for the elimination of radioactive surface hotspots whilst the high hydrophilicity should assist in the prevention of lateral radionuclide spread.

Current literature into hydrogel radionuclide decontamination details hydrogels of differing composition and does not consider the loading of more aggressive reagents

such as nitric acid. This project also aimed to fill some of these uninvestigated voids; especially since there is considerable prior art on the effectiveness of such decontamination reagents but they typically rely on solution based deployment methods rather than investigating the advantages of a solid gel applicator.

Whilst neutron poisons are commonly employed in nuclear reactors in the form of control rods and shielding materials there is no documented use of neutron poisons in emergency situations beyond the dumping of them into the exposed core of the Chernobyl reactor after the loss of containment. This knowledge gap holds the potential to contain a highly useful deployable contingency plan for other such fires in high neutron flux environments. A positive or negative outcome of these investigations would enhance the ability to respond to emergency situations in such environments with reduced hesitation, situation assessments and deliberation without the associated loss of control, time and potentially lives that may result.

1.7 - References

1. Calder Hall Completed. *Nature* **182,** 1708–1709 (1958).

2. Office for Nuclear Regulation. *The United Kingdom's National Report on Compliance with the Convention on Nuclear Safety.* (1998).

3. L'Annunziata, M. F. *Radioactivity : introduction and history.* (Amsterdam : Elsevier, 2007).

4. Henderson, H. *Nuclear power : a reference handbook.* (Santa Barbara, California : ABC-CLIO, 2014).

5. Sears, V. F. Neutron scattering lengths and cross sections. *Neutron News* **3,** 26–37 (1992).

6. Cottingham, W. N. and Greenwood, D. A. An Introduction to nuclear physics *Radiographics a review publication of the Radiological Society of North America Inc* **18,** 995–1007 (2001).

7. Bacon, G. E. *Neutron Physics.* (Wykeham Publications, 1969).

8. HSE. *Report by HM Nuclear Installations Inspectorate on the results of Magnox Long Term Safety Reviews (LTSRs) and Periodic Safety Reviews (PSR).* (2000).

9. Von Hippel, F. N. The radiological and psychological consequences of the Fukushima Daiichi accident. *Bull. At. Sci.* **67,** 27–36 (2011).

10. Worley, N. and Lewins, J. *The Chernobyl Accident and its Implications for the United Kingdom: Watt Committee: report.* (Taylor and Francis, 2003).

11. Bonin, B. in *Handbook of Nuclear Engineering* 3253–3419 (Springer US, 2010).

12. Woodhouse, G. J. The Contamination and Decontamination of Pond Furniture used in the Nuclear Power Industry. (University of Manchester, 2008).

13. Sellafield Ltd. *Sellafield Plan.* (2011).

14. Severa, J. and Bar, J. *Handbook of Radioactive Contamination and Decontamination, Studies in Environmental Science 47.* (Elsevier, 1991).

15. Stacey, W. M. *Nuclear reactor physics.* (Weinheim, Germany : Wiley-VCH, 2018).

16. Nikolaev, A. N., Karlina, O. K., Yurchenko, A. Y. and Karlin, Y. V. Assessment of 137Cs decontamination of concrete by the reagent method. *At. Energy* **112,** 57–62 (2012).

17. Parajuli, D. *Tanaka, Y., Hakuta, Y., Minami, K., Fukuda, S., Umeoka, K., Kamimura, R., Hayashi, Y., Ouchi, M., Kawamoto, T.* Dealing with the aftermath of fukushima daiichi nuclear accident: Decontamination of

radioactive cesium enriched ash. *Environ. Sci. Technol.* **47,** 3800–3806 (2013).

18.　Kaminski, M., Mertz, C., Ortega, L. and Kivenas, N. Sorption of radionuclides to building materials and its removal using simple wash solutions. *J. Environ. Chem. Eng.* **4,** 1514–1522 (2016).

19.　Goyal, J. and Antonarakis, E. S. Bone-targeting radiopharmaceuticals for the treatment of prostate cancer with bone metastases. *Cancer Lett.* **323,** 135–146 (2012).

20.　Laraia, M. *Nuclear decommissioning planning, execution and international experience.* (Philadelphia, Pa. : Woodhead Pub., 2012).

21.　Bayliss, C. R. (Colin R. *Nuclear decommissioning, waste management, and environmental site remediation.* (Amsterdam ; Boston : Butterworth-Heinemann, 2003).

22.　Babilas, E. and Brendebach, B. Selection and evaluation of decontamination and dismantling techniques for decommissioning of large NPPs components. *Prog. Nucl. Energy* **84,** 108–115 (2015).

23.　Demetriou, A. M., Crouch, D., Batey, H., Faulkner, S., Yeates, S., Livens, F. Using high-throughput techniques to identify complexants for ^{137}Cs, ^{60}Co and ^{90}Sr. *J. Mater. Chem.* **18,** 5350 (2008).

24.　State of the Art Technology for Decontamination and Dismantling of Nuclear Facilities. *IAEA Tech. Reports Ser. No. 395* (1999).

25.　NEA Task Group on Decontamination. *Decontamination Techniques Used in Decommissioning Activities.pdf. Decontamination Techniques Used in Decommissioning Activities* (1998).

26.　Guidi, G., Cumo, F. and de Santoli, L. LCA of strippable coatings and of steam vacuum technology used for nuclear plants decontamination. *Clean Technol. Environ. Policy* **12,** 283–289 (2010).

27.　Laraia author, M. *Advances and innovations in nuclear decommissioning.* (Kidlington, United Kingdom : Woodhead Publishing, an imprint of Elsevier, 2017).

28.　Laraia, M. in *Handbook of Advanced Radioactive Waste Conditioning Technologies* 173–204 (Elsevier, 2011).

29.　Gray, H. N., Jorgensen, B., McClaugherty, D. L. and Kippenberger, A. Smart polymeric coatings for surface decontamination. *Ind. Eng. Chem. Res.* **40,** 3540–3546 (2001).

30.　Makul, N., Rattanadecho, P. and Agrawal, D. K. Applications of microwave energy in cement and concrete - A review. *Renew. Sustain. Energy Rev.* **37,** 715–733 (2014).

31.　Buttress, A. J., Jones, D., Dodds, C., Dimitrakis, G., Campbell C., Dawson, A. Understanding the scabbling of concrete using microwave energy. *Cem.*

Concr. Res. **75,** 75–90 (2015).

32. Cavaghan, J. Decontamination and Recovery of a Nuclear Facility to Allow Continued Operation. *Radiat. Prot. Dosimetry* **173,** 118–123 (2017).

33. Kohli, R. in *Developments in Surface Contamination and Cleaning* 177–224 (Elsevier, 2010).

34. Yang, H. M., Park, C. W. and Lee, K. W. Polymeric coatings for surface decontamination and ecofriendly volume reduction of radioactive waste after use. *Prog. Nucl. Energy* **104,** 67–74 (2018).

35. Rao, S. V. S. and Lal, K. B. Surface decontamination studies using polyvinyl acetate based strippable polymer. *J. Radioanal. Nucl. Chem.* **260,** 35–42 (2004).

36. Kaminski, M. D., Lee, S. D. and Magnuson, M. Wide-area decontamination in an urban environment after radiological dispersion: A review and perspectives. *J. Hazard. Mater.* **305,** 67–86 (2016).

37. Kumar, V., Goel, R., Chawla, R., Silambarasan, M. and Sharma, R. Chemical, biological, radiological, and nuclear decontamination: Recent trends and future perspective. *J. Pharm. Bioallied Sci.* **2,** 220 (2010).

38. Ponnet, M., Klein, M., Massaut, V., Davain, H. and Aleton, G. in *Thorough Chemical Decontamination With the MEDOC Process: Batch Treatment of Dismantled Pieces or Loop Treatment of Large Components Such as the BR3 Steam Generator and Pressurizer* (2003).

39. Everett, D. H. *Basic Principles of Colloid Science. RSC Paperbacks* (Cambridge : Royal Society of Chemistry, 1988).

40. Wood, C. J. A review of the application of chemical decontamination technology in the United States. *Prog. Nucl. Energy* **23,** 35–80 (1990).

41. Tuck, M., Wray, B. and Musgrave, M. Surface and Subsurface Decontamination Technology. in *Volume 2: Facility Decontamination and Decommissioning; Environmental Remediation; Environmental Management/Public Involvement/Crosscutting Issues/Global Partnering* V002T03A036 (ASME, 2013).

42. Castellani, R., Poulesquen, A., Goettmann, F., Marchal, P. and Choplin, L. A topping gel for the treatment of nuclear contaminated small items. *Nucl. Eng. Des.* **278,** 481–490 (2014).

43. Castellani, R., Poulesquen, A., Goettmann, F., Marchal, P. and Choplin, L. Efficiency enhancement of decontamination gels by a superabsorbent polymer. *Colloids Surfaces A Physicochem. Eng. Asp.* **454,** 89–95 (2014).

44. Faure, S., Fuentes, P. and Lallot, Y. Vacuumable gel for decontaminating surfaces and use thereof. US 8636848 B2 (2014).

45. Gurau, D. and Deju, R. The use of chemical gel for decontamination during decommissioning of nuclear facilities. *Radiat. Phys. Chem.* **106,** 371–375

(2015).

46. Jung, C. H., Moon, J. K., Won, H. J., Lee, K. W. and Kim, C. K. Chemical Gel for Decontamination of Cs Surrogate on Stainless Steel Surface. in *Chemical Gel for Decontamination of Cs Surrogate on Stainless Steel Surface - 11257* (2011).

47. Nunez, L. and Kaminski, M. D. Foam and gel methods for the decontamination of metallic surfaces. (2007).

48. Nicolosi, V., Chhowalla, M., Kanatzidis, M. G., Strano, M. S. and Coleman, J. N. Liquid Exfoliation of Layered Materials. *Science.* **340,** 1226419–1226419 (2013).

49. Slimák, A. and Nečas, V. Melting of contaminated metallic materials in the process of the decommissioning of nuclear power plants. *Prog. Nucl. Energy* **92,** 29–39 (2016).

50. Rivasseau, C., Farhi, E., Atteia, A., Coute, A., Gromova, M., Cyr, D., Boisson, A., Feret, A., Compagnon, E., Bligny, R. An extremely radioresistant green eukaryote for radionuclide bio-decontamination in the nuclear industry. *Energy Environ. Sci.* **6,** 1230 (2013).

51. De Gouvion Saint Cyr, D., Wisniewski, C., Schrive, L., Farhi, E. and Rivasseau, C. Feasibility study of microfiltration for algae separation in an innovative nuclear effluents decontamination process. *Sep. Purif. Technol.* **125,** 126–135 (2014).

52. Ashworth, H., Heath, S., Bryan, N., Abrahamsen, L. and Kellet, S. Effect of Organics on Radionuclide Partitioning in Nuclear Fuel Storage Ponds. in *World Academy of Science, Engineering and Technology, International Science Index, Nuclear and Quantum Engineering* **11(6),** 147–147 (2017).

Chapter 2 – Interpenetrating polymer networks literature review

2.1 - Interpenetrating Polymer Networks

As with many new discoveries the first recorded instance of the synthesis of interpenetrating polymer networks (IPNs) by Jonas Aylesworth (Thomas Edison's chief chemist[1]) in 1914[2] was not initially recognised for its true value, the original patent neglecting to discuss IPNs or even use the word "polymer"[1,2] as would be expected in the early days of the 20th century. The interlaced network of phenol-formaldehyde and natural rubber crosslinked with sulphur was used to improve the mechanical properties of phonograph records before fading from view for many years. In fact, it was 1960 before the phrase "interpenetrating polymer network" was coined[1]. These materials have since shown great potential within fields ranging from materials separation, cleaning, decontamination, biomedical applications and many more.[1,3,4]

An interpenetrating polymer network is defined much as the name would suggest: "Two or more networks that are at least partially interlaced on a molecular scale but not covalently bonded to each other and cannot be separated unless chemical bonds are broken".[5] During their formation one polymer is either synthesised or crosslinked with another polymer (either previously crosslinked or due to undergo crosslinking) present within the reaction mix.[6] This facilitates the synthesis of a three dimensional interpenetrating network[7] to produce a material with behaviour differing from that of the parent polymeric materials[8] which can be tailored to the required task by careful selection of reagents. Such materials tend to possess greatly increased mechanical strength over single polymer networks,[9] often with one network providing the mechanical strength and a second network providing additional advantages such as energy dissipation at large strains.[10] A simplified analogy of an IPN would be to imagine a pair of interwoven nets; both individual nets are unbound to each other directly but cannot be separated without cutting the threads connecting the network.
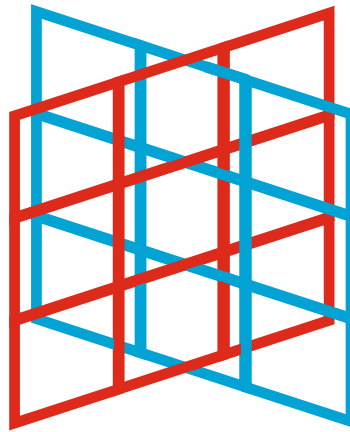
Figure 7- IPN schematic

In fact the majority of IPNs interpenetrate by the formation of separated phases to the order of tens of nanometres with many also exhibiting dual phase continuity[1,11] to the extent the different phases can be seen with the naked eye.

Suggested categories of IPNs can be determined by the synthesis method; when both networks are simultaneously synthesised using differing routes a simultaneous IPN is formed.[7] Conversely the formation of a new network around an existing polymer results in a sequential IPN,[12] a common synthetic route to the production of IPN or semi IPN hydrogels. A homo-IPN structure is also possible; with both independent networks possessing the same structure.[7]

2.2 - Double networks

The formation of a double network IPN occurs when the degree of crosslinking of two networks is asymmetrical.[6] Gong *et al* reported the first instance of this class of hydrogels in 2003, exhibiting water contents of between 60-90%, high wear resistance and fracture strength up to several tens of megapascals.[13] The greatly enhanced strength of double networks is conferred by the combination of a ductile network, with the ability to significantly extend, intertwined with a brittle "sacrificial" network which fragments into smaller segments to disperse stress, dissipate energy and cause shielding.[9] In order to achieve the composite performance the ductile network is polymerised around the brittle network and

crosslinked to a much lower degree; resulting in strengths much greater than that of the sum of the constituents. The fatigue resistance of these gels has, however, been called into question due to the mechanism of strengthening relying upon breaking the covalent bonds of the more brittle network, leading to irreversible structural changes.[10] Haque *et al* suggest in their review of double network hydrogels that the incorporation of a self-healing material (such as a substance forming physical, rather than chemical, crosslinks) into the brittle network could resolve this issue.[9] Due to the strengths exhibited, double networks are considered to have great potential for cartilage replacement.[7]

2.3 - Semi-Interpenetrating Polymer Networks

A semi-interpenetrating polymer network (semi-IPN) differs from a standard IPN by the inclusion into the synthesis of uncrosslinked linear or branched polymers;[1] resulting in physical entrainment on a molecular level of linear/branched polymer within the forming crosslinked network which could be separated without the breaking of chemical bonds.[14] Due to the relative ease of separation semi-IPNs are classified as polymer blends.[5] It is possible to convert a semi-IPN to an IPN through crosslinking of the entangled linear/branched polymer chains.[7,15,16]

Extending the previous analogy of interlinked nets a simplified visual of a semi-IPN is given below in which the network can be simplified to the principle of lengths of string threaded through and entangled within a net.
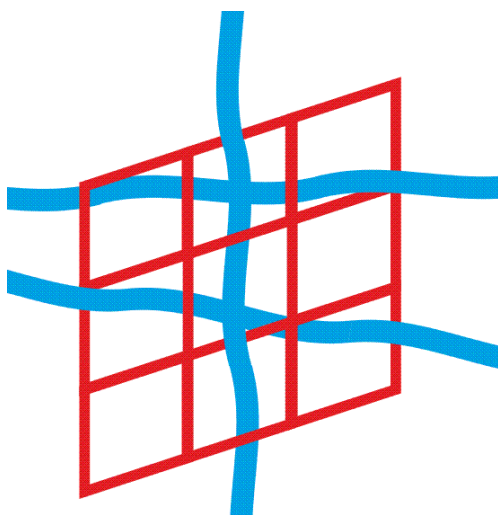
Figure 8- Semi IPN schematic with red representing the crosslinked polymer network and blue the entangled linear polymer.

An example of interest is the formation of crosslinked poly(2-hydroxyethyl methacrylate) (pHEMA) and polyvinylpyrrolidone (PVP) semi-IPN hydrogels which have been recorded in the literature for the decontamination of sensitive and delicate surfaces.[14,17,18]

2.4 - Hydrogels

Considering that a gel is a non-fluid network of either polymeric or colloidal composition (most commonly polymeric) which is swollen by a fluid element then it can be expected that the substances termed "hydrogels" are simply those whose fluid swelling agent is water.[5] These substances are therefore hydrophilic and swell to a large degree in the presence of water.[7] Hydrogels can be either IPN or semi-IPN as detailed above depending upon crosslinks present and reversibility.[3,7]

2.4.1 - Classifications of hydrogels

Further breakdown of the hydrogels family would allow the identification of several distinct branches: non-ionic, ionic and composites of hydrophilic and hydrophobic materials, each exhibiting significantly different swelling behaviours and mechanisms. Non-ionic hydrogels have been shown to swell exclusively due to interactions between the polymer network and water.[3] Cationic hydrogel swelling increases at low pH whilst anionic hydrogels swell favourably at high pH; both phenomena are due to the favourability of the degree of dissociation of the ionic chains. The swelling behaviour of amphoteric hydrogels depends upon the pH of the aqueous medium relative to the molecule's isoelectric point.[3] If we consider the composites of hydrophilic and hydrophobic hydrogels there is commonly a "backbone" with a pendant group, rotating when hydrated or dehydrated as well as with temperature changes in aqueous environments. A particularly good example of this is poly(2-hydroxyethyl methacrylate) (polyHEMA) containing a hydroxyethyl/methyl pendant which exposes the polar hydroxyethyl to water (hence the swelling) and methyl to air, making it hydrophobic. This polymer was a common component of early contact lenses.[19]
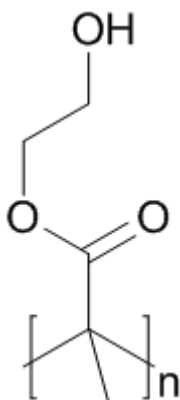
Figure 9- Structure of poly(HEMA)

Further breakdowns of classification beyond those previously detailed can be split into natural, synthetic or hybrid (a mixture of both natural and synthetic) depending on the source of the reagents in addition to homogenous (transparent), microporous and macroporous to name several possibilities.[19]

2.4.2 - Water in hydrogels

Since hydrogels are commonly formed by the swelling of polymeric network the water contained within the gel plays a significant role in the determination of hydrogel properties. The water retention of a hydrogel can be described depending upon the extent to which the water is bound and the site the water is located within the gel network (See figure 10).[3] The most integral to the hydrogel structure (and the most difficult to remove) is the bound water which is attached to the polymer chain itself via hydration of the ionic components of the chain or functional groups. This is sometimes referred to as unfreezable water.[14, 20] To the exterior of the network lies free water which has no interactions with either the polymer functional groups or ions and can be readily removed from the network, possessing the same thermodynamic properties of bulk water.[14] Between these layers lies the semi-bound water which is distant enough from the polymer chains to prevent strong interactions but yet remains close enough to prevent unhindered movement. It is often referred to as freeze-bound water as these interactions reduce the freezing point to below 0°C.[14, 20]

Interstitial water is located, as the name suggests, in the region between the sites of polymer chains. This water has no interactions with the polymer chains but remains trapped within the network nonetheless.[3]
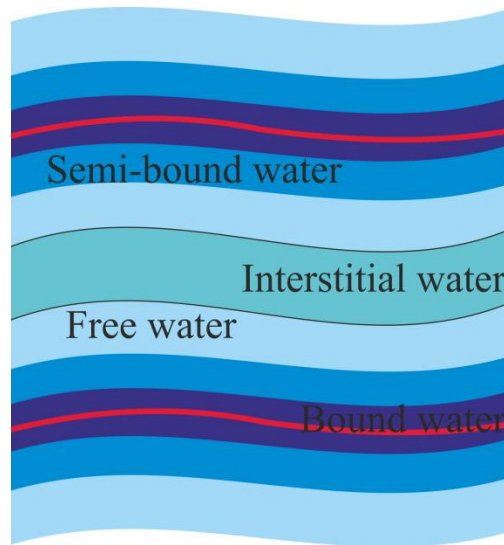
Figure 10- Hydrogel water classifications (red representing the polymer chain)

As hydrogels are defined as a non-fluid polymeric or colloidal network with water as a swelling agent[5] then it is reasonable to use a hydrogel's degree of swelling, determined by the interior cavity space capable of containing water, to characterise it. In order to do this there are three forces responsible for hydrogel swelling which must be considered: osmosis, electrostatic forces and interactions between the polymer and water.[3]

Osmotic pressure contributes to the swelling of hydrogels when they contain ionic groups. Whenever there is a difference in the concentration of ions between the hydrogel and environment then the counter ions will generate osmotic pressure, scaling with the magnitude of the difference between environments.[3]

The ions existing in hydrogels are commonly produced by the ionisation of pendant ionic groups,[3] allowing the polymer chain to become either anionic or cationic and thus repel along its length in solution; increasing the available cavities for water containment.

When considering the interactions between the polymer and water the hydrophilicity of the polymer is key. Should the hydrogel contain hydrophilic functional groups then the gels swell due to interactions between the polymer and water; increasing the hydrophilicity of the polymer will increase the magnitude of these interactions.[3]

The rate of swelling is determined by the initial stages of the swelling process; whereby the initial diffusion rate of the solvent (determined by factors such as temperature, porosity of the hydrogel network and the solvent's molecular mass) dictates the rate at which the second relaxation step occurs. The relaxation step is a slower process dependent upon the relaxation rate of the polymer chains within the hydrogel network.[3]

The controlling elements behind the swelling of hydrogels are many and varied; ranging from gel structure through drying techniques to the nature of the swelling solution itself and are so varied as to be extremely difficult to detail. The key factor of great importance, however, is the density of the crosslinks within the hydrogel network. Thankfully this is a factor over which the producer of the gel has a high degree of control and so gels possessing a high crosslink density can be formulated to pass large volumes of water through the network.[3]

2.4.3 - Hydrogel synthesis

In order to synthesise a hydrogel the three most integral components are monomer, initiator and crosslinker. In many cases it is pertinent to include linear, uncrosslinked polymer should the formation of a semi-IPN be the objective. This would necessitate the formation of an aqueous solution in order to allow incorporation into the growing crosslinked polymer network but water or a suitable aqueous solution may be used to tailor final hydrogel properties after preparation in another solvent.[3] Hence it is greatly advantageous for the reagents to possess at least some degree of solubility in water. Varying the quantities of these components, their relative ratios and the nature of each component reagent can greatly alter the physical characteristics of the hydrogels. As can changes to reaction conditions such as temperatures, times and even the nature of the reaction vessel itself. The method used in the main body of this work is a solution method using a homogeneous mix of reagents, allowing a greater degree of control over the properties of the final hydrogel product since the temperature of the reaction is readily controlled by the solvent acting as a heat sink.[21] Prior to crosslinking the dissolved hydrophilic polymers in water are termed a hydrosol, exhibiting liquid behaviour in contrast to the solid behaviour of hydrogels.[3]

Bulk polymerisation is also possible by adding an initiator to undiluted solutions containing one or more monomers, often with a small amount of crosslinker.[21] This method results in a high degree of polymerisation but a very large increase in viscosity and temperature during the progress of the reaction; typically with a hard, glassy product which swells and softens in water.[21]

An alternate synthesis model commonly used for the production of synthetic hydrogels is via inverse dispersion where the reaction mix is heterogeneous. The suspension of differing reagents in aqueous and organic phases allows for the synthesis of small scale hydrogels (down to micron sizes[3]) although the organic solvent must be carefully selected to allow ease of removal after formation. Another method is via the aggregation of polymer chains resulting from polymeric hydrocolloids entangling and aggregating to form interactions between chains exceeding the strength of interactions with water. Suspension (oil in water) and inverse suspension (water in oil) polymerisation are also useful methods to yield hydrogels in the form of beads, powders or microspheres. [21]

Hydrogels possessing greater mechanical strength can ordinarily be achieved with an increase in crosslink density[13] and care must be given as to the choice of crosslinker since if it is soluble in the monomer this will lead to homogenous crosslinking; causing brittleness when densely crosslinked.[3] Heterogeneous crosslinking, conversely, can be induced using the inverse dispersion method containing a hydrophobic crosslinker within the continuous phase and commonly resulting in a stronger material; although both variants result in increased swollen stability.

Whilst selecting suitable reagents it must be kept in mind that "equilibrium swelling capacity of a hydrogel is a balance between swelling and elastic forces"[3] therefore a balance between high molecular weight polymers and crosslink density must be optimised for individual environments since extremes of temperature, mechanical force or pH can cause the materials to deform, fail or weaken the intermolecular forces. Generally higher-swelling hydrogels exhibit weaker mechanical properties.[3]

Once the synthesis has been completed the gel must be thoroughly washed with a large quantity of water in order to remove residual reagents, unwanted side products and, in the case of semi-IPNs, any polymer which has not been physically trapped within the forming gel network.[3]

2.4.4 - Properties and characterisation of hydrogels

Due to the composite nature of hydrogels, their physical properties are determined by the formulation proportions. The key feature used to predict and determine the resultant properties is the ratio of polymer to water; a high ratio here will result in low swelling gels and vice versa. However, the low swelling gels will exhibit increased swollen stability in contrast with high swelling counterparts. These properties are tailored by adjustment of the crosslinker to monomer ratios.[3] The effect of external pressure upon hydrogel networks can affect the swelling characteristics, with an increase in external pressure generally lowering the swelling pressure; of particular importance in the case of agricultural moisture retainers or incontinence nappies.[3]

The simplest method of swelling due to water uptake is the equilibrium water content (EWC); a mass based evaluation of the water content of a gel, given by:[17]

$$\text{EWC (\%)} = \left[\frac{M_h - M_d}{M_h}\right] \times 100$$

Equation 5- Equilibrium water content

Where M_h is the hydrated hydrogel mass and M_d is the dessicated hydrogel mass. The volume measurements of a gel can also be used to determine the dimensional swelling.[3]

Also of characteristic importance is the gel content (GC) of a gel, given by:

$$GC \text{ (\%)} = \left[\frac{M_d}{M_I}\right] \times 100$$

Equation 6- Gel content

Where M_I is the mass of the polymeric components (typically HEMA and PVP in the case of this work) in the gel synthesis mixture prior to reaction.[17] A lower GC would generally indicate loss of some of these materials prior to completion.

The mechanical strength of hydrogels is an important characteristic to analyse as most applications require certain strengths, flexibilities or ability to retain their shapes. Water retention is recorded as being an essential dependent upon the mechanical strength of hydrogels as low mechanical strength results in water leakage or structural degradation, leading to more rapid desorption.[3]

Additional characterisation of hydrogels can be gathered when gel rheology is considered: the viscoelastic response under the application of oscillatory strain/stress provides a detailed description of the solid and fluid character of the gel, rupture stress, deformation modes, viscoelasticity and general comparative strength, among other characteristics.[22]

Consideration of the G' (storage modulus) and G'' (loss modulus) can illustrate the changes in elasticity and viscous fluid behaviour,[3] revealing the dominant force and investigating the possibility of a crossover during analysis which indicates a change in properties across the region examined. A stress-strain curve analysis indicates the relative strength of the gels examined, revealing yield stresses if they occur within the range of the parameters of the test and by evaluating the shape of the curve a distinction can be made between newtonian, dilatancy (shear thicknening) and pseudoplastic (shear thinning) behaviour.[22]

An important factor used to characterise a hydrogel is to determine whether it is porous or non-porous: a non-porous hydrogel will be comprised of solid polymer and water whilst a porous hydrogel will include a third phase: air. A combination of the properties of these three phases is present in the synthesised gel, with air inclusion resulting in a deterioration of the mechanical properties yet an increase in water absorption.[3] In order to determine pore sizes and distribution the use of imaging techniques such as scanning electron microscopy (SEM) coupled with image analysis are used.

2.5 - Practical applications of hydrogels

Forward thinking is required during the synthesis of hydrogels where an application is in mind; the size of the gels produced has a significant impact on their usefulness for certain applications. For example hygiene products tend to utilise gel particles of between 150-300 mm whilst soil moistening requires large particles (to retain more moisture for longer) and seed germination applications will use smaller particles.[3] These applications all require high swelling gels where the uptake and/or retention of liquids is paramount.

2.5.1 - Drug delivery

It is often pertinent to synthesise gels with low swelling properties for drug delivery applications such as gels which change or disintegrate in response to external stimuli[23] (therefore termed "smart materials"),[6,24] digestive enzymes or facilitate diffusion-based release prior to disintegration.[25] Generally diffusion based release is the primary mechanism in water-soluble drug delivery whilst degradation is used for water insoluble drugs[26] with the potential to combine both mechanisms for bespoke drug treatments. In practice hydrogels of this type can be used to release drugs into a particular area of the human body; for example pH or salt level changes may be used to control whether release occurs in either the stomach or intestine.[27] Ingestion is the most common and easily administered method of deployment but injection is also reported[24] for both drug and gene transfection[28] in applications with a variable rate of release allowing the administration of immediate or longer term therapeutic doses.[29]

The excellent biocompatibility of hydrogels has also led to the development and use of injected hydrogels as a scaffold for tissue regeneration and bone regrowth,[30] with the ability to promote osteoblast adhesion and proliferation.[31] Gels in this form are typically injected pre-gelation in order to conform to the existing physical space and often rely upon environmental stimuli to initiate gelation and biodegrade once no longer required.[32]

2.5.2 - Dye removal

One particular area where hydrogels have found use is in the removal of soluble contaminants from waste streams. For example; Jeon *et al* reported the removal of methylene blue, methyl orange and malachite green dyes from aqueous solutions using alginate or alginate/polyaspartate hydrogel beads[33] and Mandal *et al* documented the removal of the dyes methyl violet and rhodamine B from dilute aqueous solution using a base PVA and poly(acrylic acid-co-2-hydroxyethyl methacrylate) formulation in IPN and semi-IPN forms.[7,34] The semi-IPNs were found to exhibit increased sorption over IPNs which was believed to be due to the more closely-knit network structure of the IPNs. A difference in sorption mechanisms was also observed: physical sorption in high concentration dye solutions and chemical sorption in lower concentration solutions. Uptake efficiencies of different dye molecules were dependent upon the functional groups present within both the gels and dyes; ionic repulsion being a key factor, particularly under differing pH conditions.[7] The addition of sorbents to gel networks have also been of particular use in this application: gels of chitosan and glutaraldehyde with activated carbon were reported by Gonçalves *et al* to be effective in the removal of Food Blue 2 (E133) and Food Red 17 (E129) from aqueous solutions, with the potential for five re-use cycles after dye desorption with NaOH.[35] Using a different removal mechanism the removal of acid fuchsin magenta dye from aqueous solution was reported by Zhou *et al* using a nano TiO_2/chitosan/poly(N-isopropylacrylamide) gel designed to photocatalytically degrade the dye molecules.[36]

2.5.3 - Metal ion removal

In addition to dyes, hydrogels have also been developed and used to remove metal ions from effluent waste streams and natural water courses.[12,37,38] In a similar way to dye removal, metal ion removal effectiveness depends largely upon the functional groups present within the gel structure; namely chelation and ion exchange mechanisms will vastly improve the uptake properties when compared with sorption alone,[7] with examples existing of selectivity in ion uptake due to size exclusion of

large hydrated ions.[39] Wang *et al*, for example, reported the removal of Ni^{2+}, Cu^{2+}, Zn^{2+} and Cd^{2+} with chelation and chemical adsorption faclitated by the presence of COOH, NH_2 and C=O groups.[40] Tang *et al* have also reported an increase in the uptake of heavy metal ions by the presence of COO^- groups in polyacrylate/polyethylene glycol hydrogels.[41] Ion imprinting of hydrogels has aimed to improve uptake selectivity with increased affinity for the template ion reported[42,43] and gels synthesised in this manner have been noted as particularly selective for the removal of uranyl ions,[44,45] some even incorporating thermoresponsive properties.[46] Magnetic hydrogels have also been synthesised with enhanced ease of reusability reported.[37]

2.5.4 - Nuclear decontamination

A particular decontamination gel of interest is a commercial product marketed as "SuperGel" by Argonne national laboratories. Despite most gels reporting poor effectiveness on porous substrates, it has shown effectiveness on typically problematic substrates such as brick and concrete.[47] SuperGel is a hydrogel-based decontamination method consisting of engineered nanoparticles, salt, polyacrylamide and polyacrylate in an aqueous solution. It was described by the United States environmental protection agency during evaluation as "a system of super absorbing polymers containing solid sequestering agents dissolved in a non-hazardous ionic wash solution".[48] After spray application to a porous surface the wetting agents suspend contaminant radionuclides and absorbed radionuclides are removed from sorption sites by ion exchange for dissolution before fixation onto the engineered nanoparticles, resulting in increased uptake when compared to solvent only processes.[49] The formation of a highly absorbent hydrogel due to crosslinking *in situ* when contacted with wetting agents results in rapid water absorption, which prevents liquid penetration transporting contaminant radioisotopes deeper into the material. Average DFs on concrete of 3.6 ± 0.62 and 3.8 ± 0.7 are reported in different performance comparisons.[48,50] The final step is removal of the hydrogel by vacuum; the resultant gel may then be recycled, desiccated or incinerated.[48]

Yang *et al* report a varied series of hydrogel decontamination agents for the removal of ^{137}Cs radionuclides.[51–54] A calcium-alginate based hydrogel is reported containing iron oxide nanoparticles coated with copper ferrocyanide for the adsorption and removal of ^{137}Cs from painted concrete, exhibiting a DF of above 10. The gel is then removed from the surface, the hydrogel crosslinks are broken and magnetic separation is used to remove the nanoparticles. This treatment process requires initial treatment with a washing solution.[51]

A follow-up paper replaced the alginate beads with a PVA and borate complex which forms crosslinks between the borate ester and PVA hydroxyl groups.[52] This eliminated the initial washing process whilst also allowing the existing magnetic separation technique to continue without the addition of EDTA to reverse the gel crosslinks. Gels containing water and an aqueous solution of NH_4Cl (to increase Cs solubility by ion exchange) were applied to painted concrete with a maximum DF of 6.05 recorded.[52]

On a further variant by the same author a polyacrylamide and alginate hydrogel containing the aforementioned magnetic nanoparticles was reported.[53] Crosslinking was initiated by the addition of Ca^{2+} ions and post decontamination removal of this Ca^{2+} was carried out by washing with Na_2CO_3 solutions prior to magnetic nanoparticle separation. Decontamination experiments were again carried out on painted concrete with a DF of 28.9 reported.[53]

Another paper followed in 2018 using the PVA-borate hydrogel base containing Prussian blue as an adsorbent in the place of magnetic nanoparticles.[54] Further substrates are also examined: cement, aluminium and stainless steel with removal by drying and peeling. An alternative waste volume reduction step using either ultrafiltration or centrifugation rather than magnetic separation was also suggested (see Figure 11 for procedure and mechanism outline). DFs of 16.7, 47.6, 18.1 and 1.6 on painted cement, aluminium, stainless steel and cement respectively were reported after 24 hours contact. Testing of the commercially available Decongel 1101 under the same circumstances yielded lower DFs of 5.2, 28.6, 7.7 and 1.3 on these same surfaces respectively.[54]
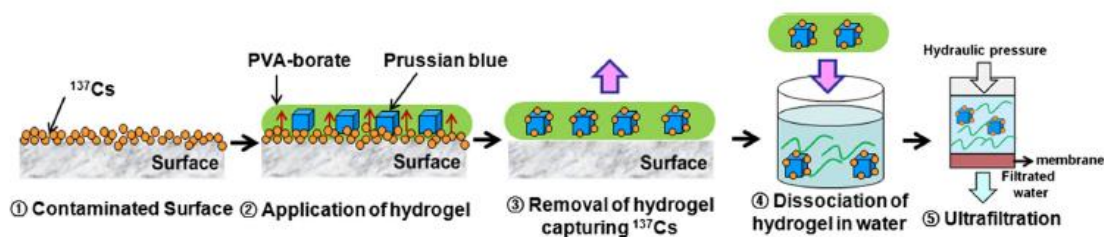
Figure 11– Mechanism of decontamination and reprocessing of Prussian blue hydrogels (taken from Yang et al)[54]

Kim *et al* also report a magnetic hydrogel for the removal of Cs^+ ions from aqueous solution.[55] A PVA base gel was used, Fe_3O_4 nanoparticles functionalised with citric acid prevent sorbent nanoparticle aggregation and potassium copper hexacyanoferrate provides the adsorption medium. The hydrogel was produced using a freeze-thaw crosslinking method with subsequent formation of the copper containing nanoparticles. 99.9% Cs^+ removal from solution was reported with separation by magnetic field for waste disposal.[55]

2.6 - Poly(NIPAM) hydrogels

The incorporation of the stimuli responsive poly(NIPAM) into hydrogels has been widely reported[56–58] as it allows the incorporation of unique thermoresponsive properties. For example the synthesis of smart gels capable of the uptake and encapsulation of metal ions with removal of water via gel contraction and gel recycling via 0.01 M HCl desorption followed by 0.1 M NaOH regeneration.[7,59] Poly(NIPAM) hydrogels co polymerised with acrylic acid and crosslinked with (+)-*N,N'*-diallyltartramide have also been reported for drug delivery applications; with documented pH and thermoresponsive properties resulting in an ability to control drug release rates in differing environments.[60] Also reported is the enantiomeric selectivity of poly(NIPAM) co polymerised with L-Phenylalanine ethyl ester in the separation of alanine, tartaric acid and phenylalanine due to the thermally controlled size reduction of the gels.[61]
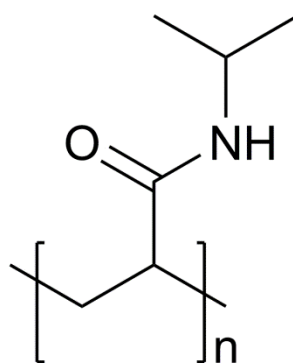
Figure 12- Structure of poly(NIPAM)

The incorporation of crown ether components on poly(NIPAM) gels was found by Dali *et al* to decrease both the magnitude of gel contraction and reusability of the gels (due to the difficult task of removing metal ions from crown ethers) but exhibited higher levels of aqueous ^{90}Sr and ^{60}Co radioisotope removal when compared with a crown ether free composite.[62] Tokuhiro *et al* also reported the use of poly(NIPAM) gels in the removal of metal ions from aqueous waste streams designed to simulate radioactive waste forms, reporting the COOH (carboxylic acid) functional group as being the most effective of those examined for ion removal.[63]

The large surface area of hydrogels, coupled with the inclusion of chelating functional groups[40] such as COOH, NH_2, C=O, SO_3^{2-}, OH, SH and $C=O(NH_2)$ makes hydrogels an extremely attractive premise for metal ion uptake and removal with additional benefits to reuse and encapsulation from thermoresponsive gel composites.

2.7 - HEMA/PVP hydrogels

As detailed earlier (see figure 9), another commonly employed polymer in the synthesis of hydrogels in poly(2-hydroxyethyl methacrylate), poly(HEMA).[64,65] Poly(HEMA) finds uses as a hydrophilic contact lens[19] when swollen to equilibrium with around 38% wt. water, a major advantage being the minimal changes in optical properties when the crosslinker composition is changed.[19] Due to its biocompatibility it is commonly used to form composites with either *N*-vinylpyrrolidone as a

copolymer or physically incorporated into a semi-IPN in the form of the highly hydrophilic and low toxicity polyvinylpyrrolidone (PVP).[3,14] While technically possible to separate this composite it is, in practice, extremely unlikely due to the high extent of entanglement and formation of hydrogen bonds between hydroxyl group of HEMA and carbonyl group of PVP.[54] The crosslinking polymerisation of HEMA by gamma radiation in the presence of PVP has been reported to produce high gel fraction semi-IPNs, with an increase in gel fraction observed up to a dose of 40 kGy.[67] Loadings of Fe_3O_4 and Ag nanoparticles were added to enhance the release of a model drug; Ciprofloxacin.

Of particular interest for the work of this project is the work carried out by Domingues *et al* in the cleaning of delicate works of art.[14,17] Poly(HEMA) and high molecular weight PVP composite hydrogels have been synthesised to combine the hydrophilicity of PVP (see figure 13) with the hydrophilic and structural properties of poly(HEMA) to form softer gel systems with high retention capabilities, no residue and a high degree of control over the area of application; resulting in a high effectiveness when applied to cleaning watercolour paintings, although requiring mechanical cleaning action.[14,17] This work aims to build upon these achievements, applying similar materials to the removal of the target radioisotopes ^{90}Sr and ^{137}Cs from stainless steel surfaces whilst maintaining ease of use, application control, structural integrity and high levels of contaminant removal.
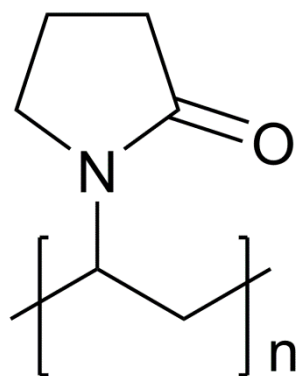
Figure 13 - Structure of PVP

2.8 - References

1. Sperling, L. H. Interpenetrating Polymer Networks: An Overview. *Interpenetr. Polym. Networks* **239,** 3–38 (1994).

2. Aylsworth, J. W. Plastic composition. 4 (1914). at http://www.google.com/patents/US1111284

3. Ottenbrite, R. M., Park, K. and Okano, T. *Biomedical Applications of Hydrogels Handbook. Climate Change 2013 - The Physical Science Basis* (Springer New York, 2010).

4. Wilson, C., Main, M., Cooper, J., Briggs, M., Cooper, A., Adams, D. Swellable functional hypercrosslinked polymer networks for the uptake of chemical warfare agents. *Polym. Chem.* **8,** 1914–1922 (2017).

5. Alemán, J. V. Chadwick, A., He, J., Hess, M., Horie, K., Jones, R., Kratochvil, P., Meisel, I., Mita, I., Moad, G., Penczek, S., Stepto, R. Definitions of terms relating to the structure and processing of sols, gels, networks, and inorganic-organic hybrid materials (IUPAC Recommendations 2007). *Pure Appl. Chem.* **79,** 1801–1829 (2007).

6. Haq, M. A., Su, Y. and Wang, D. Mechanical properties of PNIPAM based hydrogels: A review. *Mater. Sci. Eng. C* **70,** 842–855 (2017).

7. Dragan, E. S. Design and applications of interpenetrating polymer network hydrogels. A review. *Chem. Eng. J.* **243,** 572–590 (2014).

8. Kim, S. J., Yoon, S. G. and Kim, S. I. Synthesis and characteristics of interpenetrating polymer network hydrogels composed of alginate and poly(diallydimethylammonium chloride). *J. Appl. Polym. Sci.* **91,** 3705–3709 (2004).

9. Haque, M. A., Kurokawa, T. and Gong, J. P. Super tough double network hydrogels and their application as biomaterials. *Polymer.* **53,** 1805–1822 (2012).

10. Peak, C. W., Wilker, J. J. and Schmidt, G. A review on tough and sticky hydrogels. *Colloid Polym. Sci.* **291,** 2031–2047 (2013).

11. Lyngaae-Jørgensen, J. and Utracki, L. A. Dual phase continuity in polymer blends. *Makromol. Chemie. Macromol. Symp.* **48–49,** 189–209 (1991).

12. Wang, J. J. and Liu, F. Enhanced adsorption of heavy metal ions onto simultaneous interpenetrating polymer network hydrogels synthesized by UV irradiation. *Polym. Bull.* **70,** 1415–1430 (2013).

13. Gong, J. P., Katsuyama, Y., Kurokawa, T. and Osada, Y. Double-network hydrogels with extremely high mechanical strength. *Adv. Mater.* **15,** 1155–1158 (2003).

14. Domingues, J., Bonelli, N., Giorgi, R., Frantini, E., Gorel, F., Baglioni, P. Innovative hydrogels based on semi-interpenetrating p(HEMA)/PVP networks for the cleaning of water-sensitive cultural heritage artifacts. *Langmuir* **29,** 2746–2755 (2013).

15. Dragan, E. S., Lazar, M. M., Dinu, M. V. and Doroftei, F. Macroporous composite IPN hydrogels based on poly(acrylamide) and chitosan with tuned swelling and sorption of cationic dyes. *Chem. Eng. J.* **204–205,** 198–209 (2012).

16. Yin, L., Fei, L., Tang, C. and Yin, C. Synthesis, characterization, mechanical properties and biocompatibility of interpenetrating polymer network–super- porous hydrogel containing sodium alginate. *Polym. Int.* **56,** 1563–1571 (2007).

17. Domingues, J., Bonelli, N., Giorgi, R. and Baglioni, P. Chemical semi-IPN hydrogels for the removal of adhesives from canvas paintings. *Appl. physics. A, Mater. Sci. andamp; Process.* **114,** 705–710 (2014).

18. Baglioni, P., Carretti, E. and Chelazzi, D. Nanomaterials in art conservation. *Nat Nano* **10,** 287–290 (2015).

19. Kopecek, J. Hydrogels: From soft contact lenses and implants to self-assembled nanomaterials. *J. Polym. Sci. Part A Polym. Chem.* **47,** 5929–5946 (2009).

20. Li, X., Cui, Y., Xiao, J. and Liao, L. Hydrogel–hydrogel composites: The interfacial structure and interaction between water and polymer chains. *J. Appl. Polym. Sci.* **108,** 3713–3719 (2008).

21. Ahmed, E. M. Hydrogel : Preparation , characterization , and applications : A review. *J. Adv. Res.* **6,** 105–121 (2015).

22. Kavanagh, G. M. and Ross-Murphy, S. B. Rheological characterisation of polymer gels. *Prog. Polym. Sci.* **23,** 533–562 (1998).

23. Alvarez-Lorenzo, C., Blanco-Fernandez, B., Puga, A. M. and Concheiro, A. Crosslinked ionic polysaccharides for stimuli-sensitive drug delivery. *Adv. Drug Deliv. Rev.* **65,** 1148–1171 (2013).

24. Deen, G. and Loh, X. Stimuli-Responsive Cationic Hydrogels in Drug Delivery Applications. *Gels* **4,** 13 (2018).

25. Ashley, G. W., Henise, J., Reid, R. and Santi, D. V. Hydrogel drug delivery system with predictable and tunable drug release and degradation rates. *Proc. Natl. Acad. Sci.* **110,** 2318–2323 (2013).

26. Omidian, H. and Park, K. Swelling agents and devices in oral drug delivery. *J. Drug Deliv. Sci. Technol.* **18,** 83–93 (2008).

27. Tokarev, I. and Minko, S. Stimuli-responsive porous hydrogels at interfaces for molecular filtration, separation, controlled release, and gating in capsules and membranes. *Adv. Mater.* **22,** 3446–3462 (2010).

28. Guo, S., Qiao, Y., Wang, W., He, H., Deng, L., Xing, J., Xu, J., Liang, X., Dong, A. Poly(ε-caprolactone)-graft-poly(2-(N, N-dimethylamino) ethyl methacrylate) nanoparticles: pH dependent thermo-sensitive multifunctional carriers for gene and drug delivery. *J. Mater. Chem.* **20,** 6935 (2010).

29. You, J., Almeda, D., Ye, G. J. and Auguste, D. T. Bioresponsive matrices in drug delivery. *J. Biol. Eng.* **4,** 15-27 (2010).

30. Kim, J., Lee, K., Hefferan, T., Currier, B., Yaszemski, M., Lu, L. Synthesis and Evaluation of Novel Biodegradable Hydrogels Based on Poly(ethylene glycol) and Sebacic Acid as Tissue Engineering Scaffolds. *Biomacromolecules* **9,** 149–157 (2008).

31. Dey, R. E., Wimpenny, I., Gough, J. E., Watts, D. C. and Budd, P. M. Poly(vinylphosphonic acid- co -acrylic acid) hydrogels: The effect of copolymer composition on osteoblast adhesion and proliferation. *J. Biomed. Mater. Res. Part A* **106,** 255–264 (2018).

32. Amini, A. A. and Nair, L. S. Injectable hydrogels for bone and cartilage repair. *Biomed. Mater.* **7,** 24105 (2012).

33. Jeon, Y. S., Lei, J. and Kim, J.-H. Dye adsorption characteristics of alginate/polyaspartate hydrogels. *J. Ind. Eng. Chem.* **14,** 726–731 (2008).

34. Mandal, B., Ray, S. K. and Bhattacharyya, R. Synthesis of full and semi Interpenetrating hydrogel from polyvinyl alcohol and poly (acrylic acid-co-hydroxyethylmethacrylate) copolymer: Study of swelling behavior, network

parameters, and dye uptake properties. *J. Appl. Polym. Sci.* **124,** 2250–2268 (2012).

35. Gonçalves, J., Santos, J., Rios, E., Crispim, M., Dotto, G., Pinto,L. Development of chitosan based hybrid hydrogels for dyes removal from aqueous binary system. *J. Mol. Liq.* **225,** 265–270 (2017).

36. Zhou, J., Hao, B., Wang, L., Ma, J. and Cheng, W. Preparation and characterization of nano-TiO2/chitosan/poly(N-isopropylacrylamide) composite hydrogel and its application for removal of ionic dyes. *Sep. Purif. Technol.* **176,** 193–199 (2017).

37. Ozay, O., Ekici, S., Baran, Y., Aktas, N. and Sahiner, N. Removal of toxic metal ions with magnetic hydrogels. *Water Res.* **43,** 4403–4411 (2009).

38. Chauhan, G. S., Chauhan, S., Sen, U. and Garg, D. Synthesis and characterization of acrylamide and 2-hydroxyethyl methacrylate hydrogels for use in metal ion uptake studies. *Desalination* **243,** 95–108 (2009).

39. Chauhan, G. S. and Mahajan, S. Use of novel hydrogels based on modified cellulosics and methacrylamide for separation of metal ions from water systems. *J. Appl. Polym. Sci.* **86,** 667–671 (2002).

40. Wang, W., Kang, Y. and Wang, A. One-step fabrication in aqueous solution of a granular alginate-based hydrogel for fast and efficient removal of heavy metal ions. *J. Polym. Res.* **20,** 101-112 (2013).

41. Tang, Q., Sun, X., Li, Q., Wu, J. and Lin, J. Synthesis of polyacrylate/polyethylene glycol interpenetrating network hydrogel and its sorption of heavy-metal ions. *Sci. Technol. Adv. Mater.* **10,** 15002 (2009).

42. Firlak, M., Çubuk, S., Yetimoğlu, E. K. and Kahraman, M. V. Recovery of Au(III) ions by Au(III)-imprinted hydrogel. *Chem. Pap.* **70,** 757–768 (2016).

43. Wang, J. and Liu, F. Enhanced and selective adsorption of heavy metal ions on ion-imprinted simultaneous interpenetrating network hydrogels. *Des. Monomers Polym.* **17,** 19–25 (2014).

44. Liu, Y., Cao, X., Hua, R., Wang, Y., Liu, Y., Pang, C., Wang, Y. Selective adsorption of uranyl ion on ion-imprinted chitosan/PVA cross-linked hydrogel. *Hydrometallurgy* **104,** 150–155 (2010).

45. Ulusoy, H. İ. and Şimşek, S. Removal of uranyl ions in aquatic mediums by using a new material: Gallocyanine grafted hydrogel. *J. Hazard. Mater.* **254–255,** 397–405

(2013).

46. Wang, J. J. and Liu, F. Thermoresponsive Ion-Imprinted Hydrogels with Interpenetrating Network Structure for Removal of Heavy Metal Ions. *Adv. Mater. Res.* **643,** 83–86 (2013).

47. Parra, R. R., Medina, V. F. and Conca, J. L. The use of fixatives for response to a radiation dispersal devise attack - a review of the current (2009) state-of-the-art. *J. Environ. Radioact.* **100,** 923–934 (2009).

48. Environmental Protection Agency, U. S. *Argonne National Laboratory Argonne SuperGel for Radiological Decontamination.* (2011). at <https://cfpub.epa.gov/si/si_public_record_report.cfm?address=nhsrc/anddirEntryId=236310>

49. Kohli, R. in *Developments in Surface Contamination and Cleaning* 177–224 (Elsevier, 2010).

50. Drake, J., James, R. R. and Demmer, R. Waste Management Symposia 2011. in *Side-by-Side Performance Comparison of Chemical-Based Decontamination Products for Dirty Bomb Cleanup* (2011).

51. Yang, H., Hong, S., Park, C., Lee, K., Choi, Y., Yu, J., Seo, B. Magnetic Adsorbents Embedded in Hydrogel Bead for Surface Decontamination. *J. Nanosci. Nanotechnol.* **16,** 8569–8574 (2016).

52. Yang, H., Hwang, K., Park, C., Lee, K. Polyvinyl alcohol-borate hydrogel containing Prussian blue for surface decontamination. *J. Radioanal. Nucl. Chem.* **109,** 1–8 (2018).

53. Yang, H. M., Park, C. W. and Lee, K. W. Polymeric coatings for surface decontamination and ecofriendly volume reduction of radioactive waste after use. *Prog. Nucl. Energy* **104,** 67–74 (2018).

54. Yang, H. M. Hwang, K., Park, C., Lee, K, Polyvinyl alcohol-borate hydrogel containing Prussian blue for surface decontamination. *J. Radioanal. Nucl. Chem.* 1**09,** 1–8 (2018).

55. Kim, Y. K., Kim, T., Kim, Y., Harbottle, D. and Lee, J. W. Highly effective Cs+removal by turbidity-free potassium copper hexacyanoferrate-immobilized magnetic hydrogels. *J. Hazard. Mater.* **340,** 130–139 (2017).

56.   Zhu, X. F., Yang, M., Zhang, H. X. and Nie, Y. J. The Synthesis and Feature Rearch on the Thermosensitive Hydrogels (NIPA-co-AAm). *Mater. Sci. Forum* **704–705,** 913–917 (2011).

57.   Zhuang, Y., Wang, G., Yang, H., Zhu, Z., Fu, J., Song, W., Zhao. Radiation polymerization and concentration separation of P(NIPA-co-AMPS) hydrogels. *Polym. Int.* **54,** 617–621 (2005).

58.   Danyuo, Y. Dozie-Nwachukwu, S., Obayemi, J., Ani, C., Odusanya, O., Oni, Y., Anuku, N., Malatesta, K., Soboyejo, W. Swelling of poly(N-isopropylacrylamide) P(NIPA)-based hydrogels with bacterial-synthesized prodigiosin for localized cancer drug delivery. *Mater. Sci. Eng. C* **59,** 19–29 (2016).

59.   Yamashita, K., Nishimura, T. and Nango, M. Preparation of IPN-type stimuli-Responsive heavy-Metal-Ion adsorbent gel. *Polym. Adv. Technol.* **14,** 189–194 (2003).

60.   Cuggino, J. C., Contreras, C. B., Jimenez-Kairuz, A., Maletto, B. A. and Alvarez Igarzabal, C. I. Novel Poly(NIPA- co -AAc) Functional Hydrogels with Potential Application in Drug Controlled Release. *Mol. Pharm.* **11,** 2239–2249 (2014).

61.   Chen, J. J., Jiang, L., Zhao, Y. P., Zhang, Q. S. and Chen, L. Chiral Recognizable Properties of Thermosensitive Poly(NIPA-*co*-NALPE) Hydrogels. *Adv. Mater. Res.* **160–162,** 13–18 (2010).

62.   Deli, D., Law, K., Liu, Z., Crouch, D., Livens, F, Yeates, S. Selective removal of ^{90}Sr and ^{60}Co from aqueous solution using N-aza-crown ether functional poly(NIPAM) hydrogels. *React. Funct. Polym.* **72,** 414–419 (2012).

63.   Tokuhiro, T., Akella, S. S., Carey, J. W. and Tokuhiro, A. T. Icone15-10163 Metal binding capability of functionalized thermo-sensitive polymer networks and application of hydrogels to low-level radioactive waste processing. *Proc. Int. Conf. Nucl. Eng.* **2007.** 150-163, (2007).

64.   Krezović, B. D., Dimitrijević, S. I., Filipović, J. M., Nikolić, R. R. and Tomić, S. L. Antimicrobial P(HEMA/IA)/PVP semi-interpenetrating network hydrogels. *Polym. Bull.* **70,** 809–819 (2013).

65.   Chappard, D., Montheard, J.-P. and Chatzopoulos, M. 2-Hydroxyethyl Methacrylate (HEMA): Chemical Properties and Applications in Biomedical 2-Hydroxyethyl Methacrylate (HEMA): Chemical Properties and Applications in B iomed i ca I

Fields. *J. Macromol. Sci. Part C Polym. Rev.* **32,** 1–34 (1992).

66.   Huang, Y. and Yang, J. *Novel Colloidal Forming of Ceramics*. (Springer Berlin Heidelberg, 2010).

67.   Abou El Fadl, F. I., Maziad, N. A., El-Hamouly, S. H. and Hassan, H. R. Synthesis and characterizations of various polyvinyl pyrrolidon/hydroxyl ethyl methacrylate nanocomposite hydrogels as drug delivery systems. *J. Macromol. Sci. Part A* **55,** 107–115 (2018).

Blank page

Chapter 3- Decontamination of Caesium and Strontium from stainless steel surfaces using hydrogels

J. J. Moore,[a] T. Raine,[a] A. Jenkins,[b] F. Livens,[c] K. Law,[c] K. Morris,[d] G. Law[c] and S. G. Yeates[a]

a. Organic Materials Innovation Centre, School of Chemistry, The University of Manchester, Oxford Road, Manchester, M13 9PL, United Kingdom.

b. Decontamination Centre of Expertise, Sellafield Ltd., Sellafield, Cumbria, CA20 1 PG, United Kingdom.

c. Centre for Radiochemistry Research, School of Chemistry, The University of Manchester, Oxford Road, Manchester, M13 9PL, United Kingdom.

d. School of Earth and Environmental Science, The University of Manchester, Oxford Road, Manchester, M13 9PL, United Kingdom

3.1 - Abstract

Current surface methods for the decontamination of radioactively contaminated material in nuclear facilities tend to rely on the use of liquid based agents to remove highly mobile radionuclides. However this results in the generation of large volumes of liquid waste which must then be processed. For the first time we report a polymer hydrogel based approach which gives a high decontamination factor for the removal of ^{137}Cs and ^{90}Sr on 304L grade stainless steel with minimal liquid waste and no lateral spread or increased penetration of radionuclides. Once dried these gels are able to retain the contaminants for treatment as solid waste resulting in a concentrated, less mobile waste form.

3.2 – Introduction

Nuclear power is a well-established method of energy generation in global use; offering significant benefits such as low carbon emissions and a higher energy density over plant lifetimes than conventional combustion-based or

renewable power sources[1]. However, the generation of significant volumes of radioactive waste material presents a unique challenge as fission products are frequently highly mobile, particularly in aqueous solutions. Of particular concern are the fission products ^{137}Cs and ^{90}Sr due to their decay largely by β-emission, half-lives of 30.2 and 28.8 years respectively[2], high solubility in salt form and likelihood of contaminating commonly used plant materials such as steels[3] (often penetrating below surface layers[4]) in storage ponds or waste streams. These factors result in an increased risk of exposure to local workers, an increased risk of environmental exposure and significant challenges in the decontamination and decommissioning of plant material.

Many previous gel based decontamination methods have focussed on either the removal of radioisotopes and other contaminants from aqueous solutions[5–8] or the application of spreadable gels,[9] many of which crosslink in situ and dry to form peelable coatings[10–13] such as the commercially available Decongel.[14] Despite their documented effectiveness (e.g. Yoon *et al* of up to 92% decontamination efficiency for the removal of ^{137}Cs from 304L grade stainless steel[15]) many of these techniques require multiple applications[9,10] and removal by methods such as vacuuming or brushing,[16,17] which increases the risk of mobile residues or particulates.

The use of hydrogels in radioisotope decontamination aims to address some of the issues commonly associated with chemical-based decontamination techniques: namely safe handling difficulties, increased radionuclide penetration, lateral spread of contamination and the generation of significant volumes of liquid waste requiring further treatment.[18] These gels also aim to reduce the requirement for repeat applications and prevent residue deposition on treated surfaces.

Hydrogels used and investigated herein are categorised as semi-interpenetrating networks (s-IPN) created by the physical entrainment on a molecular level of linear/branched polymer within a forming crosslinked network.[19] Whilst the possibility exists to separate this network[20] without the breaking of chemical bonds this is unlikely in practice due to the large degree of entanglement. 304L grade stainless steel was selected due to the widespread employment on the UK Sellafield nuclear reprocessing site in waste and reprocessing streams.[21]

3.3 – Experimental

3.3.1 – Materials

Polyvinylpyrrolidone (PVP, m. wt. 1300 kDa), N,N'-methylenebisacrylamide (MBAM), azobisisobutyronitrile (AIBN), dioctylsulphosuccinate and $^{88}Sr(NO_3)_2$ were purchased from Sigma Aldrich Ltd., U.K. and used as received.

Further surfactants were obtained from DuPont Ltd., U.K. and used as received.

2-Hydroxyethyl methacrylate (HEMA) was purchased from Sigma Aldrich Ltd., U.K. and filtered through basic Al_2O_3 before use.

$^{90}SrCl_2$ in and $^{137}CsCl$, both in 0.1 M HCl, were purchased from Areva Cerca LEA, France and used as received.

70 % nitric acid, hexane and toluene were purchased from Fischer Scientific Ltd., U.K. and used as received.

N-Isopropylacrylamide (NIPAM) was purchased from Flurorochem Ltd., U.K. and recrystalised from a 40:60 mixture of hexane:toluene before use.

3.3.2 - Synthesis of Hydrogels

Gel H06: PVP (49.8 g) was dissolved with deionised water (99.6 g) and to this was added HEMA (50.0 g, 0.384 mol), MBAM (0.4 g, 0.003 mol) and AIBN (0.2 g, 0.001 mol). The mixture was stirred until homogenous before centrifugation at 2,000 rpm to remove any bubbles present. This method was employed for successive gels.

The highly viscous solution was then transferred to well plates (5.2 mL volume) and placed into an oven at 60 °C for 4 hours.

Once cured the gels were removed from the well plates and washed in deionised water for 7 days to remove any unreacted starting materials or unbound polymer. Where hydrogels were loaded with decontamination agents soaking was carried out

in aqueous solutions of these reagents. EDTA, dioctylsulphosuccinate, Synperonic NP-30, Capstone FS-50 and FS-51 were used at concentrations of 0.5 mg mL^{-1}.

3.3.3 - Rheological characterisation

Gels of reduced volume (2 mL) were prepared using the above method.

Rheological characterisation was carried out using an Ares LN2 rheometer (TA Instruments, Hertfordshire, U.K.) with parallel-plate geometry of 25 mm diameter. Measurements were carried out at a constant temperature of 20 °C. Strain sweep tests were performed at a frequency of 1.0 Hz with an increasing strain level from 1 to 100%. Changes in the storage modulus (G') and storage and loss modulus (G") were recorded. From this data a value within the linear viscoelastic region (LVE) was selected and frequency tests carried out central to this region, typically 50%. The oscillatory frequency was then increased from 0.1 to 5.0 Hz whilst recording the G' and G" data as a function of frequency.

3.3.4 - Steel sample contamination

304(L) stainless steel coupons with a cold-rolled 2B finish (40 mm x 40 mm x 0.5 mm, RS components, UK) were contaminated with a known volume of a 400 Bq/mL sln of $^{137}CsCl_2$ or $^{90}SrCl_2$ in deionised water and allowed to dry.

3.3.5 - Decontamination experiments using Autoradiography

Autoradiography was carried out on contaminated coupons using a BAS-IP super resolution storage phosphor screen at a distance of 2 mm from the sample and exposure time of 18 hours.

Autoradiography plates were developed using a Typhoon 9410 molecular imager (GE Amersham, Buckinghamshire, U.K.).

Hydrogel samples were placed on the contaminated coupons for a controlled time before removal, allowing the coupon to dry and repetition of autoradiography analysis.

The standard measure of decontamination used for evaluation is the decontamination factor (DF) defined as:

$$DF = \frac{\text{Initial contamination level}}{\text{Contamination level after decontaminating process}}$$

Equation 7 - Calculation of the decontamination factor[22]

3.3.6 - Decontamination experiments using GD-OES

Samples of 304(L) stainless steel were polished to a 1 μm finish before contamination by exposure to 3M HNO_3 containing 500 ppm $Sr(NO_3)_2$ at 60 °C for 30 days in an analogue of PUREX waste streams.[4,22]

A GD-Profiler 2 (Horiba Jobin Yvon) was used to perform elemental depth analysis using a glow discharge area of 4 mm, applied power of 35 W and Ar gas pressure of 635 Pa.

The elemental emission lines used for analysis were (nm) Fe I 371.999, Cr I 425.439, Ni I 341.482, O II 130.223, Sr II 460.739 and Al I 396.157. Calibration was carried out using an Al sheet (depth 1mm) with polychromator focal length of 500 mm and 30 optical windows.

Hydrogel samples were applied to the surface for a controlled time before a repeat GD-OES analysis.

3.3.7 - SEM of hydrogels

Secondary electron scanning electron microscopy (SE-SEM) was carried out on Au/Pd coated cryogenically fractured hydrogel samples. Samples were either freeze dried or dried at ambient temperature prior to examination. All samples were

examined in high vacuum mode with 5 kV accelerating voltage on a FEI Quanta 250 FEG SEM. Image analysis was carried out using BoneJ.[23]

3.3.8 - Electron microprobe analysis

Measurements were run on a JEOL JXA-8530F FEG-EPMA equipped with four wavelength dispersive spectrometers. Elements were analysed at 15 kV 165 nA, focused beam, under the following conditions:

Element, emission line (order)	Diffracting crystal	Standard used	Counting time (on peak/ off peak)
Sr La (1)	TAP	SrCO3	30s/15s
Si Ka (1)	TAP	Si	20s/10s
Mn Ka (1)	LIFL	Mn	25s/10s
Ni Ka (1)	LIFL	Ni	10s/10s
Cr Ka (2)	PETL	Cr	20s/15s
Mo La (1)	PETL	Mo	20s/15s
Fe (balance)	unmeasured	-	-

Table 2 - Electron microprobe analysis parameters

3.4 - Results and discussion

3.4.1 - Synthesis of Hydrogels

The hydrogel synthesis is based upon the work of Baglioni *et al* [19,24–26] in the restoration of fine art. Modifications have been made to the composition of the gels ranging from ratio modifications to reagent replacement. Removal of large air bubbles from the gels was necessary in order to synthesise a more structurally sound gel free of large voids; centrifugation being chosen as a method more suitable for the

high molecular weight of the polymers used in the precursor solution due to the well-known damaging effects of ultrasound upon such polymers.[27,28] The use of well plates as moulds ensures consistency of volume and size in an easy to manipulate gel "puck". Gels can be formed into any reasonable shape using a suitable mould.

The HM01 and H06 hydrogels were produced *via* a crosslinking free radical polymerisation of HEMA/MBAM in the presence of high molecular weight hydrophilic PVP to produce a semi-interpenetrating polymer network.[29] The presence of HEMA allows the gels to expand and contract reversibly in the presence of water; the OH group extending outwards and methyl retracting inwards (see figure 14). This effect is reversed as the gel is dehydrated and hydrogen bonding between OH groups within the gel structure becomes more favourable.[30]
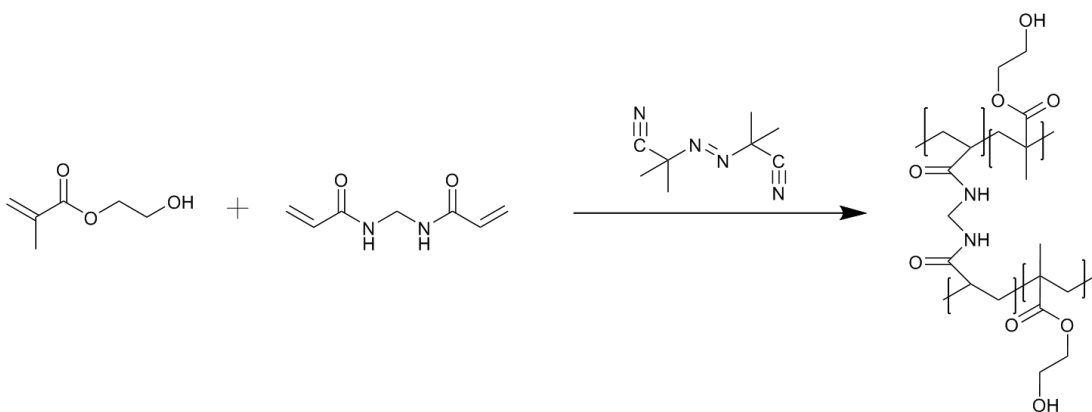
Figure 14 - Formation of radical initiated crosslinked pHEMA hydrogels

Additionally, NIPAM based gels were also investigated building upon prior art[31] with modifications to the incorporated polymer and combinations of a HEMA/PVP/NIPAM "hybrid" gel, HHN06 (and HHN04) to investigate the potential for the incorporation of the thermoresponsive properties of polyNIPAM with a more rheologically favourable gel structure.

% wt.	HEMA	NIPAM	MBAM	AIBN	PVP	Water
HM01	24.94	0	0.20	0.25	24.84	49.77
H06	25.00	0	0.20	0.10	24.90	49.80
HHN06	24.83	2.76	0.22	0.28	16.56	55.35

Table 3 - Abridged table of formulations, PVP molecular weight 1300 kDa

3.4.2 - Rheological characterisation

Rheological characterisation was used as a screening tool to assess the suitability of the gels for use under application conditions. Gels were eliminated at this stage where stress was measured to be below 4000 Pa at 50% strain or complex viscosity indicated that yield stress was reached over the frequency range examined. Several gels were further eliminated during use where application to surfaces led to rupture. Figure 15 shows the crossover point between the storage (G') and loss (G") modulus where viscous fluid behaviour exceeds elastic properties[32] at a strain rate of 25% as well as the yield stress of gel H06 in the same region. When compared with other gel formulations, it can be noted that this crossover point (G_c) shows the most significant increase upon major reduction of the HEMA monomer concentration; although these gels were discounted on the basis of handling and structural integrity deficiency.
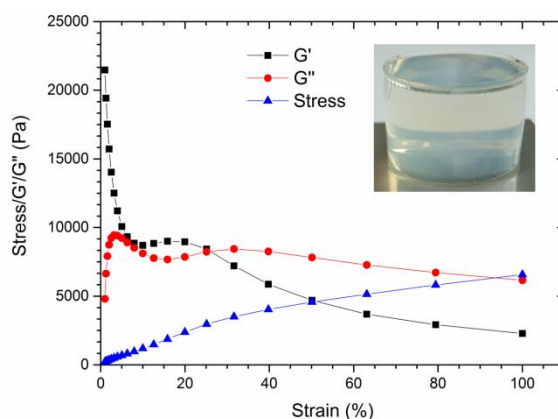
Figure 15 - Gel H06 stress-strain and G' G" plots. Inset: H06 hydrogel "puck" on steel containing 2% (0.5 M) HNO₃.

3.4.3 - SEM of swollen hydrogel

The examination of a freeze-dried sample of gel H06 enabled the visualisation of the open pore structure of the hydrated gel which posessed a mass equilibrium water content (EWC) of 73%.[19]
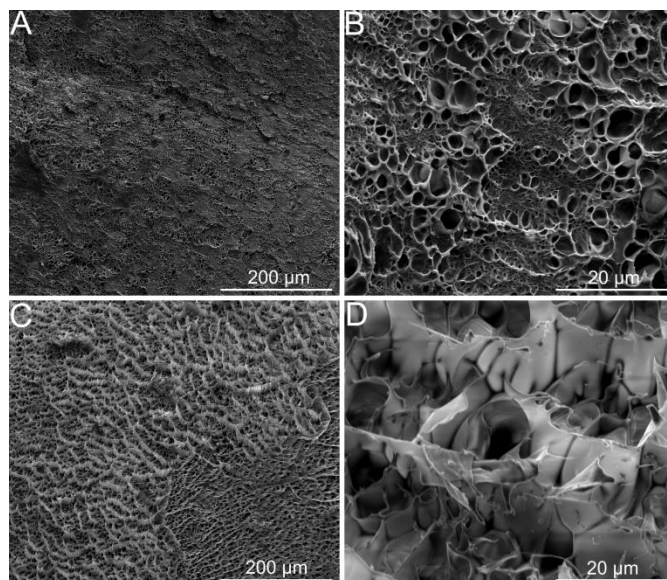
Figure 16 - SEM images of freeze dried H06 gel interior 500 X (A), 5000 X (B), exterior 500 X (C) and 5000 X (D).

The interior of the gel features pores ranging from 5.65 μm to 0.06 μm with an average pore size of 0.70 μm and solid volume fraction of 38% in a continuous network; allowing efficient water uptake with a significant surface area. Since this internal surface area is composed of functional groups containing significant electron donor properties it is therefore expected to have a strong affinity for the retention of metal ions present in solution.[8] When examining the pore structure of the gel exterior a membranous protrusion can be seen across the majority of the gel surface. This is believed to result from the final stages of polymerisation process as the supply of monomer becomes limited.

3.4.4 - Surface decontamination of stainless steel

The application of gels to a 200 Bq contaminated smooth stainless steel coupon and subsequent analysis by autoradiography (a technique whereby a storage phosphor $BaFCl \cdot Eu^{2+}$ screen is used to visualise and quantify the distribution of radioisotopes via exposure and absorption followed by laser induced development) demonstrated up to an 81% reduction in measured ^{137}Cs activity, DF of 5.1, using gels loaded with water alone and rapid removal from the steel surface. This can be attributed to the high solubility of Cs in salt form[33] and retention capability of the hydrogels; a desorption treatment is typically required to remove encapsulated metal ions.[8]

Upon application of the same gel formulation to ^{90}Sr contaminated steel samples the effectiveness of the gels reached 87%, DF of 7.5, despite exhibiting a reduced initial rate of decontamination. Since both ^{137}Cs and ^{90}Sr are initially present in each sample at a level of 200 Bq the increased intensity of exposure present in ^{90}Sr contaminated samples is attributed to the β decay of this isotope to a second radioactive product, ^{90}Y (t½ 64 hours) , which further β decays to the stable isotope ^{90}Zr.[2] The residual ^{90}Sr after application was confined to within the circumference of the initially contaminated area, demonstrating no lateral spread of radionuclides.

	Blank	3	15	45	60	90	120	180
T								
DF	-	3.1	4.6	4.8	5.6	6.5	6.7	7.5
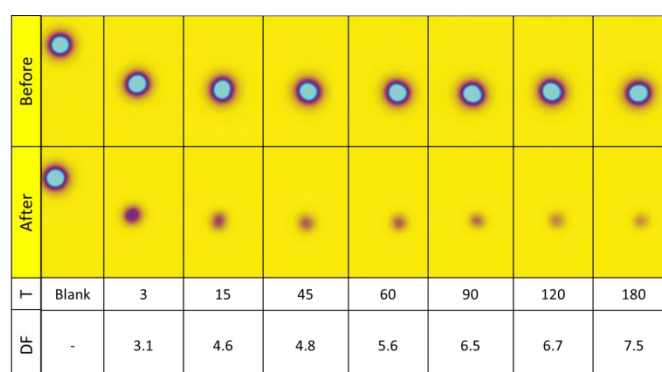
Figure 17 - Autoradiography images of 200 Bq ^{90}Sr before (above) and after (below) H06 with water application over time intervals 3 minutes to 3 hours.

Further development of the H06 hydrogel centred on the raising of the decontamination effectiveness beyond that of the water loaded gels alone. To this end multiple gels and decontamination agents were screened for their ability to

enhance the uptake of Cs and Sr from steel surfaces. Comparisons between ^{137}Cs and ^{90}Sr contamination removal returned DFs of 13.2 and 3.9 respectively with 1 hour contact of gel H06 loaded with water. This increased decontamination of ^{137}Cs over ^{90}Sr was again observed when various surfactants and EDTA solutions were loaded into gels.

Owing to the well documented use of nitric acid to decontaminate steels and dissolve radionuclides in plant processes,[22] various concentrations of nitric acid were examined. Average DFs of 15.9 and 20.0 were obtained with 35% (7.9 M) nitric acid in gel H06 on ^{137}Cs and ^{90}Sr respectively. Yang *et al* report a similar hydrogel method using Prussian blue as the active component with a DF of 18.1 on stainless steel. The evaluation by this group of the commercially available Decongel 1101 under identical conditions yielded a lower DF of 7.7.[12]

In order to investigate potential degradation of the gel structure H06 was exposed to differing concentrations of nitric acid. Figure 18 suggests up to 10% (2.3 M) nitric acid induces minimal material degradation whilst at or above 35% (7.9 M) the OH functionality peak present at 3300 cm^{-1} is significantly broadened, with diminishing of the ester peak at 1750 cm^{-1} and amide peak at 1650 cm^{-1} suggesting destruction by hydrolysis of the ester and amide groups in the peptide bond[34] of the crosslinker. The ester would be expected to be more susceptible than the amide to acid hydrolysis with the formation of carboxylic acid and exhibition of significant hydrogen bonding. This would be consistent with the observed increase in the swollen volume of gels exceeding 35% HNO$_3$.
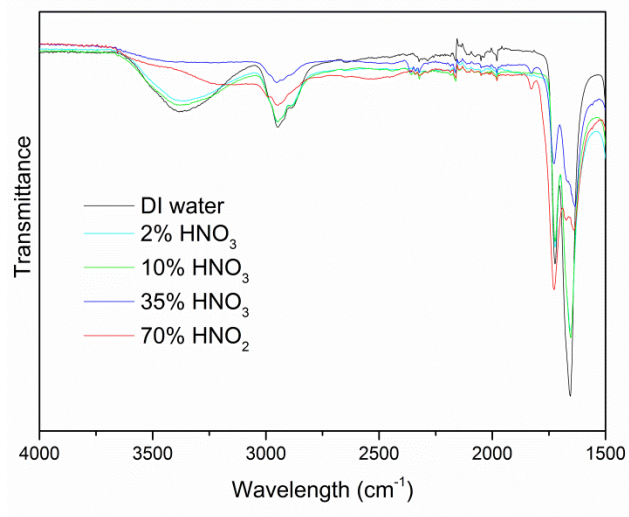
Figure 18 - FT-IR spectra of gel H06 after immersion in various HNO$_3$ concentrations for 7 days and subsequent desiccation.

2% (0.5 M) HNO$_3$ was considered as suitable for gel loading due to the limited degradation effects observed upon sufficient exposure to reach absorption equilibrium. Upon 1 hour contact application to ^{137}Cs and ^{90}Sr contaminated steel the observed activity levels were reduced to between 6% and 1% of initial levels, equating to an estimation of between 2-12 Bq of activity (see figure 19).

Sample	Cs blank	Cs 1 hour	Cs 1 hour	Cs 1 hour	Sr blank	Sr 1 hour	Sr 1 hour	Sr 1 hour
DF	-	17.1	17.1	95.1	-	19.2	23.0	24.3
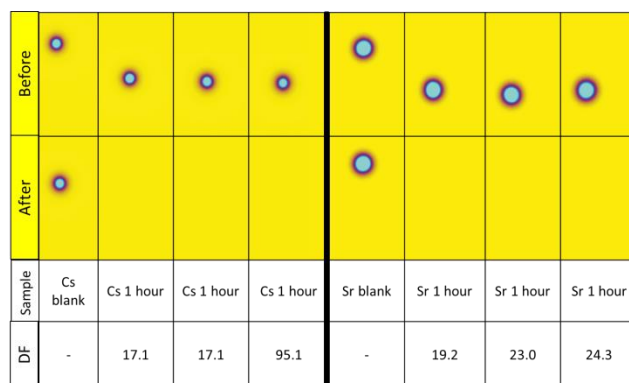
Figure 19 - Autoradiography images of 200 Bq ^{137}Cs (left) and ^{90}Sr (right) before and after H06 with 2% HNO$_3$ application for 1 hour.

Following on from this level of effectiveness the contamination levels of ^{90}Sr were increased in order to examine the scalability of these gels. Upon doubling the activity to 400 Bq a similar level of effectiveness by percentage removal was observed, with estimated activity levels of 12-16 Bq recorded and DFs of up to 30.9.

SEM imaging of desiccated H06 gel showed significant structural differences, both interior and exterior, when compared with freeze-dried hydrated gels. The absence of pores or voids would strongly suggest that the gels are, once dried, able to encapsulate the radionuclides removed from the steel surfaces and retain them for ease of removal, transport and eventual disposal. This can be attributed to the collapse of the pore structure upon the removal of the large liquid volume fraction of the hydrated gel's composition.
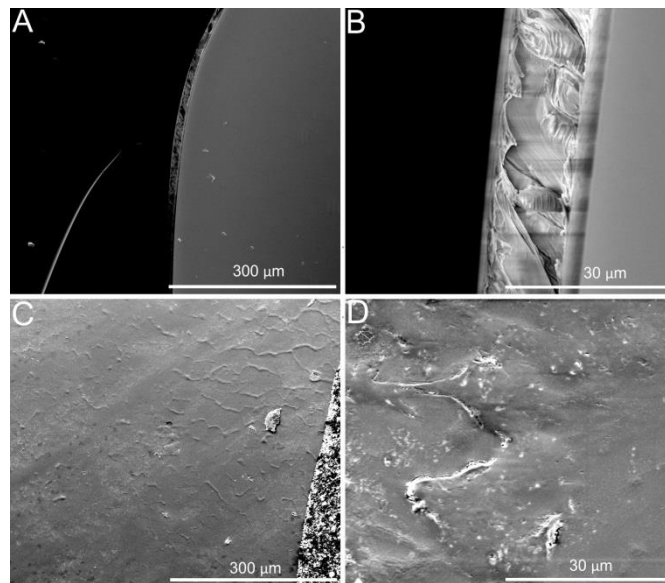
Figure 20- SEM images of desiccated H06 gel interior 500 X (A), 5000 X (B), exterior 500 X (C) and 5000 X (D).

3.4.5 - Sub-surface decontamination of stainless steels

Further investigations centred upon the penetration of radioisotopes to greater depths of stainless steel structure, as is commonly observed in reactor and plant waste streams during both standard operating and decommissioning activities. Samples of 304L stainless steel contaminated with stable [88]Sr under acidic conditions mirroring those typical of plant conditions (prepared in a method pioneered by Lang *et al*[4]) showed strontium to be concentrated within the passive Cr_2O_3 layer (see figure 21) by comparison of the Cr and O abundance peaks, indicative of the inhibiting properties this layer exerts upon the penetration process.[4] Cs was not investigated using the GD-OES method as it could not be reliably measured under any of the examined parameters and has previously proven evasive.[4]
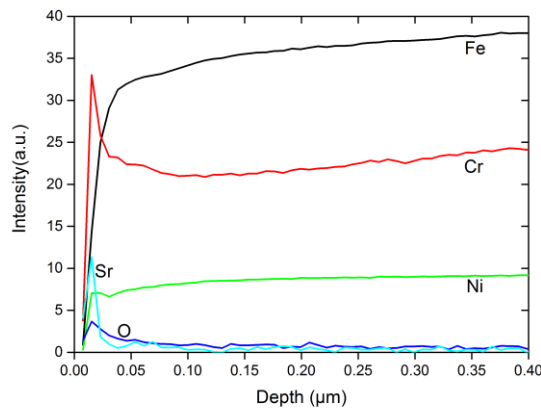
Figure 21 - Sr contaminated steel GD-OES profile (Note: O peaks are scaled by a factor of 10 and Sr by a factor of 100 for clarity).

Despite the qualitative nature of GD-OES analysis, upon gel application for 1 hour the measured Sr peaks were seen to diminish across the selection of samples examined (further details in section 4.6) with no evidence of increased Sr penetration beyond the Cr_2O_3 layer depth of 0.013-0.015 μm. This would suggest a reduced level of Sr when coupled with autoradiography data. The application of gel H06 containing 35% HNO_3 to 304L stainless steel also showed no sign of increased Sr penetration beyond the Cr_2O_3 layer. Observed instead was the absence of a Cr peak around 0.013-0.015 μm depth (see figure 22); suggesting corrosive attack of this layer by the high concentration of HNO_3 used.
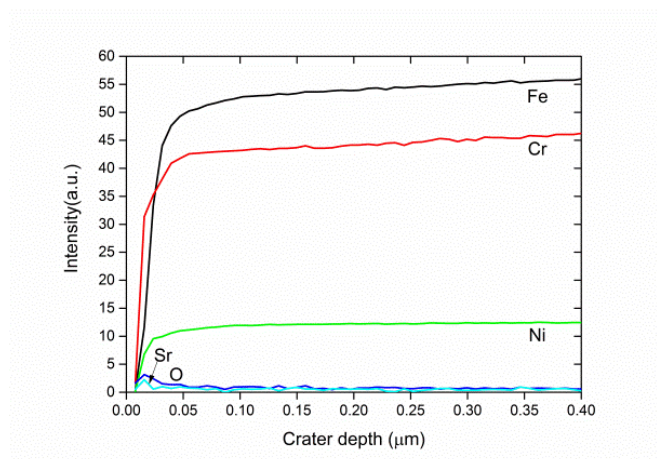
Figure 22 - Sr contaminated steel GD-OES profile after 35% HNO_3 gel application (Note: O peaks are scaled by a factor of 10 and Sr by a factor of 100 for clarity).

Further investigation into levels of Sr in the surface layers was carried out using electron microprobe analysis. 100 measurements at a spacing of 20 μm returned an average strontium % wt. composition of 1.44% ±0.01% prior to gel application and 1.26% ±0.01% after the application of gel H06 containing 2% HNO$_3$ with 1 hour contact time. The reduction in effectiveness (DF 1.1) can be attributed to the increased difficulty in the removal of Sr embedded within the oxide layer compared to the simplicity of surface decontamination. This would suggest that subsurface contamination would require multiple applications to achieve a satisfactory DF.

3.5 – Conclusions

In this study a new hydrogel-based chemical decontamination procedure appropriate for use on steel surfaces has been developed through gel rheological screening selection and an autoradiography investigation for effectiveness in the removal of ^{137}Cs and ^{90}Sr. Decontamination factors of up to 95 on surface contamination have been observed upon loading gels with 2% (0.5 M) nitric acid without inducing further radionuclide penetration into the steel surfaces or lateral spread of radionuclides. Partial subsurface decontamination has been demonstrated and SEM studies have confirmed pore structure collapse leading to contaminant encapsulation.

The results of this study have produced a reagent loadable, non-degrading hydrogel treatment which minimises liquid waste and provides a more localised decontamination technique to reduce the mobility and volume of radioisotope waste whilst achieving a high DF.

3.6 - Conflicts of interest

There are no conflicts to declare.

3.7 – Acknowledgements

3.8- References

1.   Cheng, V. K. M. and Hammond, G. P. Life-cycle energy densities and land-take requirements of various power generators: A UK perspective. *J. Energy Inst.* **90,** 201–213 (2017).

2.   Shultis, J., Faw, Richard E, and McGregor, D. S. *Fundamentals of Nuclear Science and Engineering.* (CRC Press., 2016).

3.   Agency, I. A. E. Management of Spent Fuel from Nuclear Power Reactors. *Manag. Spent Nucl. Fuel from Nucl. Power React.* 506 (2006).

4.   Lang, A., Engelberg, D., Smith, N., Trivedi, D., Horsfall, O., Banford, A., Martin, P., Coffey, P., Bower, W., Walther, C., Weiß, M., Bosco, H., Jenkins, A., Law, G. Analysis of contaminated nuclear plant steel by laser-induced breakdown spectroscopy. *J. Hazard. Mater.* **345,** 114–122 (2018).

5.   Deli, D., Law, K., Liu, Z., Crouch, D., Livens, F, Yeates, S.. Selective removal of ^{90}Sr and ^{60}Co from aqueous solution using N-aza-crown ether functional poly(NIPAM) hydrogels. *React. Funct. Polym.* **72,** 414–419 (2012).

6.   Wang, J. J. and Liu, F. Enhanced adsorption of heavy metal ions onto simultaneous interpenetrating polymer network hydrogels synthesized by UV irradiation. *Polym. Bull.* **70,** 1415–1430 (2013).

7.   Bhattacharyya, R. and Ray, S. K. Enhanced adsorption of synthetic dyes from aqueous solution by a semi-interpenetrating network hydrogel based on starch. *J. Ind. Eng. Chem.* **20,** 3714–3725 (2014).

8.   Dragan, E. S. Design and applications of interpenetrating polymer network hydrogels. A review. *Chem. Eng. J.* **243,** 572–590 (2014).

9.   Nunez, L. and Kaminski, M. D. Foam and gel methods for the

decontamination of metallic surfaces. US 2006/0217584 A1 (2007).

10. Gurau, D. and Deju, R. The use of chemical gel for decontamination during decommissioning of nuclear facilities. *Radiat. Phys. Chem.* **106,** 371–375 (2015).

11. Castellani, R., Poulesquen, A., Goettmann, F., Marchal, P. and Choplin, L. Efficiency enhancement of decontamination gels by a superabsorbent polymer. *Colloids Surfaces A Physicochem. Eng. Asp.* **454,** 89–95 (2014).

12. Yang, H. M. Hwang, K., Park, C., Lee, K. Polyvinyl alcohol-borate hydrogel containing Prussian blue for surface decontamination. *J. Radioanal. Nucl. Chem.* **109,** 1–8 (2018).

13. Yang, H. M., Park, C. W. and Lee, K. W. Polymeric coatings for surface decontamination and ecofriendly volume reduction of radioactive waste after use. *Prog. Nucl. Energy* **104,** 67–74 (2018).

14. Gurau, D. and Deju, R. Radioactive decontamination technique used in decommissioning of nuclear facilities. *Rom. J. Phys.* **59,** 912–919 (2014).

15. Yoon, S., Kim, C., Jung, C., Choi, B., Choi, W., Lww, K., Moon, J. Effect of alkyl alcohol on viscosity of silica-based chemical gels for decontamination of radioactive contaminations. *Asian J. Chem.* **25,** 7023–7027 (2013).

16. Faure, S., Fuentes, P. and Lallot, Y. Vacuumable gel for decontaminating surfaces and use thereof. US 8636848 B2 (2014).

17. Castellani, R., Poulesquen, A., Goettmann, F., Marchal, P. and Choplin, L. A topping gel for the treatment of nuclear contaminated small items. *Nucl. Eng. Des.* **278,** 481–490 (2014).

18. NEA Task Group on Decontamination. *Decontamination Techniques Used in Decommissioning Activities.pdf. Decontamination Techniques Used in*

Decommissioning Activities (1998).

19.   Domingues, J., Bonelli, N., Giorgi, R., Fratini, E., Gorel, F., Baglioni, P. Innovative hydrogels based on semi-interpenetrating p(HEMA)/PVP networks for the cleaning of water-sensitive cultural heritage artifacts. *Langmuir* **29,** 2746–2755 (2013).

20.   Alemán, J. V. Chadwick, A., He, J., Hess, M., Horie, K., Jones, R., Kratochvil, P., Meisel, I., Mita, I., Moad, G., Penczek, S., Stepto, R. Definitions of terms relating to the structure and processing of sols, gels, networks, and inorganic-organic hybrid materials (IUPAC Recommendations 2007). *Pure Appl. Chem.* **79,** 1801–1829 (2007).

21.   Shaw, R. D. Corrosion prevention and control at Sellafield nuclear fuel reprocessing plant. *Br. Corros. J.* **25,** 97–107 (1990).

22.   Choppin, G. and Choppin author, G. R. *Radiochemistry and nuclear chemistry*. (Amsterdam [Netherlands] : Elsevier, 2013).

23.   Doube, M., Klosowski, M., Arganda-Carreras, I., Cordelieres, F., Dougherty, R., Jackson, J., Schmid, B., Hutchinson, J. BoneJ: Free and extensible bone image analysis in ImageJ. *Bone* **47,** 1076–1079 (2010).

24.   Baglioni, P., Bonelli, N., Chelazzi, D., Chavalier, A., Dei, L., Domingues, J., Fratini, E., Giorgi, R., Martin, M. Organogel formulations for the cleaning of easel paintings. *Appl. Phys. A Mater. Sci. Process.* **121,** 857–868 (2015).

25.   Domingues, J., Bonelli, N., Giorgi, R. and Baglioni, P. Chemical semi-IPN hydrogels for the removal of adhesives from canvas paintings. *Appl. physics. A, Mater. Sci. andamp; Process.* **114,** 705–710 (2014).

26.   Baglioni, P., Carretti, E. and Chelazzi, D. Nanomaterials in art conservation. *Nat Nano* **10,** 287–290 (2015).

27.   Suslick, K. S. and Price, G. J. Applications of ultrasound to materials chemistry. *Annu. Rev. Mater. Sci.* **29,** 295–326 (1999).

28.   Wheeler, J. S. R., Reynolds, S. W., Lancaster, S., Sanchez, V. and Yeates, S. G. Polymer degradation during continuous ink-jet printing. *Polym. Degrad. Stab.* **105,** 116–121 (2014).

29.   Sperling, L. H. Interpenetrating Polymer Networks: An Overview. *Interpenetr. Polym. Networks* **239,** 3–38 (1994).

30.   Chappard, D., Montheard, J.-P. and Chatzopoulos, M. 2-Hydroxyethyl Methacrylate (HEMA): Chemical Properties and Applications in Biomedical 2-Hydroxyethyl Methacrylate (HEMA): Chemical Properties and Applications in B iomed i ca I Fields. *J. Macromol. Sci. Part C Polym. Rev.* **32,** 1–34 (1992).

31.   Zhang, J., Cheng, S.-X. and Zhuo, R.-X. Poly (vinyl alcohol)/ poly (N-isopropyl- acrylamide) semi-interpenetrating polymer network hydrogels with rapid response to temperature changes. *Colloid Polym Sci* **281,** 580–583 (2003).

32.   Dey, R. E., Wimpenny, I., Gough, J. E., Watts, D. C. and Budd, P. M. Poly(vinylphosphonic acid- co -acrylic acid) hydrogels: The effect of copolymer composition on osteoblast adhesion and proliferation. *J. Biomed. Mater. Res. Part A* **106,** 255–264 (2018).

33.   Ashraf, M. A., Akib, S., Maah, M. J., Yusoff, I. and Balkhair, K. S. Cesium-137: Radio-Chemistry, Fate, and Transport , Remediation , and Future Concerns. *Crit. Rev. Environ. Sci. Technol.* **44,** 1740–1793 (2014).

34.   Singh, B. R. in *ACS Symposium Series* (ed. Singh, B. R.) **750**, 2–37 (1999).

Blank page

Chapter 4 - Supporting Information: Decontamination of Caesium and Strontium from stainless steel surfaces using hydrogels

J. J. Moore,[a] T. Raine,[a] A. Jenkins,[b] F. Livens,[c] K. Law,[c] K. Morris,[d] G. Law[c] and S. G. Yeates[a]

a. Organic Materials Innovation Centre, School of Chemistry, The University of Manchester, Oxford Road, Manchester, M13 9PL, United Kingdom.

b. Decontamination Centre of Expertise, Sellafield Ltd., Sellafield, Cumbria, CA20 1 PG, United Kingdom.

c. Centre for Radiochemistry Research, School of Chemistry, The University of Manchester, Oxford Road, Manchester, M13 9PL, United Kingdom.

d. School of Earth and Environmental Science, The University of Manchester, Oxford Road, Manchester, M13 9PL, United Kingdom

4.1 - Hydrogel formulations

Many formulations were conceived, synthesised and analysed in an effort to develop a gel with superior hydrophilic properties, structural rigidity, ease of handling and lack of excessive bubbles. Gels with formulation numbers not detailed here were either formulated but not synthesised, used in early small scale development experiments or were slightly reformulated to a more refined gel formulation which is included below. Gels featuring the prefix "HM" or "H" were based upon literature precedent.[1] EWC was not recorded in earlier gels examining degassing effects and bubble formation.

% wt.	Formulation	HEMA	MBAM	AIBN	PVP	PVP mol. Wt.(kDa)	Water	Vazo 67	EWC
	HM01	24.94	0.20	0.25	24.84	1,300	49.78		74
	HM02	25.01	0.20		24.76	1,300	49.78	0.25	-
	H06	25.00	0.20	0.10	24.90	1,300	49.80		73
	H10	24.73	0.20	0.99	24.63	1,300	49.46		-
	H11	25.02	0.20	0.25	24.78	1,300	49.75		-
	H12	25.02	0.20	0.25	24.78	1,300	49.75		-
	H13	17.65	0.21	0.18	26.37	1,300	55.58		-
	H14	16.81	0.20	0.17	25.04	1,300	57.77		-
	H15	10.49	0.20	0.10	24.37	1,300	64.83		-
	H16	10.49	0.20	0.10	24.37	1,300	64.83		-
	H17	24.98	0.20	0.25	24.83	360	49.75		-
	H18	10.47	0.20	0.25	24.34	360	64.74		84
	H19	24.91	0.20	0.25	24.81	40	49.83		58
	H20	10.49	0.20	0.10	24.37	40	64.83		-
	H21	27.01	0.19	0.24	24.15	10	48.40		53
	H29	25.00	0.20	0.50	24.90	1,300	49.41		75
	H30	25.00	0.20	0.05	24.90	1,300	49.85		74
	H31	15.15	0.20	0.10	24.90	1,300	59.65		83
	H32	10.00	0.20	0.10	24.90	1,300	64.81		87
	H33	20.00	0.20	0.10	24.90	1,300	54.81		79
	H34	20.00	0.16	0.10	24.90	1,300	54.84		75
	H35	15.00	0.12	0.10	24.90	1,300	59.89		84
	H36	10.00	0.08	0.10	24.90	1,300	64.91		89
	H37	25.00	0.20	0.32	24.90	1,300	49.59		74
	H41	25.00	0.50	0.10	24.90	1,300	49.50		70
	H42	25.00	1.00	0.10	24.90	1,300	49.00		67
	H43	25.00	0.30	0.10	24.90	1,300	49.70		72
	H44	25.00	0.10	0.10	24.90	1,300	49.90		74
	H45	25.00	0.20	0.10	30.00	1,300	44.70		76
	H46	25.00	0.20	0.10	21.00	1,300	53.70		70
	H47	25.00	0.20	0.10	15.00	1,300	59.70		67

Table 4- PVP/PHEMA hydrogel formulations

Formulation HM01 was devised as a basic method development gel for use with initial scaling, moulding, uptake and decontamination measurements whilst screening of further gel formulations was ongoing. This allowed a greater throughput with regards to method development, baseline comparison data and gel loading investigations as experiments could be carried out concurrently.

Formulations H11-H16 were compared to investigate the effects of AIBN:HEMA upon the bubble formation within the polymerising gels and simultaneously to

investigate various means of degassing the highly viscous gel solution. Through these formulation experiments a lower AIBN concentration was noted as being essential to limit bubble formation (the decomposition of AIBN to form radicals releases N_2 gas) and no degassing or various methods of degassing via sonication were discounted due to polymer decay[2] or inadequate degassing.

H17-H21 were used to investigate the effects of PVP molecular weight ranging between 10, 40 and 360 kDa PVP.

Formulations HM01, H06, H10, H29 and H30 were compared to investigate the effect of AIBN concentrations, with the highest concentration of 0.99% AIBN being immediately discounted due to the large number of bubbles produced resulting in buoyancy in water and reduction in structural integrity. AIBN levels at or below 0.1% showed no visible bubbles within the gel structure and thus this level was maintained through successive formulations.

Formulations H06, H31, H32 and H33 were compared to investigate the effects of HEMA concentration variation with a constant MBAM proportion. Whilst H31 and H32 both possess the highest EWCs of this series they were found to be more fragile during handling, application and removal than higher HEMA formulations. In order to determine whether this was due to the increasing crosslink density caused by the constant MBAM proportion gels H34, H35 and H36 were synthesised with a constant MBAM;HEMA ratio consistent with the ratio of gel H06. An increase in crosslinker proportion was observed to result in a decreased EWC, most likely due to a decrease in pore size.[3] Gel H36 exhibited the least disintegration during handling.

H37 was a repeat of a literature formulation[1] with a fixed 1:0.01 HEMA:AIBN ratio. H06 was very similar to this gel but with a reduced quantity of AIBN than the literature precedent[1] in order to reduce the excessive formation of bubbles.

H41-H44 were used to investigate the effects of varying MBAM crosslinker concentrations (and therefore crosslink density in the synthesised gels) relative to H06.

H45, H46 and H47 were used to investigate the effects of PVP concentration relative to H06. Since PVP is the hydrophilic component of these gels a predictable trend of

reduced PVP concentration resulted in reducing EWCs of 76, 70 and 67% corresponding to PVP reductions of 30, 21 and 15%.

% wt.	Formulation	HEMA	MBAM	AIBN	PVP	PVP mol. Wt. (kDa)	Water	NIPAM
	HHN04	13.88	0.22	0.28	16.66	1,300	55.08	13.88
	HHN06	24.83	0.22	0.28	16.56	1,300	55.35	2.76

Table 5 - PHEMA/PNIPAM "hybrid" hydrogels

HHN04 and HHN06 were successful attempts to form a HEMA/NIPAM hybrid gel using the existing PHEMA gels as a base formulation. HHN04 formed an opaque, white, brittle gel whilst HHN06 formed a pearlescent, more rubber like gel.

When heated in water to 40 °C no significant size decrease was observed.

% wt.	Formulation	NIPAM	MBAM	Ammonium persulphate	TEMED	PVP	PVA	Polymer mol. Wt. (kDa)	Water
	HNP01	5.97	0.09	0.15	1.39				92.40
	HNP02	4.18	0.09	0.15	1.39	1.79		1,300	92.40
	HNP03	4.18	0.09	0.15	1.39		1.79	124-186	92.40

Table 6 - PNIPAM hydrogels

The "HNP" series of gels was an investigation into the suitability of literature precedent[4] PNIPAM hydrogels either alone (HNP01) or with the hydrophilic polymers PVA and PVP. These gels were more transparent and faster to form than PHEMA based gels but were significantly less user friendly with regards to handling and extremely hard to effectively remove from surfaces once applied (further discussion in rheology SI section).

When heated in water to 40 °C these gels were all found to decrease in size with limited decreases in HNP01 and HNP02 and an extremely large size reduction in HNP03.

4.2 - Equilibrium water content (EWC) calculation

EWCs were calculated gravimetrically using the following method:

$$EWC = \left(\frac{M_h - M_d}{M_h}\right) \times 100$$

Equation 8- Equilibrium water content

Where M_h is the mass of the hydrated hydrogel at equilibrium and M_d the mass of the desiccated hydrogel.[1,3,5,6] This a quantifying guide to the hydrogel's hydrophilicity.

4.3 - Rheological screening

Formulations were profiled using the rheometer. Several gels could not be examined on the rheometer due to the large number of bubbles present resulting in structural voids within the gel.

The figures 23-29 (A) below detail stress-strain curves for gel series examined. The extent of the curves with no abrupt decline indicates that the rupture point has not yet been reached over the course of the range investigated and from the curvature of each plot plastic deformation can be observed.[7] It is also noteworthy that H06 was generally a stronger gel than the others examined (exceptions H41 and H43 which both have increased crosslinker compositions of 0.5 and 0.3% respectively) but is generally less flexible than many of the other gels. In practice those gels which were more flexible often presented handling difficulties wheras H06 proved flexible enough to apply to and remove from a surface without deforming to fracture.

Comparing the "HNP" series found a significantly lower strength of gels which discounted them from further use. Within the "HHN" gels HHN06 was found to be stronger, the addition of NIPAM to this existing base formulation yielding negative strength returns.

Figures 23-29 (B) show the change in complex viscosity (η^*) across a frequency range of 0.1 to 4.5 Hz for multiple formulation variants, over which increase in range the complex viscosity decreases. The decrease in complex viscosity is indicative of structural deformation of the hydrogel network under conditions of high frequency shear strain, these gels can all be described as shear thinning and pseudoplastic[8] as the complex viscosity decreases after yield stress is reached. Gels HM01, H31, 34, 41, 43, 44, 46, HNP01 and HHN06 show a yield stress (viscosity maximum) within the measurable region, prior to this point the material is viscoelastic and is expected to return to this state at rest.

Examining the complex viscosity plots of figures 23-27 would suggest that gel H06 exhibits a reduced deformation due to frequency increases and that, therefore, this formulation is comparatively resistant to structural deformation with minimal shear thinning. Whilst figure 24 (B) would suggest the superior structural properties of gel H31 in resistance to structural deformation it was found in practice to suffer under relatively low compressive force due to manual surface application. It must also be considered, due to the solely parallel nature of the oscillations during rheology measurements, that rheology studies may not fully evaluate the suitability of gels in this application and should be considered guiding but not authoritative measures of structural suitability; particularly since gels are not expected to encounter such oscillatory forces during decontamination procedures.

The complex viscosity of figure 28 ("HNP" series of gels) reports complex viscosities of two orders of magnitude lower than observed in the series of "H" gels, indeed these gels are much more fragile and gelatinous, whilst still exhibiting shear thinning pseudoplastic behaviour and appearing to flow upon the application of stress as has been observed in previous samples. HNP01 is the only one of this series of gels to exhibit a visible yield stress within the measured range.

The HEMA/NIPAM hybrid gels ("HHN" series) detailed in figure 29 also exhibit the pseudoplastic, shear thinning behaviour previously discussed with an initially higher complex viscosity than gel H06; suggesting a greater magnitude of shear thinning effect.

Figure 23 - A- AIBN variance hydrogel stress-strain curves B- Complex viscosity C-G' (open markers) and G'' (filled markers) plots.
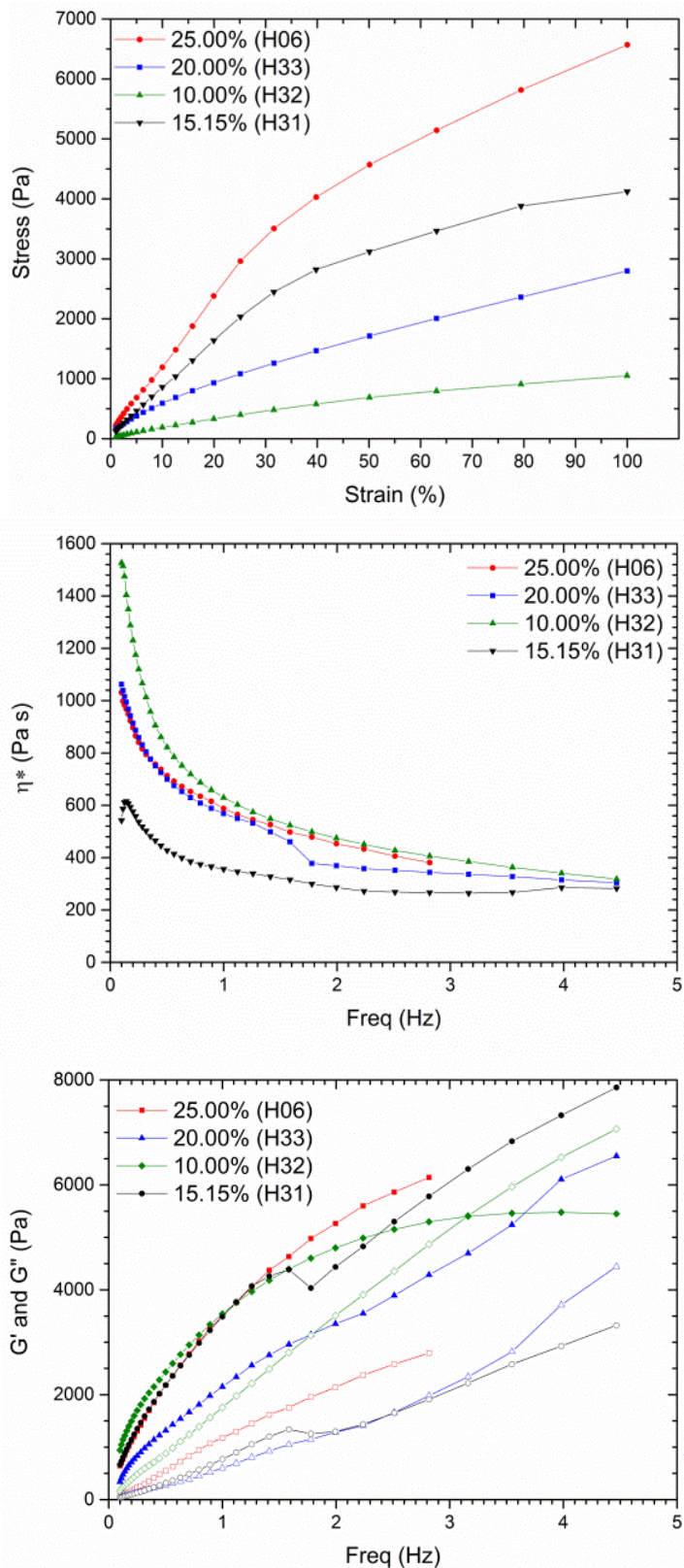
Figure 24 - A- HEMA variance (fixed MBAM) hydrogel stress-strain curves curves
B- Complex viscosity C- G' (open markers) and G'' (filled markers) plots.
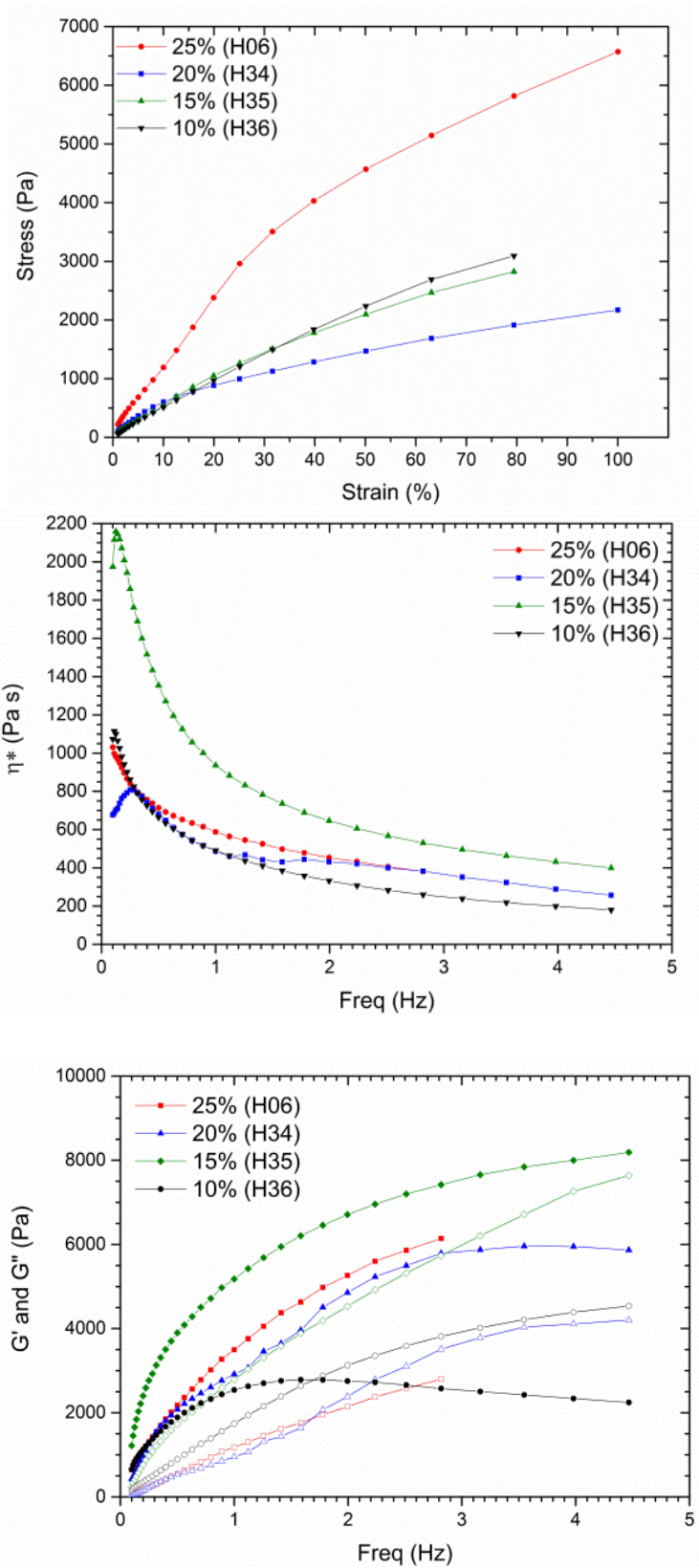
Figure 25 - A- HEMA variance (constant MBAM:HEMA ratio) hydrogel stress-strain curves B- Complex viscosity C- G' (open markers) and G'' (filled markers) plots.

Figure 26 - A- MBAM variance hydrogel stress-strain curves B- Complex viscosity C- G' (open markers) and G'' (filled markers) plots.

Figure 27 - A- PVP proportion variance hydrogel stress-strain curves B- Complex viscosity C- G' (open markers) and G'' (filled markers) plots.
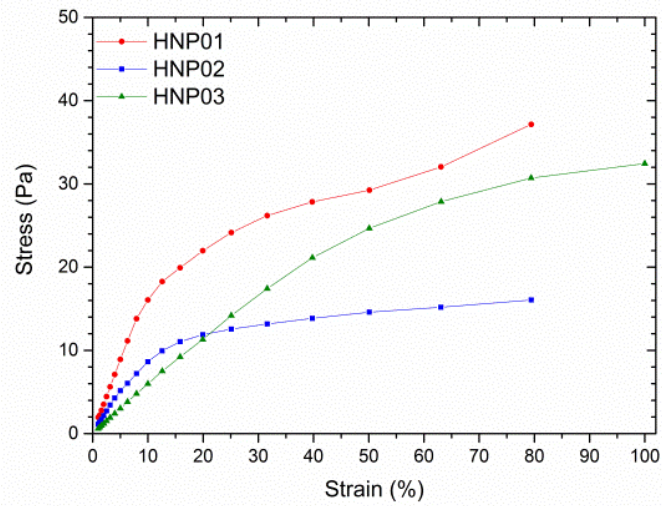
Figure 28 - A- HNP formulations hydrogel stress-strain curves B- Complex viscosity C- G' (open markers) and G'' (filled markers) plots.
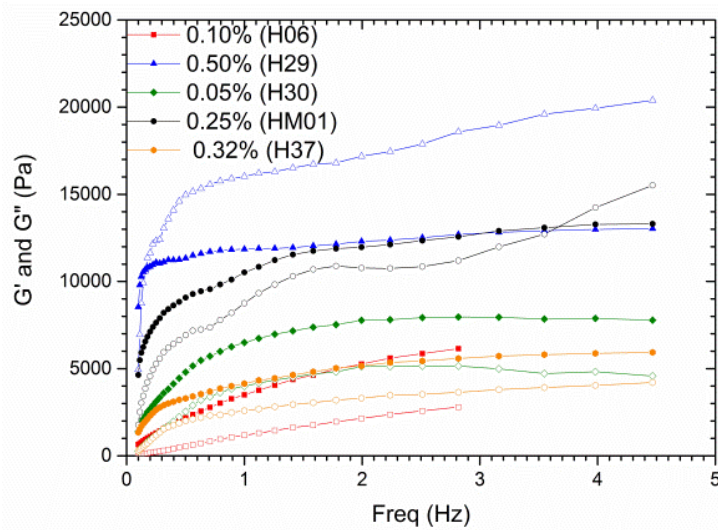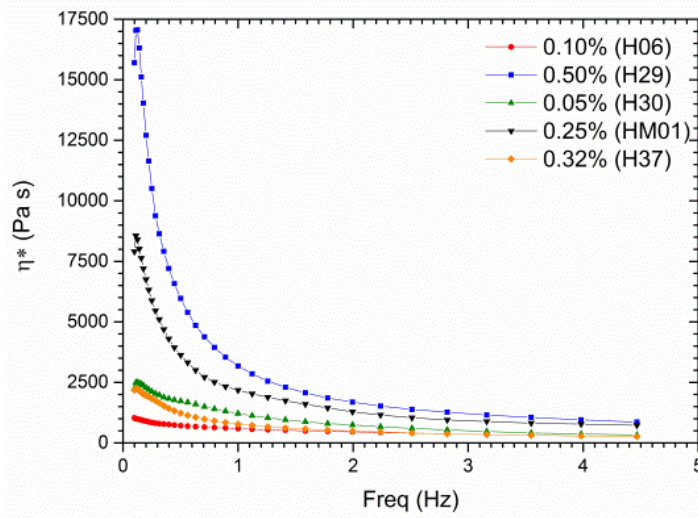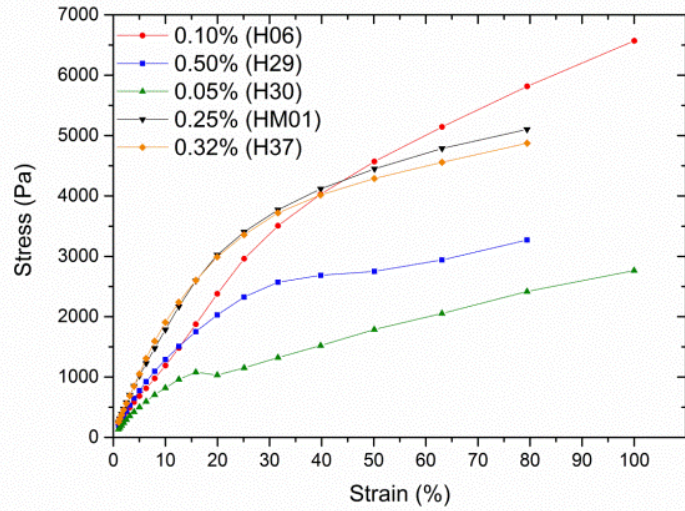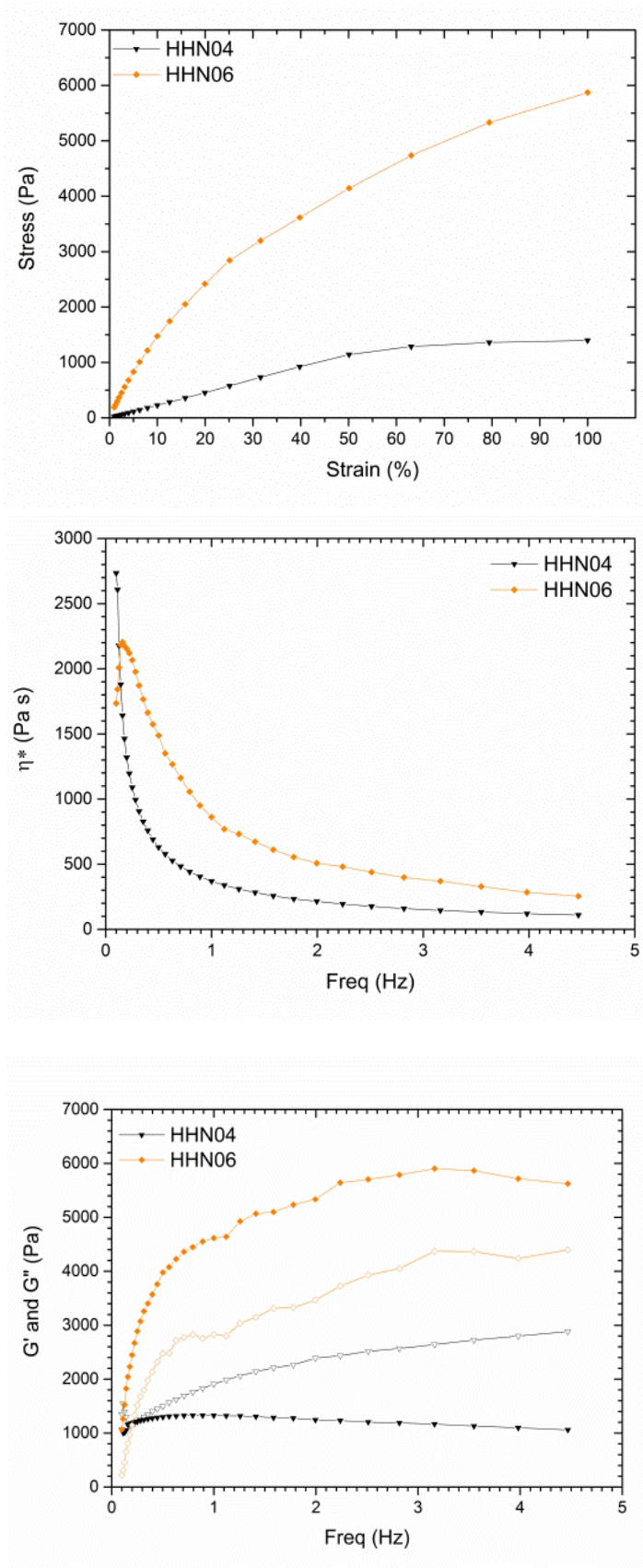
Figure 29 - A- HHN formulations hydrogel stress-strain curves B- Complex viscosity C- G' (open markers) and G'' (filled markers) plots.
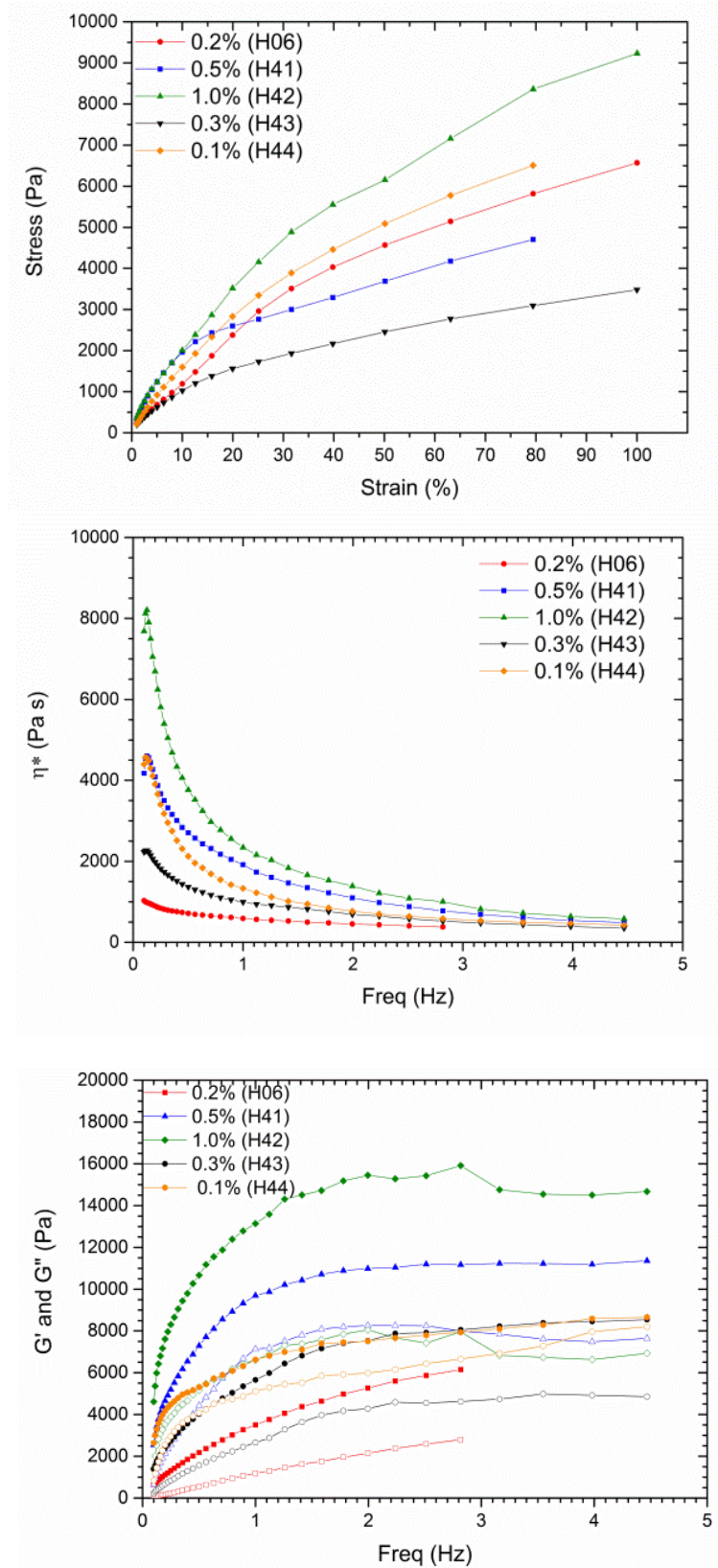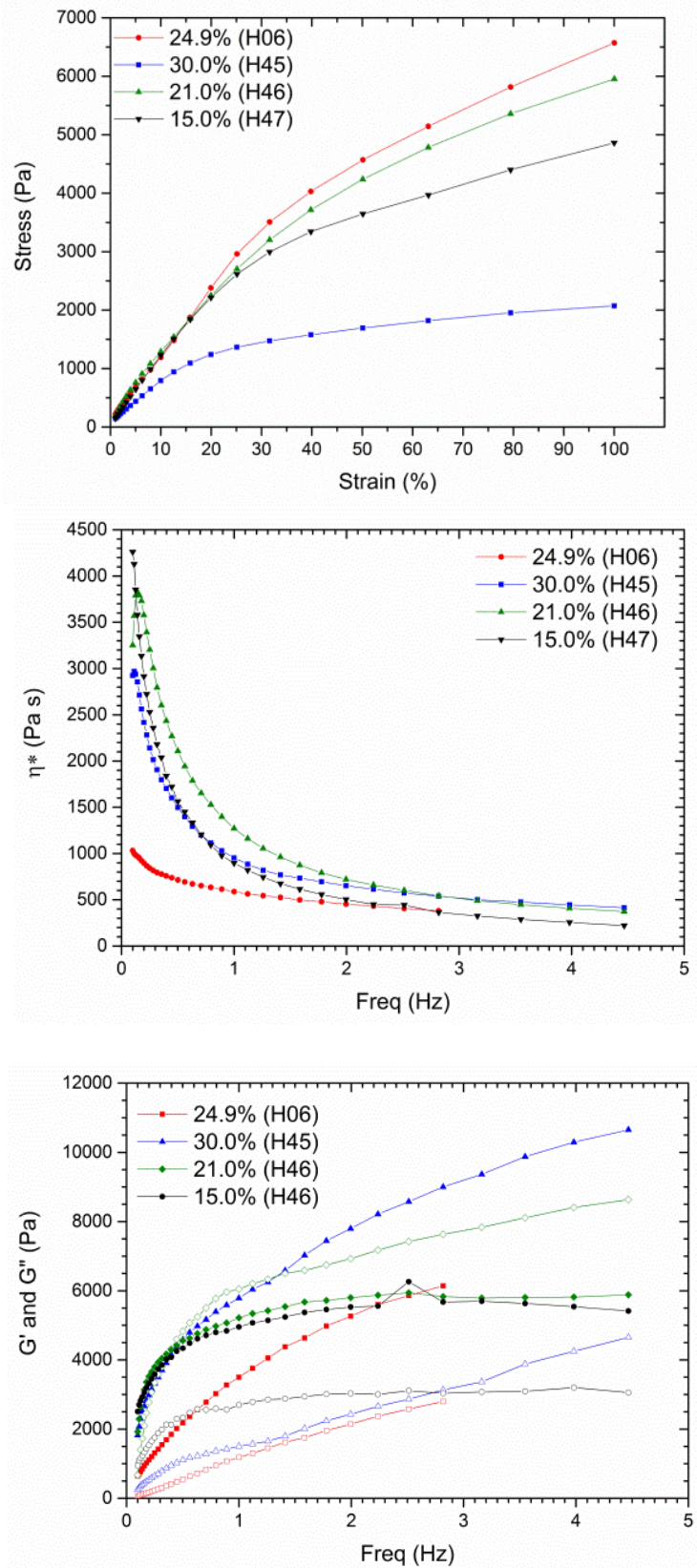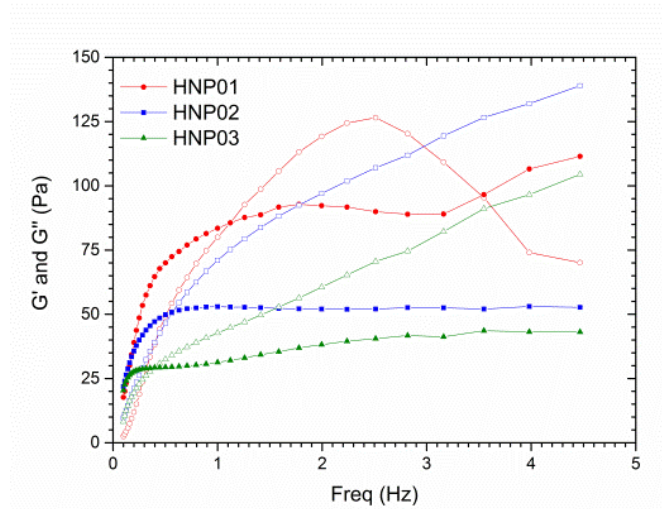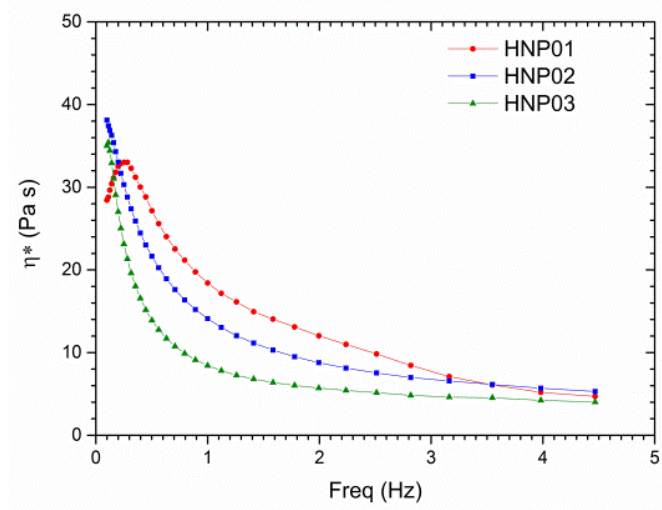
Figures 23-29 (C) show the storage (G') and storage and loss (G") moduli of gels with G' represented as open markers and G" as filled markers.[9] The position of G' relative to G" for each gel describes the characteristic properties of each gel; where G' is greater behaviour is more solid-like and where G" is greater behaviour is more akin to a fluid.[7]

When examining figures 23-27 G" for each gel can be noted as greater than G' which would categorise gels as possessing viscous fluid behaviour. The notable exceptions to this are gels H29 and H46. Gel 29, however contains a significant number of bubbles which result in voids in the structure which can cause errors during rheology measurements.

Figures 28 and 29 show G' increasing beyond G" during the frequency sweep; suggesting that at high strain frequency these highly aqueous and fragile gels take on a more solid like characteristic.

4.4 - Autoradiography screening

Formulation HM01 was used in initial experiments to determine blank loading (water only) effectiveness over time and the effects of loading the gels during the equilibrium soaking phase with various decontamination agents; ranging from surfactants to the EDTA ligand and nitric acid due to literature and industrial precedent.[10–13] Strontium was selected for the majority of further screening experiments to streamline the process, with the reincorporation of caesium in later stages of screening.

The data collected would suggest that the loading of gels with the surfactant Synperonic NP-30 or the hexadentate ligand EDTA has no significant effect upon either the decontamination rate or total removal level of strontium. The gels showed an unexpected disparity between effectiveness on strontium or caesium between the very similar formulations HM01 and H06. The minor formulation variances between these gels would suggest that this variance is, despite repeats, due to experimental or instrumental error. The standard error for this technique of decontamination analysis has been calculated as 4%.

The contact times examined show the majority of gels reach a pseudo-plateau level of effectiveness within 15 minutes, with nitric acid gel exhibiting a longer initial latency period. In all cases the pseudo-plateau level is reached within 40 minutes with smaller increases in effectiveness observed beyond this point and, in certain cases, gels exhibiting moderate adhesive properties to the surface upon drying. It was therefore decided to fix further experimental contact times to 1 hour to ensure a consistent level of decontamination and prevent adhesion of the gel to the surface.
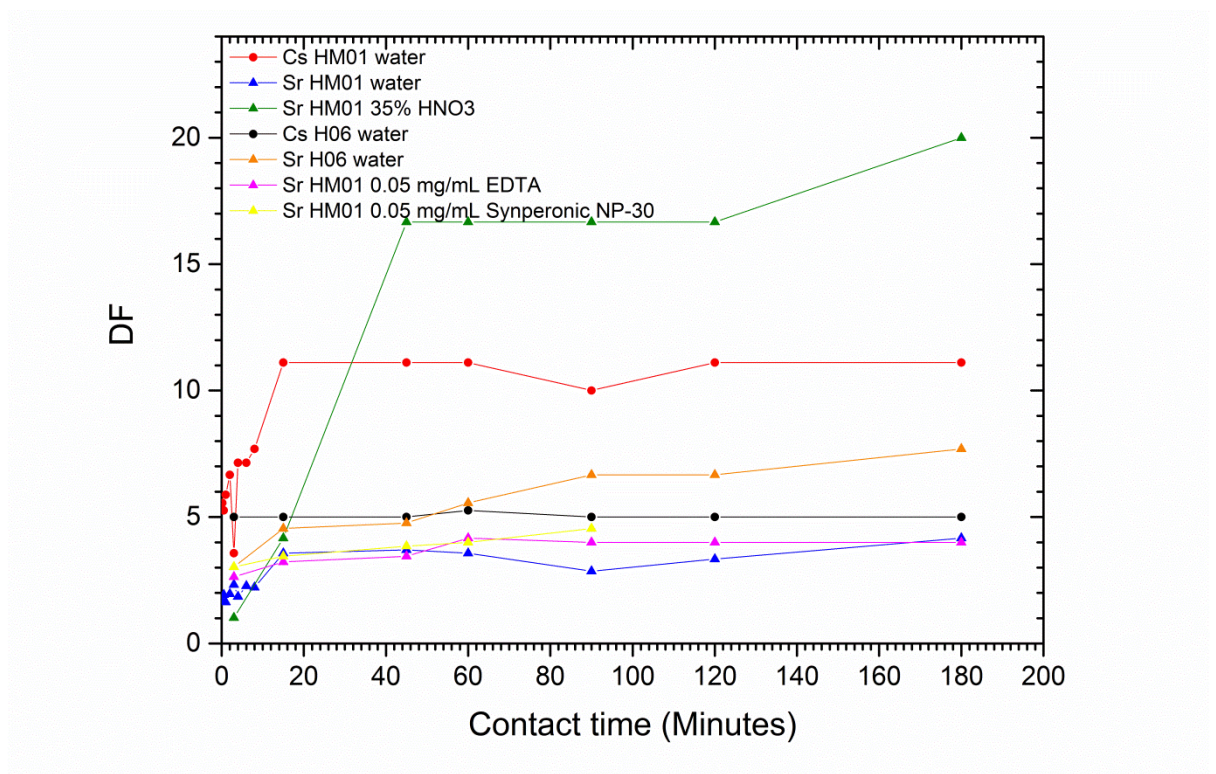
Figure 30 - Decontamination effectiveness of blank and loaded gels as a function of contact time
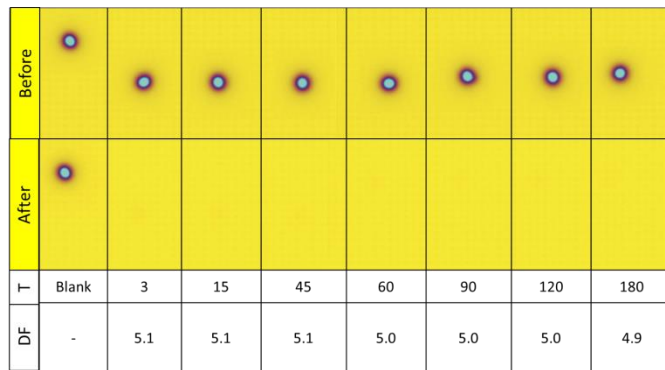
Figure 31 - Autoradiography images of 200 Bq ^{137}Cs before (above) and after (below) H06 with water application over time intervals 3 minutes to 3 hours.

Further experiments were carried out with 1 hour contact time on ^{90}Sr contaminated steels. EDTA and the surfactants Capstone FS-50, FS-51, Synperonic NP-30 and dioctylsulphosuccinate were loaded into gels from an aqueous solution of concentration 0.05 mg mL^{-1} during the 7 day gel equilibration period.
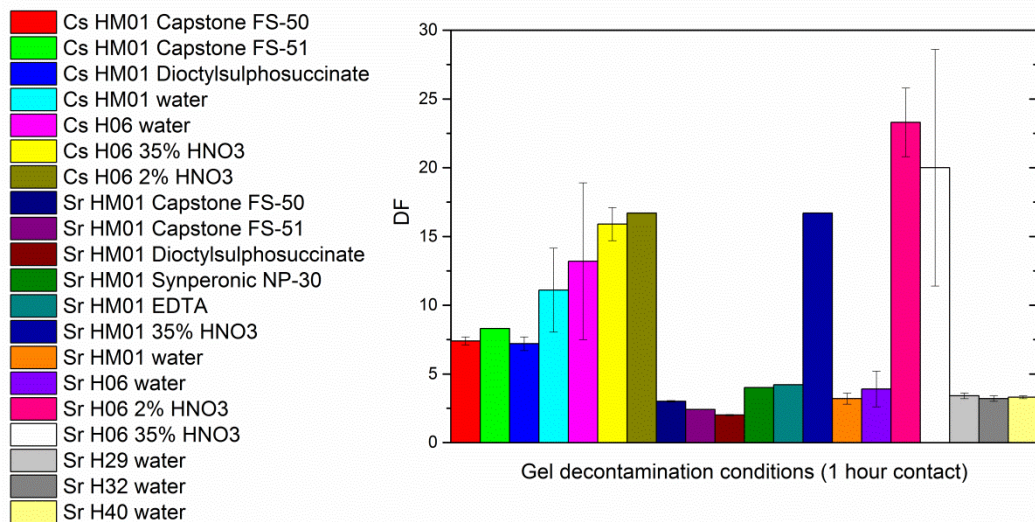
Figure 32 - Decontamination effectiveness of differently loaded gels at 1 hour contact time.

The 1 hour contact data suggests the decontamination of ^{137}Cs on 304L stainless steel with these gels to be more effective than ^{90}Sr. Further screening investigations were therefore focused more heavily on ^{90}Sr due to the increased challenge in the

decontamination of this isotope. In certain cases error bars are unavailable due to lack of DF variation in repeats or, in the case of Cs H06 2% HNO$_3$, unrealistic distortion of the error bars caused by the nature of the top heavy fraction during the calculation of the DF.

Examining the effectiveness of these gels it can be observed that the surfactant loading is ineffective in ^{137}Cs and ^{90}Sr removal and may in fact retard the uptake of gels containing only water, possibly due to the presence of dissolved solids in the water preventing dissolution or prevention of interaction with the gel surface by these additives.

The negligible differences in DFs achieved between H29, H32 and H40 on 200 Bq ^{90}Sr demonstrate that variations in the water content of each gel do not cause significant variations in decontamination effectiveness; with EWCs of 75, 87 and 64% respectively.

The major increases in DF come as a result of the use of HNO$_3$ of concentrations 35% (7.9 M) and 2% (0.5 M). 70% (15.8 M) HNO$_3$ was investigated but discounted after the 7 day equilibration period as the gels began to excessively swell to extreme fragility, hypothesised to be due to destruction of the crosslinking peptide bond by the concentrated acid. Attempts to load the gels with aqueous NaOH solutions resulted in brittle, opaque gels with little to no liquid uptake and were thus discounted.
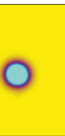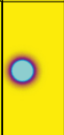
Sample	Blank	Sr 1 hour	Sr 1 hour	Sr 1 hour
DF	-	24.0	26.9	30.9

Figure 33 - Autoradiography images of 400 Bq ^{90}Sr before (above) and after (below) H06 with 2% HNO$_3$ application for 1 hour.

4.5 - HNO$_3$ IR of H06

Gels were immersed in HNO$_3$ of differing concentrations beyond the standard 7 day equilibration in order to investigate the potential for short term storage, potentially resulting in a shelf life allowing transport of a gel based "decontamination package".
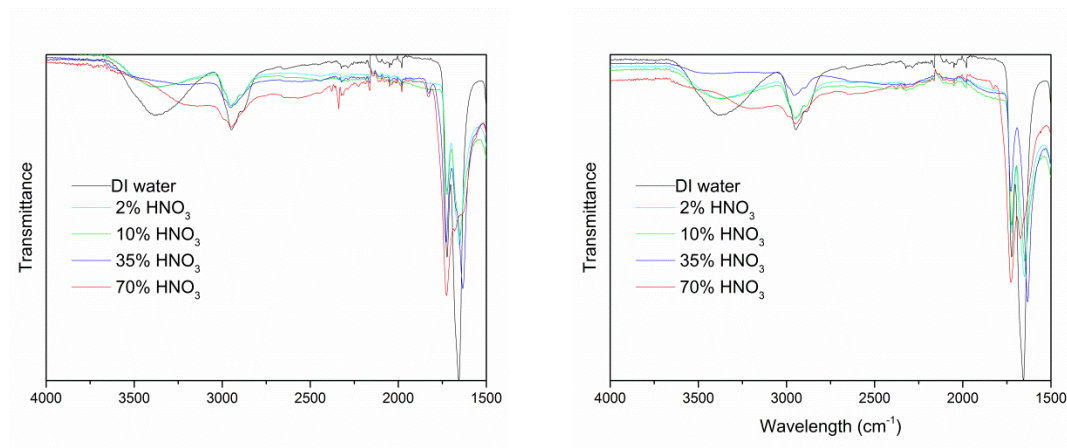
Figure 34 - FT-IR spectra of gel H06 after immersion in various HNO$_3$ concentrations for 14 (L) and 21 (R) days and subsequent desiccation

Results suggest that storage beyond the 7 day equilibration period leads to increased hydrolysis of the ester functionality present at 1750 cm^{-1} and a reduced amine peak around 1650 cm^{-1} corresponding to the peptide bond[14] and suggesting damage to the crosslinking units of the gels. The broadening of the OH group around 3300 cm^{-1} suggests the formation of carboxylic acid leading to increased hydrogen bonding.

4.6 - GD-OES profiling

GD-OES profiling of steel samples was used to analyse at which position within the steel samples the ^{88}Sr contamination was present. In all of the following graphs the values for O have been scaled by a factor of 10 and values for Sr scaled by a factor of 100 for clarity.
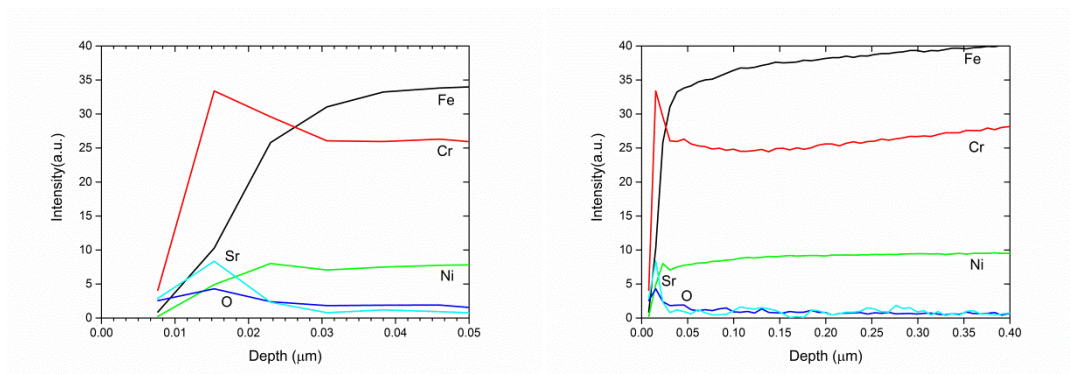
Figure 35 - GD-OES analysis of Sr-contaminated 304L steel samples prepared in

3 M HNO₃
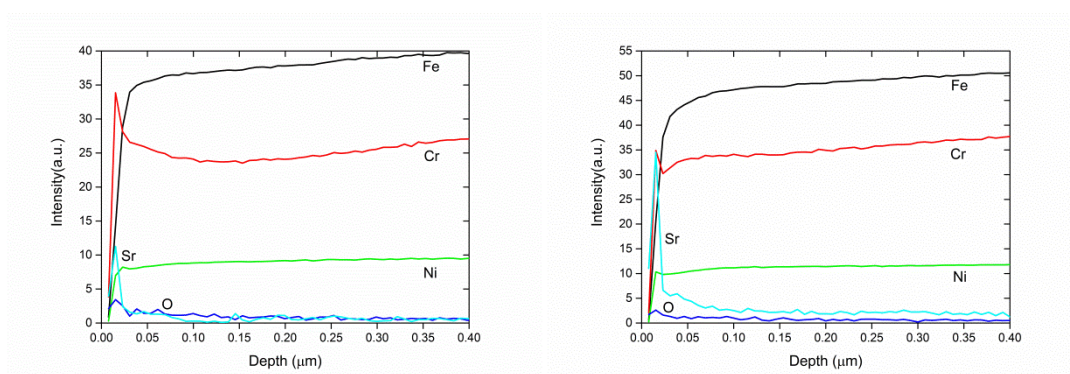
Figure 36 - GD-OES analysis of Sr-contaminated 304L steel samples prepared in

6 M HNO₃

The examination of samples prepared in 3 M and 6 M HNO_3 all showed the Sr contamination to be present largely in the Cr_2O_3 layer (indicated by the presence of both Cr and O peaks at the same location near to the steel surface),[15] residing between 0.013-0.015 μm within the steel surface. Despite the increase in concentration from 3 M to 6 M HNO_3 no further significant penetration was observed, suggesting that Sr either has an affinity for the oxide layer or that this passive layer constitutes a significant barrier to further Sr penetration.

Gels containing 2% (0.5 M) and 35% (7.9 M) HNO_3 were applied to these steel surfaces before they were rinsed with DI water and IPA, allowed to dry and reanalysed to investigate whether this treatment would result in further penetration of the Sr into the steel samples.
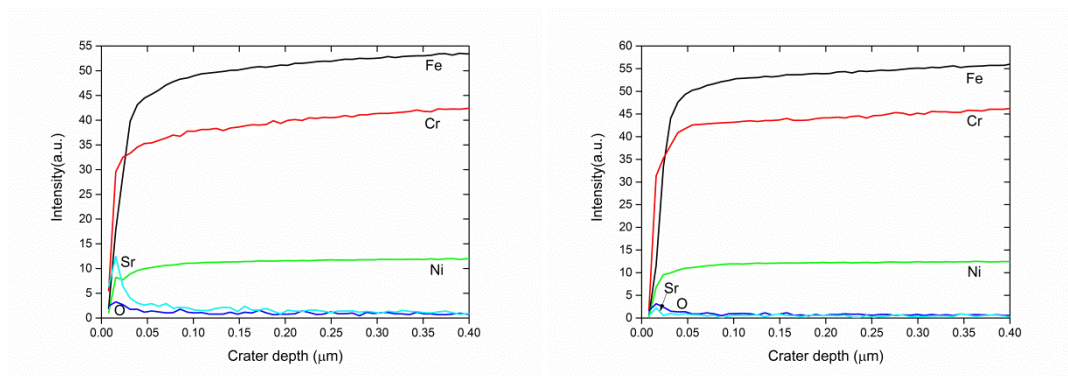
Figure 37 - GD-OES profiles of 304L steel after treatment with gels containing 35% (7.9 M) HNO$_3$
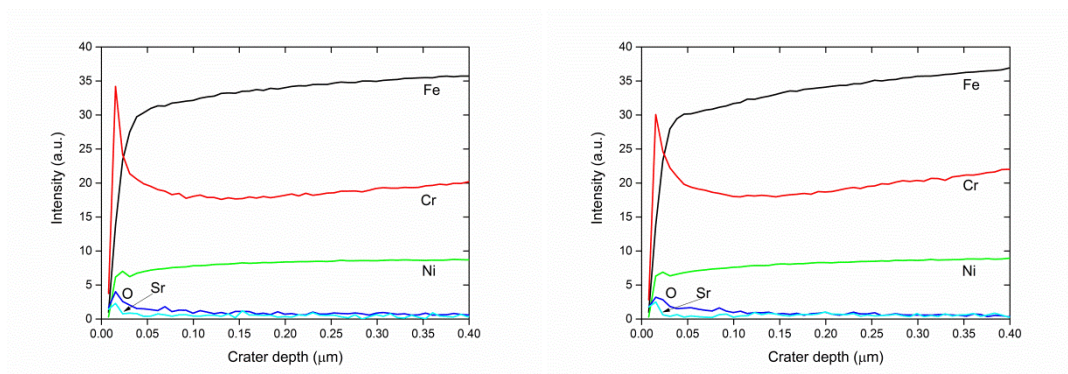
Figure 38 - GD-OES profiles of 304L steel after treatment with gels containing 2% (0.5 M) HNO$_3$

From the data plots above the major difference observed between figure 37 (35%, 7.9 M HNO$_3$) and figure 38 (2%, 0.5 M HNO$_3$) is the absence of a large Cr peak around 0.013-0.015 μm depth of the steel sample in the former figure. This would suggest destruction and solubilisation of the Cr$_2$O$_3$ layer at 35% HNO$_3$, however the continued presence of an O peak would suggest some oxide presence (possibly a reduced proportion of Cr$_2$O$_3$ and Fe$_2$O$_3$).

This development alone would be a reasonable basis to discount the use of HNO$_3$ at levels up to and above 35% strength to prevent damaging the passive layer of the steel surface which is likely to cause future concerns if materials are to be reused. Coupled with the destructive activity of this concentration of acid on the gel structure (see figure 38) these gels can be discounted from practical use.

The experiments carried out using 2% HNO_3 would suggest, due to the very visible presence of a strong Cr peak in the layer of depth between 0.013-0.015 μm, to cause little or no noteworthy damage to the Cr_2O_3 layer of the steel. The presence of the Sr peak at this same position would indicate less than 100% decontamination has taken place (as indeed is also noted when 35% HNO_3 gels are applied) but the penetration depth of the Sr into the steel has not been increased by the application of gels containing this weaker HNO_3 concentration.

4.7 - Interferometer depth maps

Depth profiles for each crater produced by GD-OES analysis were measured using a ContourGT-X 3D optical profiler white light interferometer with Vision64 Map software (Bruker Ltd. Massachusetts, U.S.). The resulting depth data was used to calibrate the sample measurement depth of GD-OES analysis.
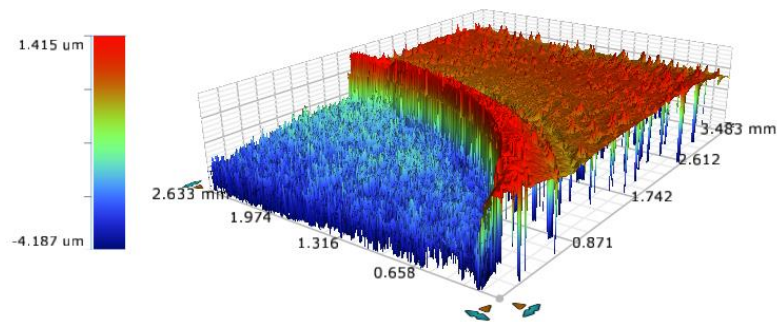
Figure 39 - Interferometer depth map of GD-OES crater.

Multiple craters were profiled of known sample measurements in order to provide an ablation depth estimate for each crater.

4.8 - References

1. Domingues, J., Bonelli, N., Giorgi, R., Fratini, E., Gorel, F., Baglioni, P. Innovative hydrogels based on semi-interpenetrating p(HEMA)/PVP networks for the cleaning of water-sensitive cultural heritage artifacts. *Langmuir* **29,** 2746–2755 (2013).

2. Suslick, K. S. and Price, G. J. Applications of ultrasound to materials chemistry. *Annu. Rev. Mater. Sci.* **29,** 295–326 (1999).

3. Mandal, B. B., Kapoor, S. and Kundu, S. C. Silk fibroin/polyacrylamide semi-interpenetrating network hydrogels for??controlled drug release. *Biomaterials* **30,** 2826–2836 (2009).

4. Zhang, J., Cheng, S.-X. and Zhuo, R.-X. Poly (vinyl alcohol)/ poly (N-isopropyl- acrylamide) semi-interpenetrating polymer network hydrogels with rapid response to temperature changes. *Colloid Polym Sci* **281,** 580–583 (2003).

5. Li, X., Cui, Y., Xiao, J. and Liao, L. Hydrogel–hydrogel composites: The interfacial structure and interaction between water and polymer chains. *J. Appl. Polym. Sci.* **108,** 3713–3719 (2008).

6. Mandal, B., Ray, S. K. and Bhattacharyya, R. Synthesis of full and semi Interpenetrating hydrogel from polyvinyl alcohol and poly (acrylic acid-co-hydroxyethylmethacrylate) copolymer: Study of swelling behavior, network parameters, and dye uptake properties. *J. Appl. Polym. Sci.* **124,** 2250–2268 (2012).

7. Kavanagh, G. M. and Ross-Murphy, S. B. Rheological characterisation of polymer gels. *Prog. Polym. Sci.* **23,** 533–562 (1998).

8. Dey, R. E., Wimpenny, I., Gough, J. E., Watts, D. C. and Budd, P. M. Poly(vinylphosphonic acid- co -acrylic acid) hydrogels: The effect of copolymer composition on osteoblast adhesion and proliferation. *J. Biomed. Mater. Res. Part A* **106,** 255–264 (2018).

9. Zuidema, J. M., Rivet, C. J., Gilbert, R. J. and Morrison, F. A. A protocol for

rheological characterization of hydrogels for tissue engineering strategies. *J. Biomed. Mater. Res. - Part B Appl. Biomater.* **102,** 1063–1073 (2014).

10. State of the Art Technology for Decontamination and Dismantling of Nuclear Facilities. *IAEA Tech. Reports Ser. No. 395* (1999).

11. Laraia, M. *Nuclear decommissioning planning, execution and international experience*. (Philadelphia, Pa. : Woodhead Pub., 2012).

12. Laraia, M. in *Handbook of Advanced Radioactive Waste Conditioning Technologies* 173–204 (Elsevier, 2011).

13. Laraia, M. *Advances and innovations in nuclear decommissioning*. (Kidlington, United Kingdom : Woodhead Publishing, an imprint of Elsevier, 2017).

14. Singh, B. R. in *ACS Symposium Series* (ed. Singh, B. R.) **750** 2–37 (1999).

15. Lang, A., Engelberg, D., Smith, N., Trivedi, D., Horsfall, O., Banford, A., Martin, P., Coffey, P., Bower, W., Walther, C., Weiß, M., Bosco, H., Jenkins, A., Law, G. Analysis of contaminated nuclear plant steel by laser-induced breakdown spectroscopy. *J. Hazard. Mater.* **345,** 114–122 (2018).

Blank page

Chapter 5 – Foams literature review

5.1 - Colloidal dispersions

A colloid is defined as a substance in which one component is dispersed in another, with the discontinuous (or dispersed) phase of the approximate size range of 1-1000 nm in a continuous (or dispersion) phase. Due to the small size of components of colloidal dispersions they possess extremely high surface areas, meaning the study of surface chemistry and effects is of paramount importance.[1] Common examples include pigment based inks (solid pigment suspended in a liquid), aerosol sprays (liquid suspended in a gas) and foams (gas suspended in a liquid or, occasionally, solid).

Due to the large surface areas of colloids there is a tendency to spontaneously aggregate into larger phases in order to minimise surface area and thus free energy.[1] In order to prevent this, the energy barrier of the repulsive forces must be of sufficient magnitude that the attractive forces causing aggregation are unable to breach it. Common means of stabilisation of sols (solids suspended in liquids) are steric (by polymers) and electrostatic (often charged) stabilisation. Although no colloid is predicted to be stable indefinitely there remains in existence more than one sample of gold colloid prepared by Michael Faraday over 150 years ago.[1]

The particular emphasis of this body of work is upon the properties and applications of foams and as such there will be limited attention paid to other forms of colloid.

5.2 - Foams

Foams are a particular subset of colloid wherein the discontinuous phase is a gas which is suspended in a continuous (often liquid) phase; although the size of the discontinuous phase does, however, sit outside the range generally assigned to the preponderance of colloids[2] foams are considered colloidal due to the thickness of the lamellae lying within this range.[3] The majority of people will be familiar with

foams as domestic products in forms such as: washing up liquid (where the produced foam, of normally very significant bubble size distribution, sits upon a bulk liquid phase of dilute detergent and below a second bulk phase of atmospheric gas), shaving foam (where pressurised containers produce bubbles of lesser varied bubble sized distribution which, when ejected, is isolated from the bulk liquid phase) and bath sponges (which are examples of solid foams, in this case containing an open pore structure rather than the also observable closed pore structure).

In a case where a gas is introduced into a liquid at a rate faster than that at which bubble drainage can occur; there is the potential for a foam to form. A surfactant (or some form of impurity) is required in order produce a foam by slowing the usually rapid rate of bubble coalescence.[4] The stability of a foam is variable depending on the content of the liquid, although it should be noted that no foam is thermodynamically stable and given time all liquid foams will collapse.[2]

The two key forms taken by foams are "wet" foams; with liquid fractions of above approximately 15% and featuring relatively small, spherical bubble systems with close packing of spheres[5] which are separated by liquid to the extent that each bubble has minimal influence on other bubbles and "dry" foams; which exhibit polyhedral bubbles separated by almost flat thin films of liquid as can be seen by the representation in figure 40.
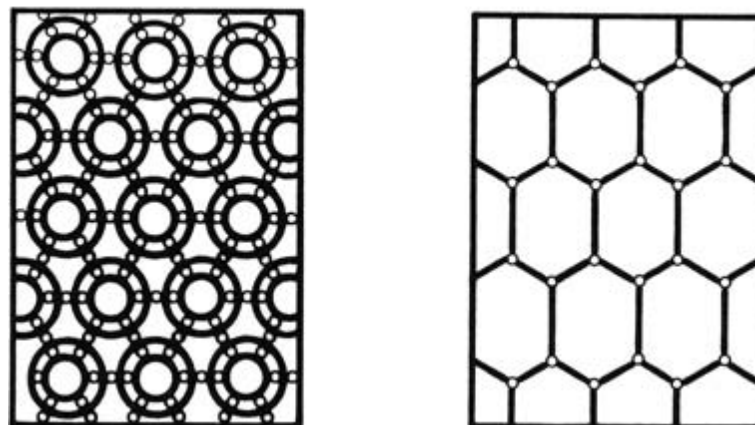
Figure 40 - Representative 2D images of a wet foam (left) and dry foam (right)[4]

In order to determine whether a foam is either dry or wet it is necessary to consider the bubble size in comparison with the capillary length (l_0):

$$l_0^2 = \frac{\gamma}{\Delta \rho g}$$

Equation 9 - Capillary length

In this equation $\Delta \rho$ represents the difference in density between the gas and liquid components, γ represents the surface tension and *g* represents the acceleration due to gravity.[5] A smaller average bubble diameter than capillary length is indicative of wet foam whereas dry foams, inversely, are in equilibrium under gravity and contain larger bubbles.

The schematic in figure 41 below aims to relate the terminology used to describe foams to a simplified 2D dry foam polyhedral structure.
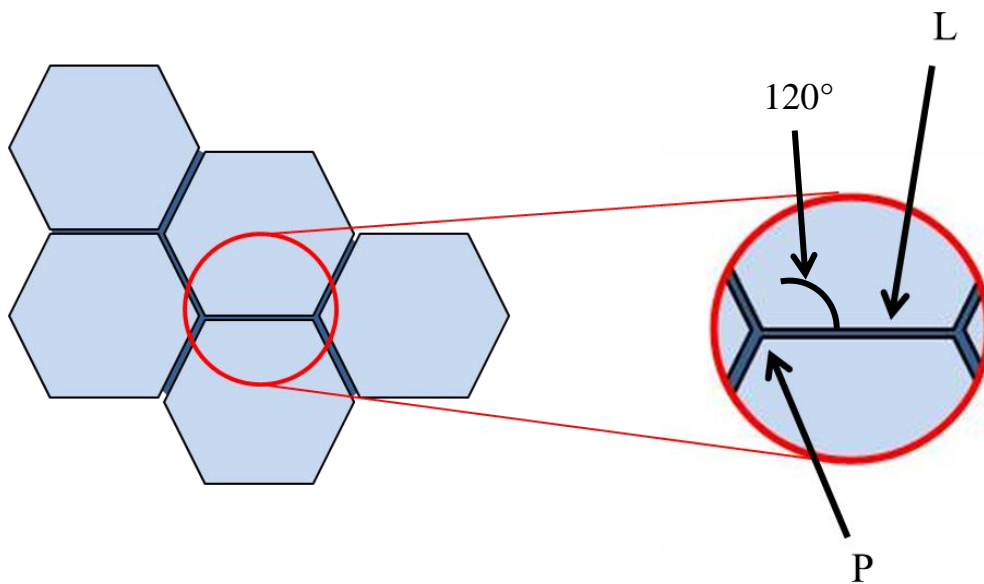
Figure 41 - Basic schematic of foam structure where light blue hexagons are gas bubbles; P represents a plateau border (sometimes known as a node) and L represents a lamella (often referred to as film, or wall)

Dry foams are ordinarily more stable than the wet variety, with the potential for wet foams to dehydrate via drainage to exhibit dry foam characteristics. Of particular note is the relatively regular structure adopted by dry foams, particularly that three films of the liquid lamella always meet and stabilise at angles of 120° and four films of the liquid lamella meet with a plateau border angle of 109° when viewed in three dimensions. Other structures are possible under conditions such as imposed strain[5] where additional, conventionally forbidden, vertexes are present but these anomalous regions are assimilated into the conventional structure rapidly after creation as the foam structure rearranges.

The predominant mechanism of rearrangement in foams is known as a T1 event. These events are often caused by straining forces on the foam structure and are classed as topological changes;[6] often occurring in cascades when an additional film meets at a vertex causing it to become energetically unstable[7], a process which has been extensively modelled.[6]

Figure 42 describes a 2D T1 transformation due to the diminishing length of a foam cell wall film, with figure 43 describing the reversible application of this event in 3D.
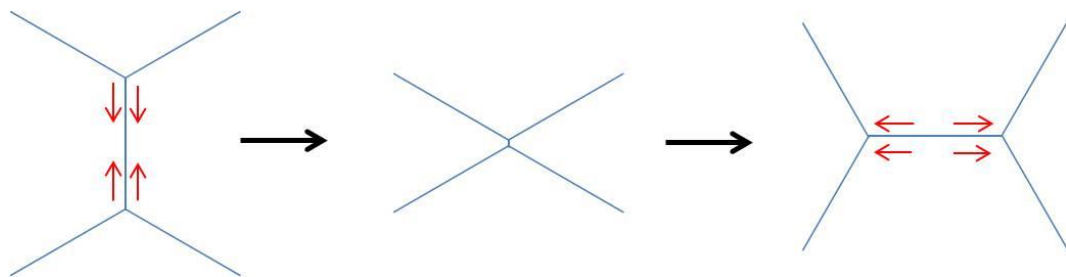
Figure 42 - A 2D representation of a T1 event. The diminishing of a lamella results in a vertex with 4 intersections which rapidly returns to a more stable configuration[8]
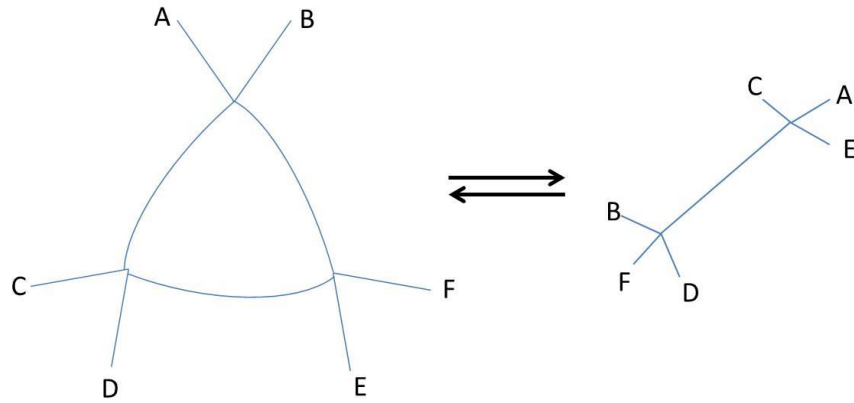
Figure 43 - A 3D representation of a T1 event. A plateau border is formed as a triangular face diminishes in size, resulting in an unstable 6 intersection vertex (and vice-versa).[5]

There are two principle categories of foam generation under which all other methods can be classed: condensation and dispersion. Condensation is the least labour intensive method but in industrial applications also tends to be the most costly, often prohibiting its use. This method of foam generation involves removing gas molecules from a saturated liquid solution either by reducing pressure or increasing temperature and is readily observable when opening a bottle of ale: as the cap is removed (the contents are depressurised) the carbon dioxide gas present in the solution due to the fermentation process forms a discontinuous gas phase in the liquid and rises to the surface to form a foam, known as a head. Dispersion as a method of foam generation relies upon agitation of a liquid in order to introduce gas from a bulk phase to form bubbles. Examples of this method include agitation via propeller (effectively the use of a blender), bubbling of a gas through a liquid or, as in the case of foams produced by washing up liquid, transfer of a liquid from one vessel (tap) to another (sink).[2]

A simple and useful measure of foaming capacity after a fixed foam-generating operation is given by Dawa *et al*:[9]

$$FC = \left(\frac{FV}{V}\right) \times 100\%$$

Equation 10 - Foaming capacity

Where FC is the foaming capacity, FV the foam volume and V the initial volume of foam-producing sample.

5.3 - Surfactants

The name "surfactant" derives from a contraction of the key property of such molecules: surface active agent. A common feature of all surfactants is the inclusion of both a hydrophilic and hydrophobic portion in a single molecule (an amphiphilic molecule); with the hydrophilic portion being composed of either an ionic or polar group to ensure compatibility with water. The hydrophobic end of the molecule, conversely, is composed of a non-polar component such as a hydrocarbon chain (although fluorosurfactants have come into more widespread use recently).[10] The hydrophilic end of the molecule is commonly referred to as the head, attached to the hydrophobic tail which is conventionally drawn to resemble a tadpole in many schematics for ease.
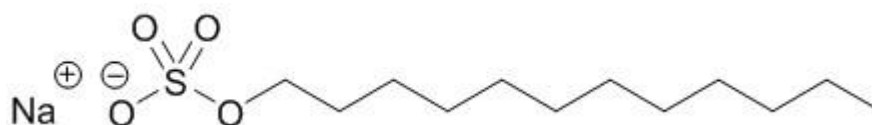
Figure 44 - Structure of SDS; a common anionic surfactant in many household applications.

Surfactants can be broken down into several groups based on the composition of the hydrophilic head portion of the molecule: anionic, cationic, non-ionic and amphoteric, although in recent years additional polymeric, silicon and fluorosurfactants have also emerged and are classified by the novel components of their hydrophobic groups.[11]

Anionic surfactants feature small cationic counter ions (such as sodium or ammonium) whereas cationic surfactants, inversely, carry counter ions such as

chloride or sulphate. The common ground between the two is the requirement that the counter ion should have minimal influence on surfactant properties.

Unlike ionic surfactants non-ionic surfactants do not dissociate into their constituent ions when formulated, with the most common members of this class being the ethoxylated variety. It is also possible to produce a mixture of anionic and cationic surfactants which behave similarly to non-ionic surfactants.

Amphoteric surfactants carry both positive and negative charges on the hydrophilic portion of the molecule, making them zwitterionic, with the pH of the formulation determining the molecule's charge.[11]

Of the speciality surfactants the silicon based variety are capable of reducing surface tensions to below those attainable with hydrocarbon surfactants (often finding use in fire extinguishing foams) but prove destructive to hydrocarbon-produced foams. Fluorosurfactants are able to lower the surface tension even further and as a result are often referred to as "superwetters".

The property for which surfactants are named is their ability to lower the surface tension of the liquid into which they are formulated by migrating to and lining up perpendicular to the air-liquid interface, causing it to spread.[12]

$$\gamma = \gamma_o - \pi$$

Equation 11 - Equation demonstrating the effect of surfactant upon surface tension

Equation 11 shows the reduction in surface tension caused by the addition of surfactant. γ represents surface tension of the solution with surfactant, γ_o the original surface tension and π the surface pressure of the surfactant.[12]

As the concentration of surfactant in solution increases the surface interface eventually becomes saturated with surfactant molecules, resulting in a large concentration of surfactant in the bulk liquid phase. Since interactions between water and the hydrophobic tails of the surfactant molecules are unfavourable, the minimisation of contact between the tails and water leads to the formation of

micelles (aggregations of surfactant molecules into large units)[8] at a concentration of surfactant termed the critical micelle concentration (CMC).
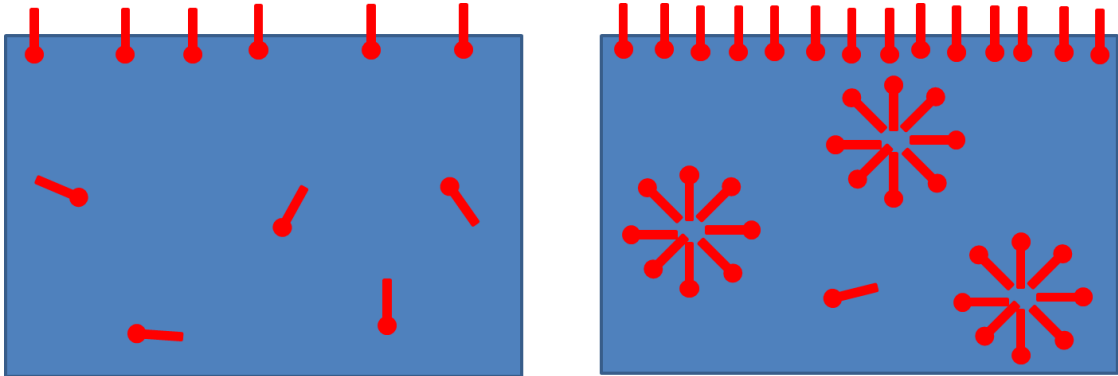
Figure 45 - Surfactant behaviour in solution at low and high concentrations. Note micelle formation at high concentrations.

In the case where the surfactant molecules are ionic the micelles formed are charged, leading to repulsive forces between similarly charged micelles.

Detection of the point at which the CMC is reached in a liquid sample containing surfactant can be determined experimentally with a simple plot of surfactant concentration vs. surface tension; the point at which there is a sharp break in the trend indicates the CMC.
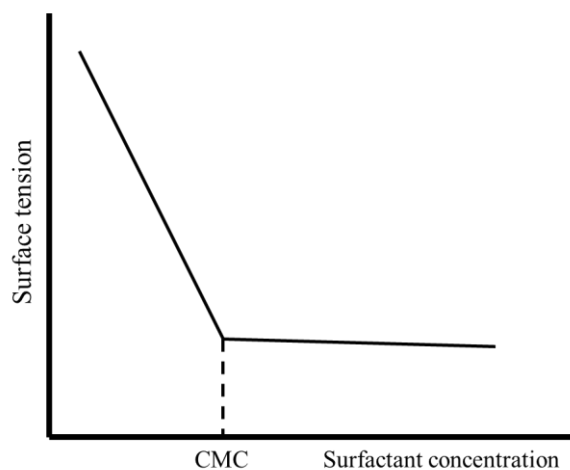
Figure 46 - Determination of CMC by plot of surface tension vs. surfactant concentration

The shape and structure of the micelles formed depends upon the geometrical constraints of the surfactant molecules, resulting in the formation of structures such as spheres, lamellae and cylinders, (see Figure 47) some of which also minimise charge repulsions between like surfactant molecules.
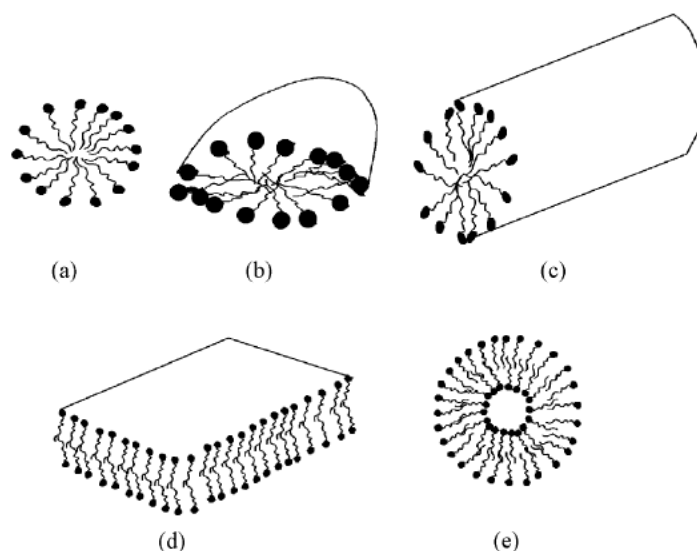
Figure 47 -Selection of possible micelle structures[13]: a) Spherical, b) Disk-shaped, c) Lamellar and e) Spherical vesicles. Taken from The basic principles of colloid science.[1]

These structures can be determined using the dimensionless value of the packing parameter (P); where V represents the volume of the hydrophobic tail group(s), a_o

126

the optimal area of polar head and l_c the critical chain length (maximum effective chain length).[13–16]

$$P = {V}/{a_o l_c}$$

Equation 12 - The packing parameter (P)[13–16]

The obtained value of P can then be compared to the following table as a guide to the structure of the micelles formed:

Micelle structure	P
Spherical	0.33
Cylindrical	0.5
Lamellar	1
Cylindrical or inverted structures	>1

Table 7 - Structure of micelles at various packing parameter values.[17]

The driving force behind micelle formation is principally entropic: since hydrophobic tails in aqueous solutions have limited degrees of freedom (due to the unfavourable interactions mentioned earlier) they aggregate together into a hydrocarbon environment where their entropy is greatly increased in addition to that of the water molecules.[1]

Once micelles have been formed in a solution the central hydrophobic cavity is capable of solubilising other hydrophobic materials within, resulting in swelling of the micelles. This is a key mechanism in the action of a detergent.[1]

5.4 - Foam rheology and drainage

Foams have been shown to exhibit viscoelastic properties in a manner similar to polymer solutions, making the study of foam rheology crucial to the understanding

of overall foam behaviour and stability. One particular use of the effective yield stresses of foams is their employment in drilling operations where they are used to prevent the uncontrolled movement of small cuttings. The foam will not move within the container in the same manner as a liquid since the packing of foam bubbles is unaffected by the deformation of individual bubbles, thus preventing significant transport. Larger, heavier particles, however, will fall through the foam in a "chaining" manner rather similar to that observable in polymeric solutions.[18]

Under conditions of increased strains and stresses foams are observed to adopt fluid like behaviour over solid like behaviour, a transition known commonly as yielding, occurring when the yield stress is exceeded and increasing as the liquid content of the foam decreases.[19] At this point the stress upon the foam (when plotted as a function of strain) begins to plateau after previously increasing to a maximum.
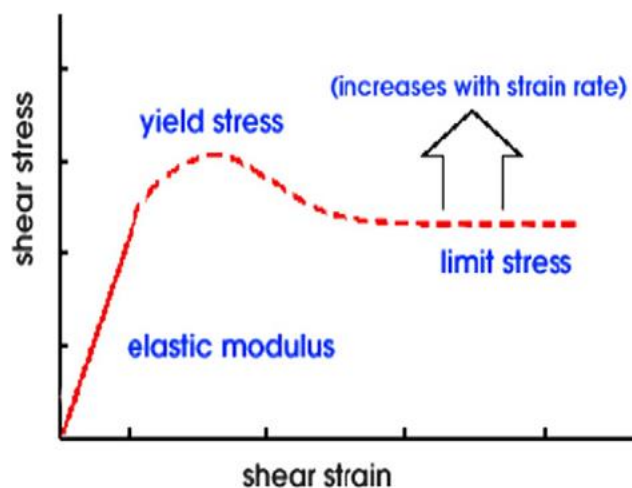
Figure 48 - Shear stress vs. shear strain-taken from "The rheology of foam"[20]

It is here that bubble packing within the structure of the foam may be influenced and the properties mentioned above with regards to the use of foams in drilling operations are lost.

Now the foam adopts a behaviour referred to as plastic flow, at which point it will permanently deform under the required levels of stress.[5] This can also facilitate more frequent T1 rearrangements, contributing to allow the foam to flow more rapidly.

The rheological behaviour of foams when in contact with confining walls or surfaces is also of interest: foams are either able to elastically deform, as expected, or slip along the surface depending upon the differences between applied stress and the foam's yield stress. Elastic deformation occurs when the yield stress of the foam is greater than the stress exerted upon the foam, whereas the slipping phenomenon exhibits viscous friction at the foam-wall interface when yield stress is the lesser force; resulting in foam flow.[5]

A key reason foams collapse over time is due to the drainage of the interlamellar liquid under gravity or pressure differences (causing liquid in the lamella to be drawn towards the plateau border)[21], resulting in thinner, more delicate lamellae with an increased probability of rupture.[22] This process is known as stratification.[10] In order to prolong the life of a foam the simple act of increasing the viscosity of the foaming solution has a significant contribution;[23–25] granting stability by ensuring the drainage of liquid is significantly retarded due to the reduced liquid flow rate, although there is the likelihood of inhibiting the production of foam as a consequence of viscosity increases.[4]

Correlations have also been observed between high surface shear viscosity[4] and foam stability in addition to high surface dilation viscosity and the stability of thin films.

The flow of gas throughout the foam structure is also of paramount importance. This process, known as coarsening, results from pressure differentials between individual bubbles and most commonly results in the diffusion of gas through lamellae from small bubbles to larger bubbles[22] with larger bubbles continuing to increase in size whilst the smaller bubbles' size decreases. A smaller bubble will possess a higher pressure than a larger bubble owing to the differences in surface curvature, a phenomenon quantified using the Laplace equation:[12]

$$\Delta P = 2\gamma/r$$

Equation 13- Pressure difference between soap bubbles using the Young-Laplace equation; where ΔP is the excess pressure, r bubble radius and γ the surface tension of the bubble.[26]

This phenomenon has the effect of eliminating small bubbles from the foam structure. In terms of a spherical bubble the excess pressure of a bubble can be shown to be inversely proportional to bubble radius.

A secondary effect of this process is the increase in the rate of liquid drainage of the lamellae by concentrating the liquid and thus thickening the lamellae, which increases the liquid flow rate.[19]

As drainage occurs and the foam adopts a more polyhedral, dry foam structure the pressure differential between adjacent bubbles is ordinarily much lower and as a result lamellae tend to exhibit reduced curvature.[12]

The composition of the gas component is a key factor in engineering the stability of a foam since gases soluble in the liquid medium will produce foams of reduced stability than insoluble gases. For example: the solubility of carbon dioxide in water based foams results in reduced stability since the transport of the gas across the foam films is faster than would be the case for an inert gas such as nitrogen.[3]

When all factors are considered, the defining factor for the rupture of lamellae is expected to be due to the statistical variation of lamellae thicknesses;[27] since when a lamella is thinned to a certain dimension it begins the process of rupture and collapse. Of course, factors such as evaporation, alien particles, shock and changes in temperature (even subtle changes in the case of certain foams) contribute to foam stability significantly.

5.5 - Foam stability

In terms of foam stability it is worth reiterating that no foam is thermodynamically stable and given time all liquid foams will collapse. There are two further classifications in use to distinguish between foams based on the timescales of their stability: foams with a lifetime of seconds are considered unstable (or transient) whereas a lifetime measured in hours or days is considered metastable (sometimes dubiously called "permanent").[10]

In order to quantify foam stability we return again to the work of Dawa *et al*:[9]

$$FS = \left(\frac{FV\Delta t}{FV_0}\right) \times 100$$

Equation 14 - Foam stability

Where FS is foam stability, $FV\Delta t$ the foam volume after 30 minutes (although in this body of work foam volume and thus stability will be measured at differing times, resulting in variable values of Δt in use) and FV_0 the initial volume of foam immediately after generation.

Evaporation of water (or other solvents) also has a significant part to play in determining the stability of foam. The thickness of foam films is reduced by evaporation, commonly resulting in areas of film with reduced stability which are more likely to rupture earlier than is desirable.[3,28,29] It is therefore common for many foaming solutions to be formulated to contain dodecanol or similar compounds possessing high boiling points to attempt to slow the rate of evaporation.

In cases where evaporation reduces foam film thickness the Marangoni effect acts as a stabilising force. When the surface thickness experiences a local reduction there is also an increase in surface area and therefore a reduction in surfactant concentration at the surface; this produces a region of increased surface tension into which more liquid is spontaneously drawn.[4] This not only replenishes the previously reduced film thickness but also returns the surface tension to a stable equilibrium value due to the presence of surfactant molecules in the transported liquid.[30] This effect also occurs during foam expansion, although it is generally more rapid in the case of thicker films (wet foams) than thinner films (dry foams) and does diminish over time. It is also possible for the reverse process to occur, where local thickening of the surface layer is reduced by the outward flow of liquid.
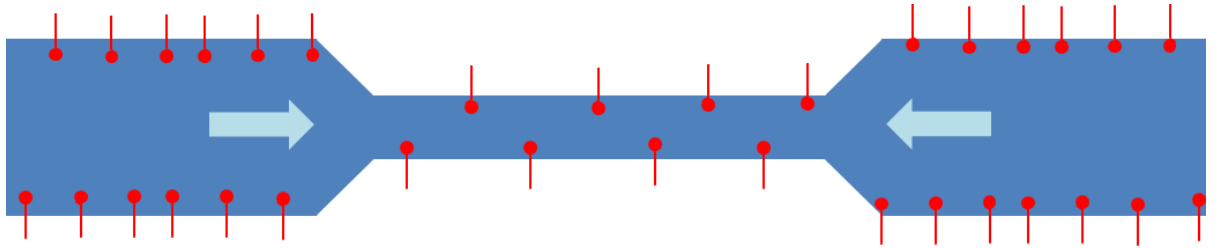
Figure 49- Stabilisation after film thinning due to the Marangoni effect. Arrows represent direction of flow.

Gibbs film elasticity (commonly denoted *E*) also acts as a stabilising force in much the same way as the Marangoni effect, although Gibbs only applies to lamella featuring surface areas larger than their thickness by multiple orders of magnitude.[31] The following equation shows how changes in surface area (A) of the lamella cause changes to the surface tension (γ), thus acting as a restorative force:[4]

$$E = 2A\left(\frac{d\gamma}{dA}\right)$$

Equation 15 - Gibbs film elasticity.

Choice of surfactant is a major consideration when attempting to formulate stable foams; short chain surfactants have a tendency to produce transient foams and therefore longer chain surfactants should primarily be considered.[10] The optimum concentration of surfactant is regarded as being at or above the CMC since, at this point, the micelles within the lamellae have the potential to form organised molecular structures which retard the rate of thinning due to repulsive interactions between micelles.[32,33]

Non-ionic surfactants often stabilise foams via their ability to form a liquid crystal structure within lamellae[34] which has not only the predictable effect of increasing viscosity but also providing a surfactant reserve at the point where it is most needed.[10]

Mixed surfactant formulations are often observed to confer more benefits than the sum of their parts; with reasons for this generally being the reduced surface tensions

available, lower CMCs, increase to surface elasticity and in particular the increase in surface viscosity.[10]

A key source of stabilisation performance in foams is the formulation of soluble polymers into the foaming solution; despite the fact that many of the polymers used are not themselves surface active (e.g. the adsorbed complexes originating from grains and sugars responsible for stabilising beer foams).[4] Polymers in solution have the effect of reducing the forces of interaction in the solution and producing flexible foam films in addition to the aforementioned viscosity increases.[35,36]

Polysaccharides are very commonly used as stabilising agents due to their ability to form hydrocolloids, resulting in increased viscosity and therefore foam stabilisation.[37] Two particularly useful examples of such polysaccharides are xanthan and acacia gums, both edible natural products, with the acacia gum originating from *Acacia Senegal* tree sap and being composed of polysaccharide and a protein-polysaccharide complex. Xanthan gum is produced as the fermentation product of the bacteria *Xanthomonas campestris* and possesses the structure of an exo-cellular polysaccharide.[9] Both are commonly used in the formulation of food products and when compared both gums possess high water solubility but offer varying degrees of viscosity increase[38] and foaming capability; with xanthan gum exhibiting no foaming capability alone in water, contrasting acacia gum's limited foaming capability.[9]

Soluble proteins are also particularly useful as agitation and adsorption often leads to denaturing, resulting in multi-molecular and rigid layers at the surface which considerably aid stability (e.g. a beaten egg white).[1] Generally it is predicted that the most effective foam stabilising additives will be those which are adsorbed at the surface slowly, after the surfactant molecules.[8]

There is additionally a basis for the use of hydrophilic solid particles (usually assumed to be spherical) in foam stabilisation[8] as if the particles are held within the film it is possible for them to pack at the film surface and prevent coalescence[1] by bridging the lamella, resulting in a low contact angle which draws liquid towards the particle via Laplace pressure (pressure difference occurring between both sides of a curved surface)[39] and opposes the lamellae thinning.[3] The increase in viscosity accompanying the incorporation of fully dispersed solid particles also adds to the stabilising effect.[40] A similar phenomenon also occurs in emulsions: a solid particle

is able to act as a bridge between multiple droplets of a dispersed phase resulting in coalescence.
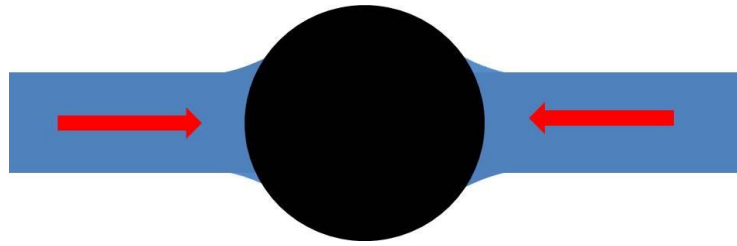
Figure 50 - Liquid is drawn towards a hydrophilic particle bridging a lamella[3]

Of particular importance is the contact angle of the lamella with a solid particle: angles below 90° at equilibrium are hydrophilic and will stabilise the foam whilst those above 90° are hydrophobic and will destabilise the foam[3] (See section 5.6). Thus the key factor in whether solid particles will stabilise a foam is the wettability.

5.6 - Antifoaming and defoaming

The matter of preventing foam formation, antifoaming, is often as simple (in principle, if rarely in reality) as reverse engineering the processes designed to stabilise foam. For example: reducing the viscosity of a foam should result in shorter-lived foams by increasing the rate of lamellae drainage, whilst increasing the rate of evaporation of the liquid lamellae should reduce the time required before rupture. Careful selection of non or low foaming surfactants is also a key consideration.

In contrast, it is often a more involved task to destroy foams once they have formed (defoaming) in unwanted places during many industrial processes,[4] methods for their destruction fall into the categories of thermal, chemical or mechanical breaking.

In the case of thermal breaking the temperature of the foam is modified in order to destabilise the foam by fluctuating the pressure within the bubbles, resulting in more rapid rupturing of lamellae. An increase in temperature is also associated with a

decreasing liquid viscosity, allowing the liquid to drain more rapidly, although the potential for destruction of or damage to the material treated does exist. [4]

Chemical breaking involves the addition of a chemical agent with the intention of destroying foam. Many foam inhibitors have been observed to disrupt the stabilising mechanism of the marangoni effect by increasing the rate at which surface tension equilibrium is attained, preventing the transport of liquid from thicker to thinner regions of the lamellae as the surface expands and thus encouraging rupture via thinning.[41] Decreasing the surface viscosity of the foaming solution, the manner of operation of tributyl phosphate, is also employed as a method of foam breaking and results in rapid draining of the interlamellar liquid.[12]

Hydrophobic solid particles are also frequently employed as a means to destabilise foams, provided they are not fully wetted. [41] When the solid particle enters the lamella and forms a contact angle of greater than 90° the increased Laplace pressure results in the flow of liquid away from the particle, causing thinning of the lamella. When paired with the non-wetting behaviour of the particle on the thinner lamella the result is rupture and thus the destruction of foam.[41]
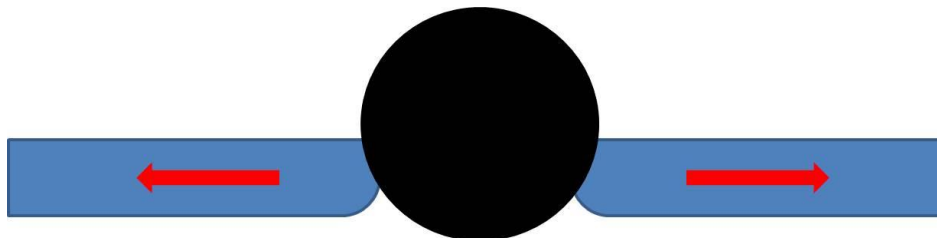
Figure 51 - Liquid flows away from a hydrophobic particle within a lamella.[3]

Oil based additives involve the localised displacement of the surfactant at the surface of the foaming solution, resulting in the formation of "blackspots" on the surface with high surface energy and, therefore, deformed lamellae in much the same way as hydrophobic solid particles; with the additional mechanism of the spreading of the oil droplet across the surface to form a lens.[3] Diethyl ether operates in this manner.

A combination of hydrocarbon or silicon oils (of particular interest are the dimethylpolysiloxanes; polymers commonly known as PDMS)[4] with hydrophobic particles is a common base for the formulation of defoamers; destroying the foam by the complementary action of the hydrophobic particles bridging the interface between oil, water and air interfaces.[3]

An easily observable example of chemical foam inhibition is the effect of hard water (water with high calcium content) on household soaps. Take for instance SDS; the calcium cation forms a calcium soap with the main body of the anionic SDS molecule[42] which produces a fragile lamella by replacing the previously elastic surface of the lamellae.[12]

As mentioned earlier mechanical defoaming is also a possibility which is usually undertaken when thermal or chemical methods would produce undesirable secondary effects.[43] In these processes the use of high shear forces via multiple mechanical means such as centrifuging or sonicating causes lamellar rupture.

5.7 - Uses of foams

5.7.1 - Decontamination foams

The concept of using foams as a decontamination medium generally relies upon two key benefits: the ability of a foam to completely fill a container of complex shape and the relatively small volume of liquid contained within a foam.[3] The idea being, much like fire-fighting applications, that a foam should be generated at the site of contamination from a concentrated solution of foaming agent combined with decontaminating reagent and directed into or over the contaminated vessel or surface in order to provide full contact. After decontaminating the surface the foam should collapse, leaving a small volume of liquid waste which is considerably easier to treat or dispose of than the large volumes of liquid generated by conventional decontamination technologies such as water jetting or solvent based systems.[44]

This approach aims to save resources, time and money in addition to improving practicality and safety (since large volumes of decontaminants need not be dealt with, nor mechanical decontamination techniques requiring human labour need be employed).

5.7.2 - Applications of decontamination foams

Decontamination foams have been formulated and tested by multiple bodies for many different applications such as industrial chemical contamination (reported in the case of illegal methamphetamine laboratories)[45], chemical or biological warfare agents, and nuclear decontamination.[46] Examples include the aqueous Allen Vanguard surface decontamination foam (designed for building decontamination), the solvent-based Sandia DF-200 decontamination foam and the U.S. military solvent-based Decon Green.[47] Both the Allen Vanguard and DF-200 utilise mildly aggressive oxidising agents as the mechanism of decontamination, with the use of foaming properties designed to effectively deliver the reagents to and coat the contaminated surface. Testing of the effectiveness of these foams on surfaces contaminated with the chemical warfare agents sulphur mustard gas, sarin, soman and VX was carried out by A.H Love *et al* in 2011.[47] If we examine the results of experiments upon these formulations as a means of comparing oxidising aqueous vs. solvent-based foam decontamination technologies it becomes apparent that all are highly effective to almost identical levels on non-permeable surfaces such as glass or stainless steel for all chemical warfare agents; with significantly different results emerging as the substances to be decontaminated become more permeable. It was noted that the aqueous Allen Vanguard tended to perform more effectively on concrete as it was better able to penetrate the pores of the concrete surface.[47] However, the solvent-based Decon Green exhibited very effective decontamination of permeable, hydrophobic polymer surfaces (vinyl and latex-painted surfaces) due to the obvious benefits of using a non-aqueous formulation on hydrophobic surfaces. The overall findings of A.H. Love *et al* would appear to highlight two key points to be taken on board by those who would wish to use or produce foams for decontamination purposes:

1-That the formulation in question must be tailored to the application at hand for most surfaces. Whilst non porous surfaces seemed easy to decontaminate, porous or permeable surfaces require considerable thought with regards to materials compatibility of the reagent delivery system. Aqueous systems have the disadvantage of corroding metals, for example.

2- That the high residual contamination remaining on many of the more porous surfaces and light residual contamination remaining on non-porous surfaces after contact times of 24 hours would indicate the need for multiple reapplications of the decontaminating agent in order to ensure 100% effectiveness.[47]

5.7.3 - Nuclear industry applications of decontamination foams

Multiple formulations exist for the use of foams for decontamination purposes either as the decontaminating method or a coating method. Rovnyi *et al*[48] describe several foam compositions intended to form coatings on contaminated surfaces to prevent the mobilisation of radionuclides as aerosols during decommissioning operations: a formulation including 7% PVA and 1% of an ethoxylated isooctylphenol surfactant (OP-10) featuring a viscosity of 56 cP, surface tension of 29.3 mN/m and density of 1.013 g/cm^3 was considered the most practical in terms of foaming ability, stability and film forming effects.[48]

In terms of decontamination reagent delivery through foams; multiple formulations exist in differing levels of detail. Costes and Gauchon[49] report in 1996 the use of a process consisting of dry foams; gassed with air, containing first NaOH with a short lifetime (described as a half-life of 8 minutes), followed by a foam containing a combination of phosphoric and sulphuric acids, completed by a mildly alkaline foam (to achieve neutral pH in the vessel to be decontaminated) to target particularly ^{60}Co and ^{137}Cs. These foams contain 0.5% of a polyethylene glycol additive which extends foam lifetimes to give a reported half-life of 14 minutes. The relatively short lifespan of these foams is not considered an issue in this case due to the continuous recirculation of the foaming solution at 30-40 °C within the vessel in processes lasting several hours with the idea being to counteract the boundary layer

phenomenon arising from wall coalescence of foams which may prevent molecules in the bulk reaching the surface.[49] Results show the majority of contamination levels to be below detectable levels. In 1993 a very similar process was successfully applied to a graphite gas-cooler of 1000 m^2 contaminated surface area containing principally the target radionuclides described above but differing in the absence of PEG additive and substitution of sulphuric for nitric acid.[50] The significant benefits of this procedure were the production of only 6 m^3 of effluents for the large surface decontaminated and the achievement of a decontamination factor of 190.

A water-based decontamination foam containing 1-hydroxyethane-1,1-diphosphonic acid (HEDPA) with significant numbers of additives, acting by dissolving oxides carrying contaminant radionuclides has also been described.[46] Decontamination factors for U and Pu are given as 890 and for other species as 136 after one application.

Also reported is a series of aqueous foams containing sulphuric acid, sodium hydroxide or phosphoric acid with polyethylene glycol, 2-pentanol, an oligosaccharide alkyl ether surfactant and a betaine-based surfactant with lifetimes of 2 hours. Decontamination factors of between 86 and above 880 are described, depending upon exact composition and the contaminated object, with up to 29 μm metal erosion observed.[51]

Additionally, reports of acidic radionuclide decontamination foams stabilised by gelling agents such as xanthan gum or gelatin have been reported to exhibit long lifetimes, often spanning several hours and have shown great promise.[44,52,53]

5.7.4 - Fire-fighting foams

A glance around any workplace or public building will show an important application of foams: fire extinguishers. To the extent that it is estimated the EU used 13,000 tons of fire-fighting foam concentrate in 2006.[54] The concept of fire-fighting foams originated in the early 1900s, formed by mixtures of inorganic powders, natural soaps and water.[5] In application it is customary for the foaming agent to be transported to the required site as a concentrated solution, at which point

it is diluted to the appropriate levels (proportioning; generally somewhere between 1-10% concentrate in water) and may be mixed turbulently with air in an aspirating process.[5] In the case of either an aspirating or non-aspirating process the key requirement is the subjection of the solution to adequate shear to produce foam, which is examined by the expansion ratio:

$$E.R. = {Volume\ of\ foam}/{Volume\ of\ solution\ used\ to\ make\ foam}$$

Equation 16 - Foam expansion ratio

Optimally the foam concentrate will require the minimum proportioning rate to reduce the quantity of foam concentrate to be transported to a site.

More modern mediums are ordinarily comprised of water, organic solvents, hydrocarbon surfactants, fluorosurfactants or silicon-based surfactants, higher alcohols, and some form of polymer. The role of the organic solvents is to provide adequate low temperature operability (where required), boost the foaming properties of the hydrocarbon surfactants and provide a method of dispersing polymers added to the solution. Higher alcohols raise the boiling point of the solution to slow the rate of foam destruction due to evaporation and also perform a secondary role increasing the viscosity of the solution. Polymers provide viscosity modification which aids in preventing foam collapse, particularly when the foam is to be used on polar fuels and they often precipitate to form a membrane between the foam blanket and combustible fuel.[5] The role of the hydrocarbon surfactants is to produce the maximum volume of foam from the minimum volume of solution; sufficient to coat the burning medium in a foam blanket and aid in wetting. Finally, fluorosurfactants are commonly employed to increase the wettability of the formulation in order to better penetrate fuels and provide greatly increased burnback defence.[5]

The general mechanism by which fire-fighting foams operate is to spread on top of the burning material and reduce the fire intensity by the evaporation of water, prevent the emission of flammable vapours from the fuel and prevent burnback by insulating the fuel from oxygen and sources of ignition.[17] Overall it has been claimed

that the insulation, heat sink and mass transfer barrier effects of foams greatly dominate the evaporation factor in terms of extinguishing mechanisms.[5]

Fire-fighting foams are ordinarily used only upon class A (Organic solids e.g. wood) and class B (flammable liquid e.g. petrol) fires[55] with each fire type having differing requirements. Class A fires require foams capable of wetting the fuel thoroughly, including surface penetration, to insulate the fuel from oxygen and sources of ignition. For the reason stated above this is considerably more effective than mere water (which acts by vaporising to displace oxygen) and additionally provides a degree of "cling" on surfaces rather than rapidly flowing away in the manner of water, hence providing a degree of burnback protection.[5] Foams for use on class B fires are required to spontaneously spread across the surface of the burning liquid to produce an insulating foam blanket and are therefore known as aqueous film forming foams (AFFF). In order to adequately spread across the surface of the liquid fuel the foam must have a specific gravity less than that of the fuel; as such most low expansion foams for use of class B fires have a specific gravity of between approximately 0.05-0.20.[5] Polar liquid fuels do have a tendency to be somewhat miscible with water based foams and as such a viscosity increaser is advantageous to help form a membranous film between the foam blanket and liquid fuel. The spreading coefficient (S.C.) may be employed to determine whether a film will form at the surface of a liquid fuel:

$$S.C. = \gamma_{a/f} - (\gamma_{a/w} + \gamma_{w/f})$$

Equation 17 - Spreading coefficient. Where a=air, w=water (to be taken as foam) and f=fuel. A positive value indicates the formation of a film over the fuel.[5]

In terms of use tailoring it is perfectly permissible to use class B foams on class A fires although the reverse is extremely ill-advised as class A foams do not form an aqueous film and can actually combine the flammable vapours from the liquid fuel and air within the foam bubbles; resulting in a flammable mixture within the bubbles which can cause significant burnback issues as the foam collapses and flash fires become a distinct possibility.[5]

The fire-fighting foam concentrate "Expandol" for use on class B fires is the key formulation of interest for the incorporation of neutron absorbers in this body of work. This concentrate is composed of ethylene glycol monobutyl ether (EGmBE) and ethylene glycol to confer freeze protection and foam boosting surfactant qualities, anionic surfactants in the form of primary alcohol ether sulphates and sulphosuccinate, a blend of primary alcohols to stabilise the foam by increasing the boiling point of the liquid with the remaining fraction being water as a balance.[56]

5.8 - References

1.   Everett, D. H. *Basic Principles of Colloid Science*. *RSC Paperbacks* (Cambridge : Royal Society of Chemistry, 1988).

2.   Schramm, L. L. *Emulsions, Foams, and Suspensions*. *Emulsions, Foams, and Suspensions: Fundamentals and Applications* (Wiley-VCH Verlag GmbH and Co. KGaA, 2005).

3.   Rivier, N. and Sadoc, J. F. Foams and emulsions. *NATO ASI Ser. Ser. E, Appl. Sci. ;* xiv, 595 p. (1999).

4.   Höfer, R., Jost, F., Schwuger, M., Scharf, R., Geke, J., Kresse, J., Lingmann, H., Veitenhansl, R., Erdwied, W. in *Ullmann's Encyclopedia of Industrial Chemistry* **15**, 572–598 (Wiley-VCH Verlag GmbH and Co. KGaA, 2000).

5.   Stevenson, P. *Foam engineering fundamentals and applications*. (Chichester, West Sussex, UK : John Wiley andamp; Sons, 2012).

6.   Satomi, R., Grassia, P. and Oguey, C. Modelling relaxation following T1 transformations of foams incorporating surfactant mass transfer by the Marangoni effect. *Colloids Surfaces A Physicochem. Eng. Asp.* **438,** 77–84 (2013).

7.   Biance, A.-L., Cohen-Addad, S. and Höhler, R. Topological transition dynamics in a strained bubble cluster. *Soft Matter* **5,** 4672 (2009).

8.   Adamson, A. W. (Arthur W. *Physical chemistry of surfaces*. (New York ; Chichester : Wiley, 1997).

9.   Dawa, Q., Hua, Y., Chamba, M. V. M., Masamba, K. G. and Zhang, C. Effect of Xanthan and Arabic Gums on Foaming Properties of Pumpkin (Cucurbita pepo) Seed Protein Isolate. *J. Food Res.* **3,** 87–95 (2013).

10.   Tadros, T. F. *Applied surfactants : principles and applications*. (Weinheim Germany : Wiley-VCH, 2005).

11.   Kosswig, K. in *Ullmann's Encyclopedia of Industrial Chemistry* **35,** 431–505

(Wiley-VCH Verlag GmbH and Co. KGaA, 2000).

12. Mollet, H. *Formulation technology emulsions, suspensions, solid forms*. (Weinheim ; New York : Wiley-VCH, 2001).

13. Israelachvili, J. N. *Intermolecular and surface forces*. (Burlington, MA : Academic Press, 2011).

14. Israelachvili, J. N., Mitchell, D. J. and Ninham, B. W. Theory of self-assembly of hydrocarbon amphiphiles into micelles and bilayers. *J. Chem. Soc. Faraday Trans. 2* **72,** 1525 (1976).

15. Evans, D. F. and Wennerstrom, H. *The colloidal domain : where physics, chemistry, biology, and technology meet*. (New York ; Chichester : Wiley-VCH, 1999).

16. Mitchell, D. J. and Ninham, B. W. Micelles, vesicles and microemulsions. *J. Chem. Soc. Faraday Trans. 2* **77,** 601 (1981).

17. Pabon, M. and Corpart, J. M. Fluorinated surfactants: Synthesis, properties, effluent treatment. *J. Fluor. Chem.* **114,** 149–156 (2002).

18. Joseph, D. D. Questions in Fluid Mechanics: Understanding Foams and Foaming. *J. Fluids Eng.* **119,** 497 (1997).

19. Neethling, S. J., Lee, H. T. and Grassia, P. The growth, drainage and breakdown of foams. *Colloids Surfaces A Physicochem. Eng. Asp.* **263,** 184–196 (2005).

20. Weaire, D. The rheology of foam. *Curr. Opin. Colloid Interface Sci.* **13,** 171–176 (2008).

21. Breward, C. J. W. and Howell, P. D. The drainage of a foam lamella. *J. Fluid Mech.* **458,** 379-406 (2002).

22. Weaire, D. Foam Physics. *Adv. Eng. Mater.* **4,** 723–725 (2002).

23. Blair, C. M. *Chem. Ind.* **5,** 538-544 (1960).

24. Reisberg, J. and Doscher, T. M.. *Prod. Mon.* **11,** 43-44 (1956).

25.   Joly, M. *Recent Progress in Surface Science*. (Academic Press, 1964).

26.   Cooper, A. and Kennedy, M. W. Biofoams and natural protein surfactants. *Biophys. Chem.* **151,** 96–104 (2010).

27.   Vrij, A. Possible mechanism for the spontaneous rupture of thin, free liquid films. *Discuss. Faraday Soc.* **42,** 23 (1966).

28.   Mysels, K. J. *Soap Films: Studies of Their Thinning and a Bibliography*. (Pergamon Press, 1959).

29.   Joye, J.-L., Hirasaki, G. J. and Miller, C. A. Numerical Simulation of Instability Causing Asymmetric Drainage in Foam Films. *J. Colloid Interface Sci.* **177,** 542–552 (1996).

30.   Scriven, L. E. and Sternling, C. V. The Marangoni Effects. *Nature* **187,** 186 (1960).

31.   Gibbs, J. W. The collected works of J. Willard Gibbs. 2 v. (1928).

32.   Johnott, E. S. *Philos. Mag.* **114,** 746 (1906).

33.   Perrin, J. *Ann. Phys. (N. Y).* **10,** 160-184 (1918).

34.   Ewers, W. E. and Sutherland, K. L. The Role of Surface Transport in the Stability and Breakdown of Foams. *Aust. J. Chem.* **5,** 697–710 (1952).

35.   Symes, K. C. The relationship between the covalent structure of the Xanthomonas polysaccharide (Xanthan) and its function as a thickening, suspending and gelling agent. *Food Chem.* **6,** 63–76 (1980).

36.   Sanderson, G. R. Polysaccharides in foods. *Food Technol.* **35,** 50–83 (1981).

37.   Sikora, M., Badrie, N., Deisingh, A. K. and Kowalski, S. Sauces and Dressings: A Review of Properties and Applications. *Crit. Rev. Food Sci. Nutr.* **48,** 50–77 (2008).

38.   Walsh, D. J., Russell, K. and FitzGerald, R. J. Stabilisation of sodium caseinate hydrolysate foams. *Food Res. Int.* **41,** 43–52 (2008).

39.   Butt, H.-J., Graf, K. and Kappl, M. *Physics and Chemistry of Interfaces*.

Wiley-VCH GmbH and Co. KGaA (2003). doi:10.1002/3527602313

40.   Pugh, R. J. Foaming, foam films, antifoaming and defoaming. *Adv. Colloid Interface Sci.* **64,** 67–142 (1996).

41.   Schick, M. J. *Nonionic surfactants.* (London : Arnold ; New York : Marcel Dekker, 1967).

42.   Smulders, E. *Laundry detergents.* (Weinheim ; Cambridge : Wiley-VCH, 2002).

43.   Zlokarnik, M. Auslegung und Dimensionierung eines mechanischen Schaumzerstörers. *Chemie Ing. Tech.* **56,** 839–844 (1984).

44.   Faure, S., Fournel, B. and Fuentes, P. Composition, foam and method for surface decontamination. (2011).

45.   Releases, S. L. N. Anthrax-killing foam proves effective in meth lab cleanup. at <https://share.sandia.gov/news/resources/news_releases/decon_foam_meth/#. VSfrUfnF9y0>

46.   Nunez, L. and Kaminski, M. D. Foam and gel methods for the decontamination of metallic surfaces. (2007).

47.   Love, A., Bailey, C., Hanna, M., Hok, S., Vu, A., Reutter, D., Raber, E. Efficacy of liquid and foam decontamination technologies for chemical warfare agents on indoor surfaces. *J. Hazard. Mater.* **196,** 115–122 (2011).

48.   Rovnyi, S. I., Arsent'eva, N. V., Emel'yanov, N. M. and Kazakevich, Y. V. Foam Compositions for Improving Radiation Conditions during Decommissioning of Nuclear Objects. *At. Energy* **93,** 893–897 (2002).

49.   Costes, J. R. and Gauchon, J. Foam decontamination of large nuclear components before dismantling. in *Research Coordination Meeting on the IAEA Coordination Research Program on New Methods and technics for IAEA optimization of decontamination for maintenance and decommissioning* 739–743 (1996).

50. Faury, M., Fournel, B., Boissonnet, G. and Privens, H. FOAMS FOR NUCLEAR DECONTAMINATION PURPOSES: ACHIEVEMENTS AND PROSPECTS. at <http://www.wmsym.org/archives/1998/html/sess18/18-37/18-37.htm>

51. Gauchon, J., Brunel, G., Costes, J. R. and Faucompre, B. Mousse de décontamination à durée de vie contrôlée. (1995).

52. Demmer, R. L., Peterman, D. R., Tripp, J. L., Cooper, D. C. and Wright, K. E. Long lasting decontamination foam. (2007).

53. Faure, S., Fournel, B. and Fuentes, P. Composition, foam and process for the decontamination of surfaces. (2003).

54. Agency, S. C. *Perfluorinated substances and their uses in Sweden*. (2006).

55. Centre, F. S. A. Fire Extinguishers – Classes, Colour Coding, Rating, Location and Maintenance. at <http://www.firesafe.org.uk/portable-fire-extinguisher-general/>

56. Angus Fire. Expandol LT SDS. (2017) at http://angusfire.co.uk/wp-content/uploads/Expandol.pdf

Blank page

Chapter 6 - Foams for neutron poisoning applications

Joshua J Moore [a], Francis Livens [b], Alex Jenkins [c] and Stephen G Yeates [a]

a - Organic Materials Innovation Centre, School of Chemistry, The University of Manchester, Oxford Road, Manchester, M13 9PL, United Kingdom

b - Centre for Radiochemistry Research, School of Chemistry, The University of Manchester, Oxford Road, Manchester, M13 9PL, United Kingdom

c - Decontamination Centre of Expertise, Sellafield Ltd., Sellafield, Cumbria, CA20 1 PG, United Kingdom

6.1 - Abstract

The issue of fires in operating areas of nuclear plant has proven to be costly beyond mere fire damage in instances such as the Windscale fire and the Chernobyl accident; which resulted in the uncontrolled release of radioactive material to the environment. Conventional fire-fighting methods employ proportioned foams in order to extinguish fires with greater efficiency than water alone but do little to shield from the radiation present in these environments. This work aims to investigate the plausibility of incorporating neutron poisoning substances into fire-fighting foams with the rationale that a reduction in neutron activity would safeguard incident responders and retard the rate of any ongoing fission reactions to reduce the temperature and therefore propagation of fire.

The results suggest the reliance upon boron based neutron poisons incorporated into foam concentrates are unlikely to provide any significant benefit beyond the remit of traditional fire-fighting foams when confronted with a fire in the presence of neutron radiation.

6.2 - Introduction

Isotopes used to capture excess neutrons are those with a high neutron absorption cross-section (probability of absorbing neutrons) such as ^{10}B, ^{155}Gd and ^{157}Gd

possessing neutron absorbing cross sections of 3835, 61100 and 259000 barns respectively[1]. These isotopes are often known as neutron poisons and many are formed during the course of reactor operation as fission products, such as ^{135}Xe.[2] The unit of 1 barn (b) is defined as 10^{-28} m^2 (100 fm^2),[1] an approximation of the cross sectional area of a Uranium nucleus.[3] The large neutron absorption cross-sections observed in many neutron poisons are not an indication of a larger nucleus than the calculated cross section, rather an increased probability of interaction when other factors such as resonance capture and the energy of the neutrons are taken into effect.[3]

Neutron poisons can be subdivided into non-burnable and burnable poisons depending on the decay products formed when reacting with a neutron. A non-burnable poison has either a small neutron absorption cross section (resulting in a relatively long life due to the low probability of absorption) or decays to a product which also exhibits a high neutron absorption cross section[2] and as such non-burnable poisons are commonly used as the key component of nuclear reactor control rods. Hafnium is an excellent example of a non-burnable poison as the absorption of a neutron forms another poison, overall having a direct succession of five poisons.

Burnable poisons, however, decay to form products which have negligible neutron absorption cross sections and therefore become less effective over time. Such poisons are frequently employed in soluble form (particularly in pressurised water reactors) to allow direct addition to the coolant, creating a much more uniform distribution throughout the reactor core. This method of neutron poisoning can be fine-tuned through the addition of more poison or dilution of the coolant in order to maintain the conditions required; usually incorporating boric acid (either containing isotopically pure ^{10}B or standard boric acid of which 20% of the boron will be ^{10}B) or gadolinium nitrate as soluble poisons.[2] When fixed in place such poisons are generally incorporated into the fuel as additives.[2,4]

$$^{10}B + {^1}n \longrightarrow {^7}Li + {^4}\alpha$$
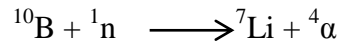
Figure 52- Neutron induced decay of ^{10}B.[5,6]

Figure 52 demonstrates the decay of ^{10}B with the emission of an alpha particle and lithium daughter nuclide of approximate energies 150 and 175 keV μm^{-1} respectively. The production of an alpha particle as a result of this process has led to the development of boron neutron capture therapy in the treatment of cancer. By creating a localised high concentration of ^{10}B within tumour cells and targeting this region with a low energy neutron beam the alpha radiation produced can be used to destroy the target tissue with minimal damage to surroundings due to the limited path lengths of decay products ranging from 4.5-10 μm in tissue or water.[5]

Another commonly used burnable neutron poison is found in gadolinium. Combined both ^{155}Gd and ^{157}Gd isotopes compose approximately 32% of naturally occurring gadolinium;[7] therefore not only do these isotopes each have a larger neutron capture cross-section than ^{10}B but also a significantly larger percentage of natural gadolinium behaves as a neutron poison which greatly enhances the usefulness of gadolinium as a poison. The neutron capture mechanisms of gadolinium are as follows:

$$^{155}Gd + {^1}n \longrightarrow {^{156}}Gd + \gamma$$

$$^{157}Gd + {^1}n \longrightarrow {^{158}}Gd + \gamma$$
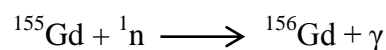
Figure 53 - Neutron capture by ^{155}Gd (15.6% of natural Gd) and ^{157}Gd (16.4% of natural Gd)[7]

The capture reactions of gadolinium, in contrast to boron, produce more penetrating gamma radiation and stable daughter gadolinium isotopes with an additional neutron.

Gadolinium has also been proposed for use in neutron capture cancer therapy in a similar fashion to boron, especially since gadolinium compounds are already

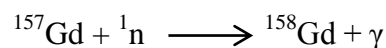commonly used as MRI contrast agents and have shown selective uptake[8]. The production of gamma radiation is more penetrating than the alpha produced by boron however and would most likely result in a larger area of effect.

Neutron poisons are commonly incorporated into aqueous solutions as materials with a large number of nuclei per unit area (namely substances containing hydrogen atoms) such as paraffin wax or water are effective neutron moderators; reducing the energy of neutrons through elastic scattering.[9] Heavy water, D_2O, is a less effective moderator due to the larger deuterium atoms although this often leads to definition as a better neutron moderator than light water when used in reactors requiring less moderation.[3]
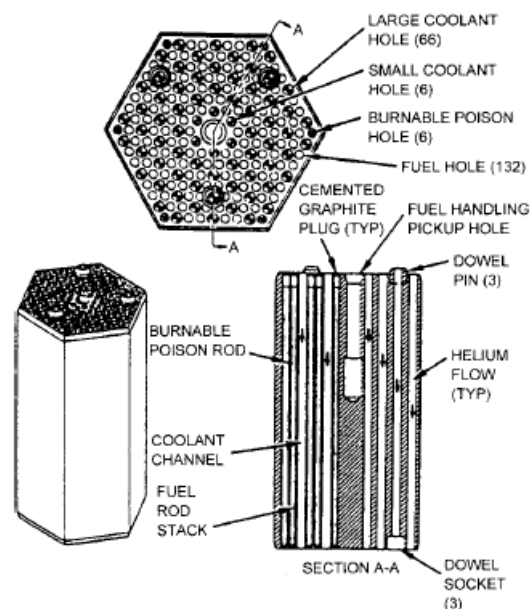
Figure 54– Fuel assembly schematic used in high temperature gas cooled reactor, illustrating the position of burnable poisons. Taken from nuclear reactor physics.[10]

In figure 54 the fuel; assembly of a high temperature gas cooled reactor details the position of burnable poison rods adjacent to the fuel rod stack, in this case the burnable poison is included within the fuel unit as an additive. Should there, however, arise the need to rapidly fill an irregular shaped vessel with a neutron poison under scenarios such as fires there are limited existing delivery mechanisms. With this in mind the consideration of a common fire fighting medium; foam, seems an ideal delivery mechanism.

Where gas is introduced into a liquid containing a surface active component more rapidly than bubble drainage occurs there exists the potential for foam formation.[11] Foams may be either wet or dry (water content above or below 15%),[12] transient or metastable (measured in lifetimes of seconds or hours/days respectively)[13] but no liquid foam is thermodynamically stable and in time all will collapse.[14]

Foams have been commonly employed as a fire fighting medium since the early 1900s, with most recent formulations being commonly deployed as a foam concentrate for dilution with water and aeration under shear forces. The mechanism of extinguishing fires is a combination of heat sink, mass transfer barrier, insulation and water evaporation displacing oxygen.[12]

In the nuclear industry foams are commonly encountered as a carrier for decontaminating reagents such as NaOH, phosphoric, nitric, 1-hydroxyethane-1,1-diphosphonic (HEDPA) and sulphuric acids[15–18] or a coating to prevent further radionuclide mobility.[19] Within these examples is a method for decontamination of large plant; reporting DFs of 190 with a multiple step treatment recirculating foam process on a 1000 m^2 graphite gas-cooler. The resulting waste effluent was a relatively small volume of 6 m^3.[16] HEDPA as an active decontaminating reagent was employed with extremely high DFs (890) recorded for U and Pu whilst other species achieved DFs of 136.[18]

The aim of this body of work has been to investigate the potential incorporation of neutron poisons into fire fighting foams in the context of an emergency scenario where fire could break out in an environment with high levels of neutron radiation. For example, the Chernobyl reactor accident required the deposition of 40 tonnes of boron carbide into the remnants of the reactor core with the goal of halting the fission reaction to mitigate the ongoing fire.[20]

A neutron poisoning foam would ideally provide the standard properties of the base fire fighting foam with regards to foam forming, wettability and stability whilst also reducing the levels neutron radiation penetrating the foam.

With regards to this objective, neutron poisons were selected based upon neutron absorption cross section, deployability, cost and availability. Poisons which are themselves radioactive, exist in gaseous form (such as ^{135}Xe) and have neutron

capture cross sections below 1000 b (barns, 10^{-28} m^2) can be immediately discounted as can toxic poisons such as cadmium. In terms of availability and cost the most deployable poisons were considered to be [10]B, [155]Gd and [157]Gd.

6.3 - Results

6.3.1 - Neutron exposure experimental configuration 1

Figure 55 – Neutron activity through aqueous poison solutions of 50 mm depth.

Figure 55 details the neutron radiation detected through aqueous samples of 50 mm depth containing boric acid in the experimental setup described as configuration 1 (see 6.6.3). Of particular note is the magnitude of effect of glass vessels and water on the neutron levels observed when contrasted with the differences observed between boron levels and isotopic concentrations which would appear to be no more significant than the base aqueous solution.
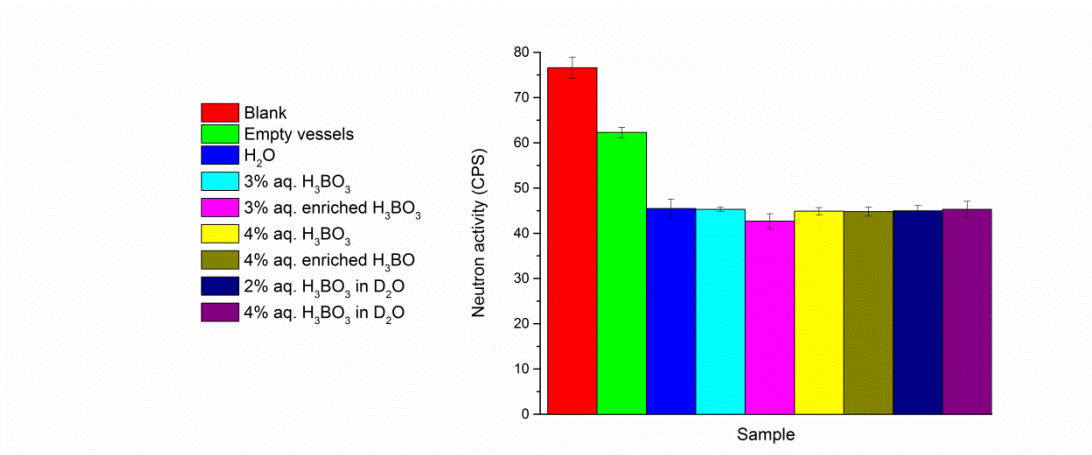
Figure 56– Neutron activity through aqueous poison solutions of 100 mm depth.

Figure 56 details the neutron radiation detected through aqueous samples of 100 mm depth containing boric acid, also in the experimental setup described as configuration 1 (see 6.6.3). Despite a doubling of the sample thickness there remained no significant observable differences between water, deuterated water, aqueous solutions of natural abundance or enriched boric acid.

6.3.2 - Neutron exposure experimental configuration 2

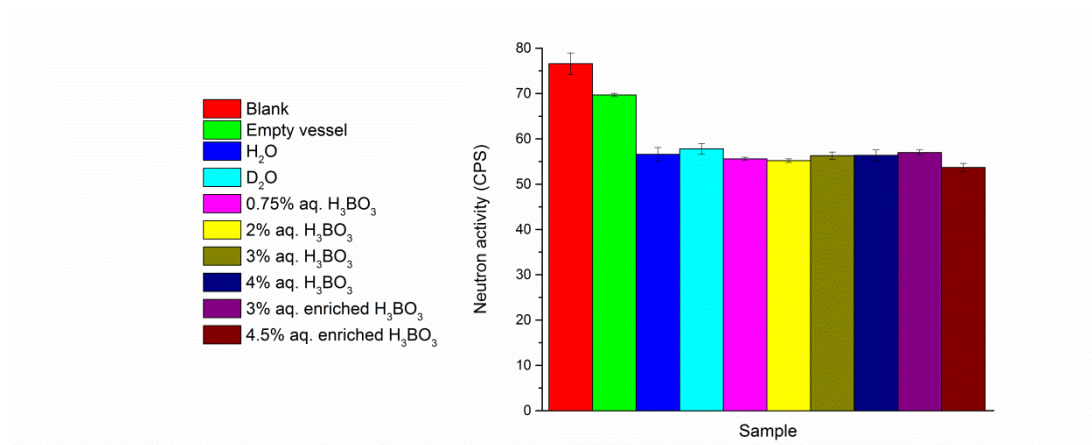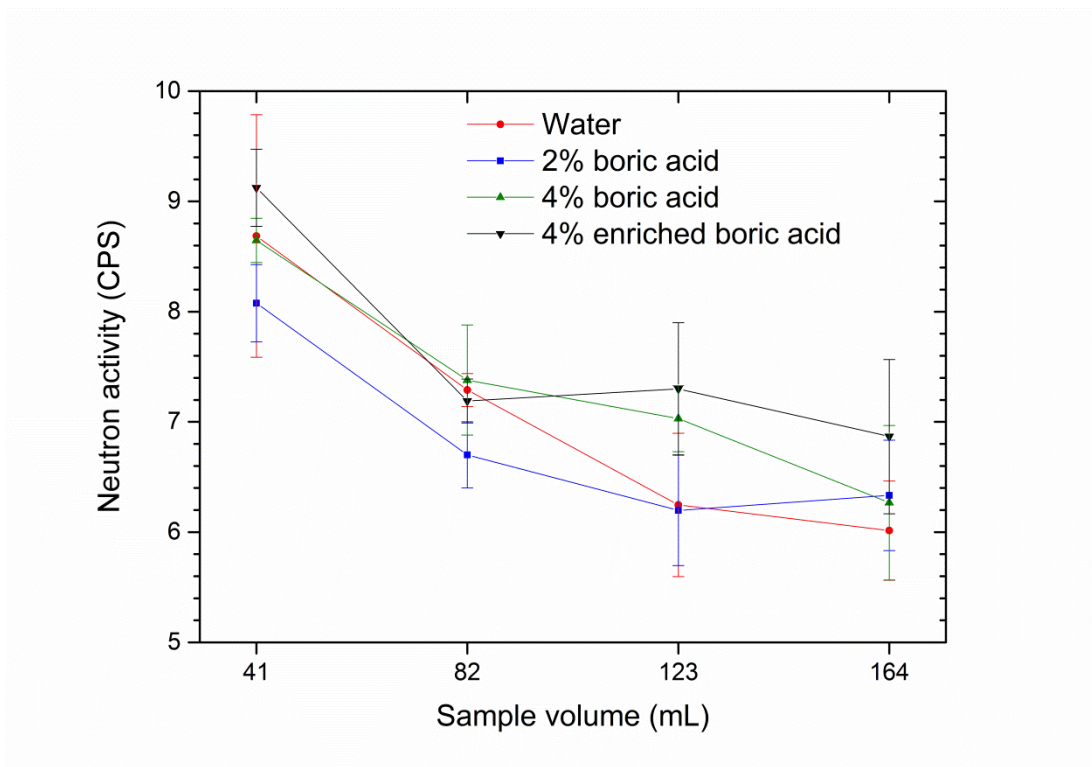*Figure 57 – Neutron activity through aqueous poison solutions.*

Figure 57 details the neutron radiation detected through aqueous samples containing boric acid in the experimental setup described as configuration 2 (see section 6.6.4). 41 mL of sample corresponds to sample depths of 61 mm, 82 mL to 122 mm, 123 mL to 183 mm and 164 mL to 244 mm. This experimental configuration was intended to eliminate the possibility of backscattering and more accurately collimate the neutrons emitted from the source. As previously observed; variations in the isotopic composition or % wt. of boric acid in aqueous solution yielded no significant differences in the neutron activity detected, with most of the measured variations lying within error regions. Boric acid was used at a maximum concentration of 4% in water to prevent saturation, which would result in precipitation in lower temperature environments.
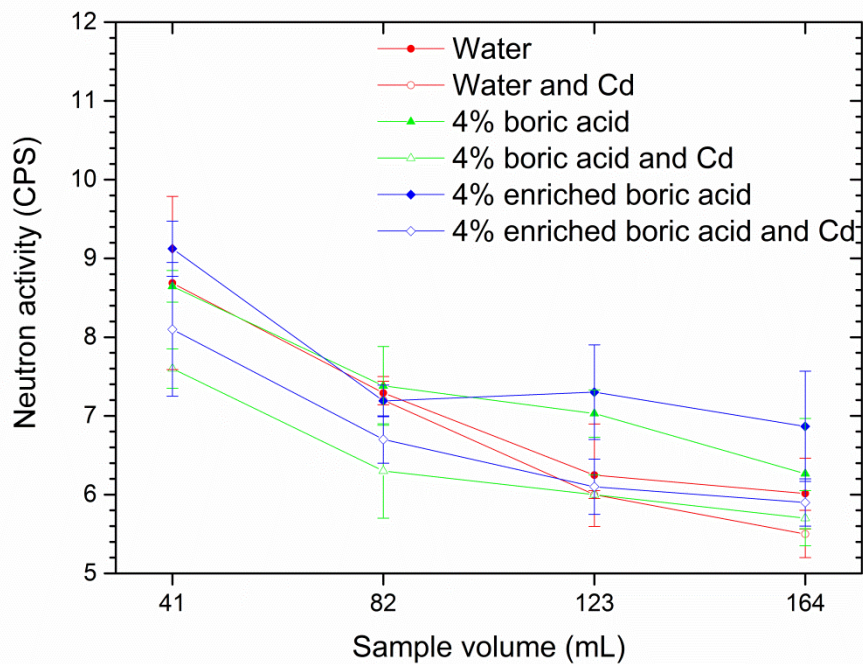
Figure 58– Neutron activity through aqueous poison solutions.

Figure 58 details investigations into the effects of Cadmium sheeting (see section 6.6.5). Whilst the cadmium does appear to offer some form of shielding, with reduced neutron levels observed when applied, there is often noticeable overlap between error regions, limiting the conclusions which may be drawn.
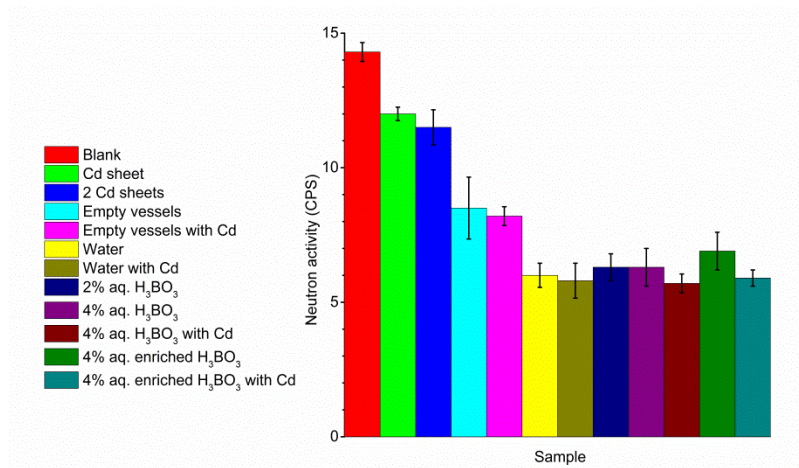
Figure 59 – Neutron activity through 164 mL of aqueous samples, depth 244 mm.

Figure 59 shows a comparison of several samples expected to illicit significant variances in neutron levels. Of particular interest is the large decrease with the application of a single cadmium sheet yet a much smaller decease upon the addition of the second, identical cadmium sheet. Further large decreases are observed with the placement of glass sample vessels when both empty and filled with water. When examining the aqueous samples of various boric acid concentrations and isotopic compositions it would be expected for the enriched boric acid samples to exhibit the lowest observed levels of neutron radiation, particularly when coupled with cadmium sheeting. Comparing all aqueous samples would be somewhat dubious due to the continual overlap of error regions between comparable samples.

6.4 - Discussion

Examination of figure 55 would suggest the most significant decrease in the measured neutron activity was due to the blank water sample, with deuterated water and boric acid solutions resulting in minimal changes which can be considered to overlap in error to the extent that there is no significant measurable difference between aqueous samples. In order to investigate whether an increased

sample volume would allow more subtle differences in activity to be observed the sample volumes were increased from 50 mL (50 mm sample depth) to 100 mL (100 mm sample depth) as shown in figure 56.

When boric acid solutions were measured it was, once again, not possible to determine whether there was any subtle reduction in neutron activity due to the presence of boron at different levels or isotopic compositions, even with the replacement of water with deuterated water. Further increases in depth of samples were not possible using this experimental configuration so an improved experimental design with an increased distance from the source to detector was devised for successive experiments.

Due to the relatively small volume of paraffin wax employed as shielding in this experimental configuration it was also considered possible for neutron back scattering to occur and therefore result in poor collimation of the neutrons through the desired samples (confirmed upon taking activity measurements at various points on the exterior of the shielded vessel); the experimental configuration 2 was designed to rectify this potential issue with an increased volume of water moderator and distance from the source. The data presented in figures 57-59 was gathered using the improved experimental configuration 2.

Figure 57 details the effect upon the neutron radiation of increasing the volume (and therefore depth) of water and boric acid aqueous solutions. Whilst the expected trend of an increase in sample volume leads to a decrease in the activity measured was observed in the case of water and 4% boric acid samples, high points in activity were observed in the cases of 4% boric and 4% enriched boric acid.

The lack of a noticeable difference in the activity of enriched boric acid (99% ^{10}B), containing five times the ^{10}B composition of typical boric acid,[5] would suggest that a boric acid containing foam is likely to be of no greater use than a standard foam in the moderation/absorption of neutrons. The large error regions which cover multiple points would suggest, once again, either no observable difference between water and various aqueous samples or differences too subtle to detect with this method due to the comparatively large margin of error. Figure 58 documents the same samples with the addition of cadmium sheeting in order to

determine whether any decreases in activity can be observed. The results show a decrease in activity observed at each point when cadmium sheeting was deployed in addition to the samples to be measured, suggesting that the lack of a reliably noticeable difference between boron samples is caused by a lack of significant poisoning effect by the boron due to the relatively small amount of ^{10}B present.

Figure 59 details the neutron activities observed through 164 mL samples of 244 mm depth in order to examine the maximum sample depth possible with the present experimental configuration. From this plot the findings from the previous experiments were replicated; suggesting a small reduction in neutron activity is provided by cadmium sheeting, a greater effect by the empty glass sample vessels and an even greater effect by these vessels filled with water. Beyond the deployment of water the inclusion of practical, achievable concentrations of common and enriched boric acid have no measurable benefit in terms of neutron activity reduction.

A noticeable trend throughout figures 57-59 is the significant initial decrease of neutron activity on the placement of a single sample and the diminishing returns in decreased activity observed concurrently. This can be explained by consideration of the energies these neutrons possess; lower energy neutrons require considerably fewer collisions in order to deplete their energy to levels which cannot penetrate the outer polyethylene layer of the ^{3}He neutron detector probe. Higher energy (fast etc.) neutrons require considerably more collisions to reduce their energy through scattering to thermal levels which are more likely to be detected.[3] So a large decrease in activity upon deployment of a sample, followed by a reduced decrease in activity upon addition of a second, identical sample would suggest that the majority of the lower energy neutrons are stopped by the first sample and further samples are only able to reduce a small number of the higher energy neutrons down to a detectable level. This could be further examined if the energies of emitted neutrons could also be examined in the experimental setup.

Gadolinium was not examined when deployed against a neutron source in the experiments detailed here due to the difficulties observed when gadolinium salts (such as the commonly deployed $Gd(NO_3)_3$)[21] were added to foam concentrates or

foaming mixtures: the rapid collapse of the foam was induced and a solid precipitate formed in the solution. This is likely due to the commonly documented phenomenon where a large cation is able to form a soap with several of the anionic surfactant molecules and is commonly observed when using soaps in hard water areas.[22] Since the collapse of the fire fighting foam would undermine the purpose of the final product other potential deployment methods were considered (details in section 7.3).

6.5 - Conclusions

The neutron absorption effects of a range of standard (^{11}B) and enriched (^{10}B) boric acid aqueous solutions have been investigated and found to be unmeasurable with any of the experimental setups or detectors available.

It would stand to reason that if the samples measured are unable to provide any measurable reductions in neutron radiation due to the effects of boric acid as a poison then the use of a foam containing considerably smaller concentrations of poisons and volumes of liquid would equally be unmeasurable by such methods. Particularly since each liquid boundary is measurable on the scale of nanometres and the maximum solubility of boric acid in proportioning foam concentrate (recommended for use at 3% with water) would result in a concentration of 0.14% boric acid.

This leads to a significant amount of doubt as to the feasibility of using foams as a neutron poison delivery mechanism and simultaneous fire-fighting medium; obtaining an effective concentration of neutron poisons in the foam or indeed enough water to moderate down the energy of the neutrons or shield from them would seem highly unlikely and thus it is recommended that alternative solutions to the problem be sought.

6.6 - Methods

6.6.1 - Chemicals

Chemicals used were purchased from Sigma Aldrich Ltd., U.K. and used as received.

6.6.2 - Foam formulation

Foam formulations detailed herein were formulated by % weight and mixed until homogeneous using a magnetic stirrer bar and hotplate stirrer at room temperature unless otherwise specified.

6.6.3 - Neutron exposure experimental configuration 1

A paraffin wax shielded cylindrical vessel of height 47.0 cm and diameter 28.5 cm containing a central hollow cylindrical core of internal diameter 5.0 cm with a depth of 22.0 cm to two AmBe neutron sources of activity 3.7 GBq (ref. date 13/04/1995) was used for the initial neutron experiments.

Samples of 50 g mass in one or more 60 mL lidded glass jars (50 mm sample depth) were lowered into the 22.0 cm deep inlet tube with or without cadmium sheeting of dimensions 1 mm x 150 mm x 150 mm covering the aperture.
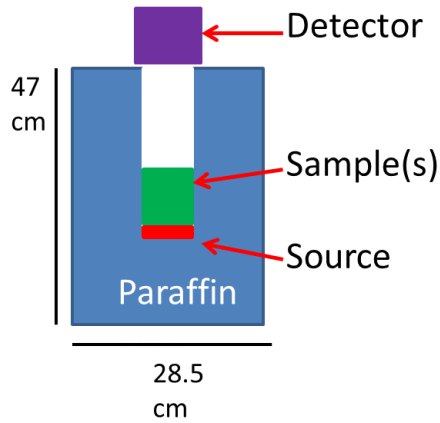
Figure 60– Neutron exposure experimental configuration 1

6.6.4 - Neutron exposure experimental configuration 2

A water-moderated cylindrical neutron tank of diameter 165.0 cm and height 98.0 cm equipped with two 4.3 cm internal diameter 3 mm thick steel pipes located 45.0 cm from the base of the tank and running parallel with the base of the tank and each other. A single AmBe neutron source (as detailed previously) was inserted into one of these tubes to a depth of 30.0 cm and samples inserted between this source and the detector contained within one or more 30 mL lidded glass jars (61 mm depth).
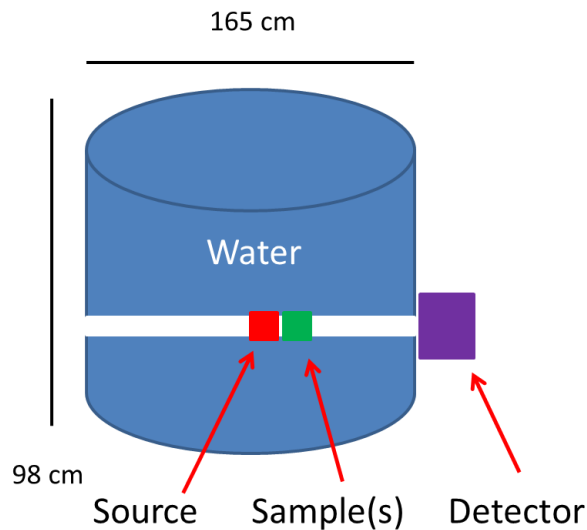
Figure 61– Neutron exposure experimental configuration 2

6.6.5 - Cadmium sheeting

Cadmium sheeting (150 x 150 x 1 mm, 99.99% purity) was deployed directly prior to the neutron detector used. Where samples were measured the cadmium was positioned after the samples yet before the detector.

6.6.6 - Neutron detectors

Detectors used include a 6 ½ inch diameter ^{3}He high density polyethylene moderated Bonner sphere (convention demands size details in inches[23]), two pieces (used individually) of 50 mm x 50 mm x 0.5 mm Indium foil of masses 9.122 g and 8.954 g and a cylindrical Canberra SN-S ^{3}He high density polyethylene moderated neutron search probe of length 34.0 cm and diameter 8.5 cm equipped with a Radiagem reader, set to a measurement integration time of 30 seconds.

6.7 - References

1. Sears, V. F. Neutron scattering lengths and cross sections. *Neutron News* **3,** 26–37 (1992).

2. US Department of Energy. DOE Fundamentals Handbook Nuclear Physics Volume 1 of 2. *Nucl. Phys.* **1,** 38 (1993).

3. Choppin, G. & Choppin author, G. R. *Radiochemistry and nuclear chemistry*. (Amsterdam [Netherlands] : Elsevier, 2013).

4. US Department of Energy. DOE Fundamentals Handbook Nuclear Physics Volume 2 of 2. *Nucl. Phys.* **1,** 36 (1993).

5. Sauerwein, W. A. G., Wittig, A., Moss, R. & Nakagawa, Y. *Neutron Capture Therapy*. (Springer Berlin Heidelberg, 2012).

6. Coderre, J. A. & Morris, G. M. The Radiation Biology of Boron Neutron Capture Therapy. *Radiat. Res.* **151,** 1–18 (1999).

7. Lapp, R. E., VanHorn, J. R. & Dempster, A. J. The Neutron Absorbing Isotopes in Gadolinium and Samarium. *Phys. Rev.* **71,** 745–747 (1947).

8. Yasui, L., Andorf, C., Schneider, L., Kroc, T., Lennox, A., Saroja, K. Gadolinium neutron capture in glioblastoma multiforme cells. *Int. J. Radiat. Biol.* **84,** 1130–1139 (2008).

9. L'Annunziata, M. F. *Radioactivity : introduction and history*. (Amsterdam : Elsevier, 2007).

10. Stacey, W. M. *Nuclear reactor physics*. (Weinheim, Germany : Wiley-VCH, 2018).

11. Höfer, R., Jost, F., Schwuger, M., Scharf, R., Geke, J., Kresse, J., Lingmann, H., Veitenhansl, R., Erdwied, W. in *Ullmann's Encyclopedia of Industrial Chemistry* 572–598 (Wiley-VCH Verlag GmbH & Co. KGaA, 2000).

12. Stevenson, P. *Foam engineering fundamentals and applications*. (Chichester, West Sussex, UK : John Wiley & Sons, 2012).

13.   Tadros, T. F. *Applied surfactants : principles and applications*. (Weinheim Germany : Wiley-VCH, 2005).

14.   Schramm, L. L. *Emulsions, Foams, and Suspensions. Emulsions, Foams, and Suspensions: Fundamentals and Applications* (Wiley-VCH Verlag GmbH & Co. KGaA, 2005).

15.   Costes, J. R. & Gauchon, J. . Foam decontamination of large nuclear components before dismantling. in *Research Coordination Meeting on the IAEA Coordination Research Program on New Methods and technics for IAEA optimization of decontamination for maintenance and decommissioning* 739–743 (1996).

16.   Faury, M., Fournel, B., Boissonnet, G. & Privens, H. Foams for nuclear decontamination purposes: achievements and prospects. at <http://www.wmsym.org/archives/1998/html/sess18/18-37/18-37.htm>

17.   Gauchon, J. ., Brunel, G., Costes, J. R. & Faucompre, B. Mousse de décontamination à durée de vie contrôlée. EP 0526305B1 (1995).

18.   Nunez, L. & Kaminski, M. D. Foam and gel methods for the decontamination of metallic surfaces. US 7166758 B2 (2007).

19.   Rovnyi, S. I., Arsent'eva, N. V., Emel'yanov, N. M. & Kazakevich, Y. V. Foam Compositions for Improving Radiation Conditions during Decommissioning of Nuclear Objects. *At. Energy* **93,** 893–897 (2002).

20.   Worley, N. & Lewins, J. *The Chernobyl Accident and its Implications for the United Kingdom: Watt Committee: report*. (Taylor & Francis, 2003).

21.   Wilde, E., Goli, M., Berry, C., Santo Domingo, J., Martin, H. Removal of Gadolinium Nitrate From Heavy Water. *WSRC-TR--99-00096*, Westinghouse Savannah River Company (2000).

22.   Smulders, E. *Laundry detergents.* (Weinheim ; Cambridge : Wiley-VCH, 2002).

23.   Thomas, D. J. & Alevra, A. V. Bonner sphere spectrometers - A critical review. *Nucl. Instruments Methods Phys. Res. Sect. A Accel. Spectrometers,*

Detect. Assoc. Equip. **476,** 12–20 (2002).

Blank page

Chapter 7 – Supporting information: Foams for neutron poisoning application

7.1 - Expandol LT foam investigations

Expandol LT foam concentrate solutions of 1, 3 and 6% concentration were formulated and their stability measured in order to examine the baseline stability of these foaming solutions at the manufacturers' recommended proportioning rates.
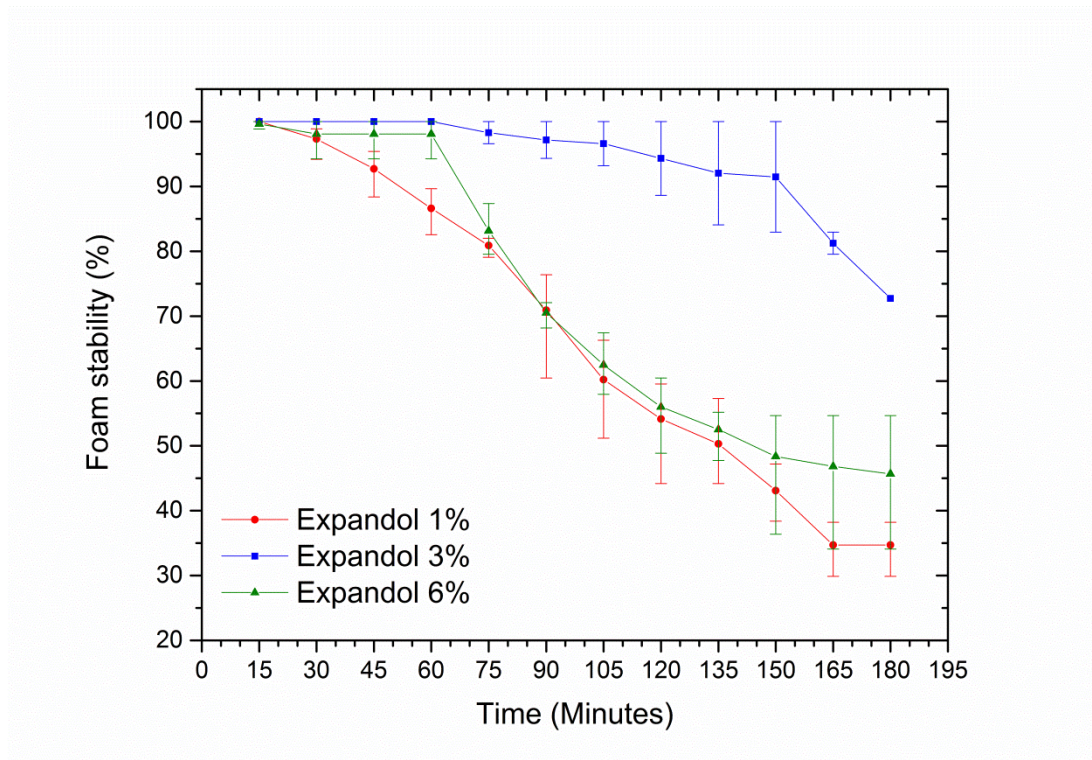
Figure 62- Expandol stability vs. proportioning rates

Observations note an initial high stability period of around 40-60 minutes followed by a period of decline featuring cascade collapse events. Increasing concentrations of Expandol tended to exhibit slightly longer initial periods of stability although the onset of collapse saw 1 and 6% solutions achieve similar levels of stability. A 3% solution as commonly used in fire-fighting applications was considered optimal due to the long lifetimes and reduced rate of collapse exhibited.

The incorporation of boric acid into both the 3% diluted Expandol foam concentrate solution and an expandol concentrate prior to proportioning with water at 3% were examined in order to examine the feasibility of this intended method of neutron poison foam formation. The pre-proportioning method produces foams with considerably lower concentrations of boric acid (0.12% when added to expandol at 4%) than previously observed but appears to show a good level of stability comparable to the expandol solution alone. The overall trends of reduced stability at higher additive levels suggests, despite limitations of large error regions, that the higher end of the boric acid solubility range would be less optimum with regards to foam properties but a stability of greater than 50% 2 hours from initial generation would not be expected to significantly hamper operability in practical use. The argument against the use of boric acid at these levels is one of implementation: in order to dissolve higher concentrations of boric acid into the foams at levels above that of a pre-proportioned mix then it must be added directly to the water at the correct proportion prior to deployment. This prevents the use of water taken directly from a hydrant during deployment and prior mixing (most likely in a fire engine water tank) delays deployment in a situation which, by its nature, demands urgency.
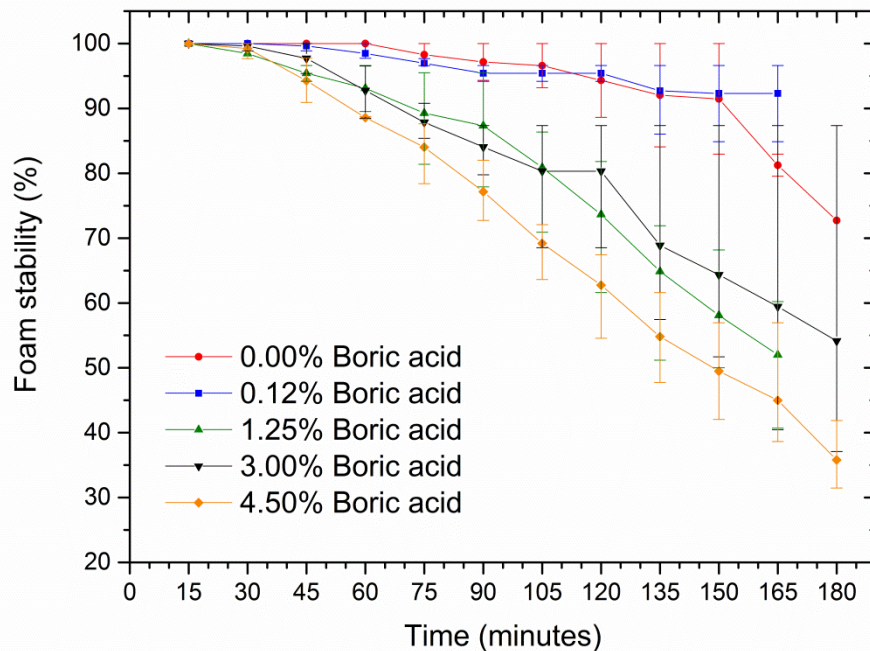
Figure 63 - Effect of boric acid on Expandol

The addition of gadolinium nitrate in the form of $Gd(NO_3)_3 \cdot 6H_2O$ to the foam concentrate immediately resulted in the formation of an insoluble precipitate due to the cationic nature of the gadolinium and anionic nature of the surfactant species used in the expandol concentrate.[1]

7.2 - Foam as a delivery mechanism

The medium for the deployment of neutron poisons is the commercially available fire-fighting foam concentrate Expandol LT produced by Angus Fire. Due to limited access to supply of this material and the need to fully detail the composition of the solution used (for the purposes of understanding); a reproduction of the formulation was attempted using composition information available from the manufacturer[2] in tandem with measurements of the properties and behaviour measured in-house.

The following formulation was developed and found to be a close match for Expandol LT (with the exception of the yellow colouration present in expandol; presumably as an identifying safety measure):

Component	% weight composition
Ethylene glycol monobutyl ether	19.9
Ethylene glycol	20.5
Dodecanol	4.0
Sulphosuccinate	5.0
Sodium dodecyl sulphate	5.0
Water	45.6

Table 8 - Expandol LT facsimile formulation

The measured surface tension of 27.9 mN/m and viscosity of 7.46 cP at 25 °C was found to be a close match to that of Expandol LT (28.2 mN/m and 7.51 cP at 25 °C) within acceptably small margins of error of 0.3 mN/m and 0.05 cP.

7.3 - Deployment of neutron poisoning foam<u>s</u>

From the shortlisted suitable materials above to be deployed they must be in a form which is either soluble or dispersible in the carrier medium; water. Although solubility is preferred over dispersibility the need to reach high concentrations of neutron poisoning materials is paramount and the inclusion of dispersed materials when solubility is problematic is considered an acceptable and necessary compromise.

7.3.1 - Deployable boron: boric acid and borax

When considering the deployability of boron the optimum starting point would be to examine the forms which have precedence within industrial applications. Boron is frequently added directly to reactor coolant in pressurised water reactors[3] in forms described as "soluble boron". These include boric acid (which can be used as either standard or enriched boric acid depending on the extent to which poisoning is required) and sodium tetraborate; more colloquially known as borax.

Attempts to incorporate boric acid into the mixture found concentrations of approximately 4.5% into aqueous systems at 20 °C to be most suitable to prevent saturation and precipitation upon small temperature changes.[4] Borax ($Na_2B_4O_7 \cdot 10H_2O$) also matches this solubility level at this temperature and has seen use in the nuclear industry but, for the same reason as detailed below, was omitted in favour of boric acid.

It would be possible to increase the loading levels by the use of sodium metaborate ($NaBO_2 \cdot 4H_2O$) which has a solubility limit of 20% at 20 °C but this was decided against as a large presence of ^{23}Na would lead to production via neutron capture of potentially problematic quantities of gamma active ^{24}Na (with a half-life of 15 hours) under conditions with high levels of neutron radiation.[5] Loadings with an almost equivalent proportion of ^{10}B to sodium metaborate can be used via the substitution of enriched boric acid; having five times the proportioning of ^{10}B compared with standard boric acid.

7.3.2 - Deployable boron: hexagonal boron nitride (h-BN)

In addition to soluble forms of boron the dispersion of boron containing materials is a viable method of delivery. Of particular interest is the use of the hexagonal form of boron nitride as this can be exfoliated into aqueous media using liquid phase exfoliation to produce stable dispersions of two-dimensional boron nitride.[6–8] From this point the material can be centrifuged out and redispersed in a smaller volume of liquid to increase the concentration of h-BN carried. The majority of work into this field has been to exfoliate material consisting of few layers for the purpose of printed electronics (usually as a substrate).

Two-dimensional h-BN has attracted considerable interest in the past few years due to its structural similarity to graphene and ability to act as an excellent dielectric[9] since it possesses a large band gap of 5.955 eV.[10] This has led to the frequent employment of h-BN as a substrate for the inkjet printing of graphene to form heterostructures.[7]

The objectives of this project, however, simply require the maximisation of stably dispersed boron-containing materials and as such flake size and material thickness are of no significant interest.
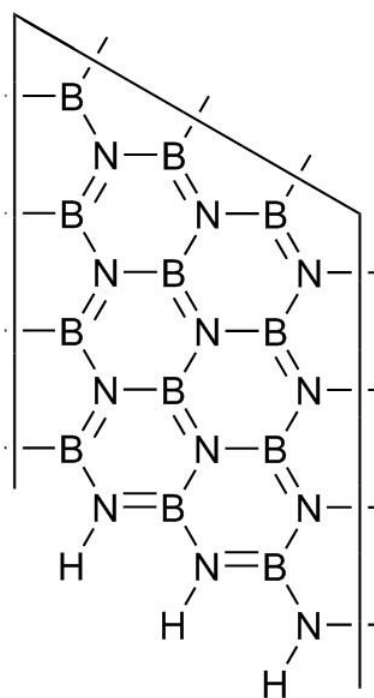
Figure 64 - Hexagonal boron nitride structure

The h-BN structure is the most common form of BN and is analogous to graphite to the extent that is has been colloquially referred to as "white graphite".[11] Its layered structure is particularly suited to exfoliation although care must be taken to ensure that the material does not re-stack once exfoliated. This material frequently finds uses as a solid lubricant, coatings, nuclear reactor shielding and furnace components due to properties such as the ability of layers to slide across one another (since atoms within each plane are bound by strong covalent bonds, whilst layers are held together by weak Van der Waals interactions), an extremely high stability in air (stable up to 1000 °C, rising to 2700 °C under certain inert gases), softness, density of 2.27 g/cm^3 and melting point of close to 3000 °C[11] in addition to those previously detailed.

7.3.3 - Sonication-assisted liquid phase exfoliation of BN

In order to produce stable dispersions of h-BN from solid powder of 1 micron approximate particle size it is necessary to reduce the size of the material. Liquid phase exfoliation is one of a variety of methods for the production of 2D materials

(others being chemical vapour deposition and mechanical exfoliation) but is of particular note due to its scalability and since it is particularly compatible with exfoliating directly into the desired aqueous medium for delivery as a foam.

The particular subcategory of liquid phase exfoliation used in this work is sonication-assisted liquid phase exfoliation whereby the layered material is sonicated within a solvent (with or without the addition of surfactants, stabilising molecules or polymer additives) creating cavities within the layered structure due to the high energy of the sonication process to separate layers into single or few layered material[91]. Should the solvent have appropriate surface energy (or the material be sufficiently stabilised by additives) then the material should remain stable against reaggregation into layered form followed by sedimentation.

The following formulations were prepared as dispersions by the method detailed in the experimental section:

Formulation reference	BN %	SDBS %	Water %	BN Conc (mg/mL)	Sonication power setting	Centrifugation speed (rpm)	Centrifugation time (min)	ZP (mV)	Mob (μmcm/Vs)	Z-Average (d.nm)	PdI	Number Mean (d.nm)
9 (2)	0.5	0.005	99.495	0.11	10	2000	20	-35.6	-2.787	357.2	0.324	245.8
9 (3)	0.499	0.005	99.496	0.43	10	2000	20	-42.2	-3.305	372.8	0.25	278.9
Blank (1)	0.5		99.5	0.63	10	2000	20	-43	-3.37	439	0.289	329.5
Blank (1)	0.5		99.5	0.24	10	3500	20	-32.2	-2.526	453.4	0.336	325.5
Blank (2)	0.5		99.5	0.23	5	2000	20	-46.2	-3.625	535.5	0.405	323
Blank (2)	0.5		99.5	0.08	5	2x cycles 2000	2x 20 min cycles	-44.8	-3.514	361.8	0.382	246.2
9 (5)	0.499	0.005	99.496	0.22	5	2000	20	-47.7	-3.737	440.3	0.369	288.2
9 (4) microfluidics	0.497	0.005	99.498	0.42	N/A	2000	20	-44.3	-3.47	297.1	0.192	241.5
Blank (3) microfluidics	0.495		99.505	0.03	N/A	2000	20	-41.9	-3.283	291.3	0.429	174.4

Table 9 - h-BN experimental formulations and measurements

BN- Boron nitride, SDBS- Sodium dodecylbenzenesulphonate, rpm- revolutions per minute, ZP- zeta potential,

PdI- polydispersity index, Z-average - intensity weighted harmonic mean size

From the data shown above (representative of the majority of data collected) an extremely large variation in the concentrations of h-BN in water can be observed. Much of this stems from inherent inaccuracies in the process of sonication as extremely small variations in the position of the probe tip or volume of liquid can lead to a significantly large difference in the forces imparted to the sample sonicated. It was hoped that the use of a probe sonicator over a bath sonicator would eliminate the positioning inconsistencies as no energy could be lost through the water bath but this appears to require further investigation.

Also of note is the expected trend of decreased concentrations at higher centrifugation speeds, the reduced concentrations after multiple centrifugations under identical conditions would also suggest either restacking has occurred between initial centrifugation and concentration measurement or simply an unintentional collection of larger material from this step.

From the particle size data collected (which must be taken as a rough guideline due to the technique of DLS technique being optimised for spherical particles) there again appears to be no clear trend between samples due to the variation of the sonication process. The results of the z and number averages obtained on the samples processed by the microfluidics apparatus are, however, apparently lower than those obtained through sonication.

If the zeta potential data is examined it can be noted that almost all of the samples measured show values indicative of good stability with the exceptions of 9 (2) and blank (1) at higher centrifugation speed which show merely moderate stability. The negative zeta potential values obtained for the blank solutions would suggest that sonication-assisted hydrolysis may have occurred to some extent[6,12–15] with a reasonable literature precedence. The use of anionic surfactant (SDBS) in the remaining samples would also be expected to contribute to this as the surfactant molecules are adsorbed onto the surface of the h-BN material.

Further investigations into the use of h-BN as a deployable neutron poison were halted due to several reasons:

- Experimental studies found them incapable of forming a stable foam whilst also retaining the suspension stability required to disperse h-BN throughout the foam.

- The low exfoliated solution concentration of h-BN could not provide sufficient boron concentration once diluted into a foam concentrate to be of use in neutron poisoning applications (especially when compared with other deployable forms such as boric acid).

- The increased cost of materials, processes and labour required to produce these dispersions was greatly exaggerated when compared with the cheaper forms of soluble boron available.

- Exfoliation of h-BN directly into expandol foam concentrate solution was not possible, preventing the most obvious, direct and simple method of delivery.

7.3.4 - Deployable Gadolinium

The most common soluble form of gadolinium used in nuclear reactor operation is the highly soluble salt gadolinium nitrate.[16] This would seem the most promising delivery mechanism however, in practice, the addition of Gd^{3+} resulted in precipitate formation (as further detailed in "Foams for neutron poisoning applications").

As a result the synthesis of gadolinium oxide nanocrystals was considered to be a viable option for investigation, especially if capping of the nanocrystals could lead to increased stability of both the suspension and foam.

The facile synthesis detailed in the experimental section was attempted with the IR analysis confirming the presence of the capping oleic acid. Although oleic acid is not miscible with water it was selected as a simple initial experiment to assess the viability of the synthesis before planned progression onto citric acid and other potential capping acids which were hoped to increase the stability of the Gd_2O_3 nanocrystals in water.

Suspension in water at a concentration of 1 mg/mL and analysis by DLS showed that the material produced was not in the nanocrystal range (1750 nm z-average diameter) but this could be reduced relatively easily by sonication of the dispersed

material. A zeta potential of 45.7 mV would suggest a good level of stability when dispersed in water but visual examination has noted sedimentation of the material from dispersant after several days which can easily be reversed with mild agitation.

Further investigations into this deployable form of gadolinium were discontinued due to sponsor concerns regarding potential environmental release of nanomaterial.

7.4 - Indium foil neutron exposure experiments

Initial tests involved use of a paraffin wax shielded drum containing two AmBe neutron sources as detailed in the experimental procedure. The top inlet was expected to provide a means of collimating the neutrons produced by the source through a sample to a detector (be it Bonner sphere, Indium foil or Canberra probe). A significant volume of Bonner sphere measurement data using this setup had to be disregarded as measurements were generated instantly with an insufficient integration time to allow the needle dial to be read accurately.

The use of Indium foil as a detection method was attempted based upon work carried out by Chao and Chiang published in 2010[17] in which Indium foils undergo neutron capture to form gamma active metastable isotopes (^{115m}In and ^{116m1}In) which can then be subjected to gamma counting to provide an indirect measurement of neutron radiation. The gamma ray spectra obtained from this method were discarded from further processing when results from the Canberra SN-S probe concluded from high levels of neutron activity to the exterior of the shielding in multiple places that this experimental configuration was not capable of accurately collimating neutrons and therefore it would not be possible to produce reliable results.

7.5 - Methods

7.5.1 - Chemicals

Unless otherwise specified all chemicals were purchased from Sigma Aldrich as used as received with the exception of Expandol LT foam concentrate solution obtained through Sellafield Ltd.

7.5.2 - Formulation procedure

Formulations detailed herein were formulated by % weight and mixed until soluble additives were dissolved using a magnetic stirrer bar and hotplate stirrer at room temperature unless otherwise specified.

7.5.3 - Foam stability tests

10ml samples to be tested were placed in sparging columns manufactured on site from borosilicate 100ml measuring cylinders fitted with a y-shaped inlet; of which one inlet was fitted with a screw-cap adapter.

Figure 65 - Sparging column

The top and second inlet were capped, a 4mm diameter glass bead introduced to the air inlet spout and compressed air introduced at a rate of 5.7ml/second using rubber tubing fitted with a Hoke gas needle valve (at setting 1.4) until the foam produced reached the 100ml mark on the measuring cylinder. A time lapse camera was used to collect foam stability measurements with interval settings appropriate to the expected lifetime of the foam. Example stability images are included below in figure 66.
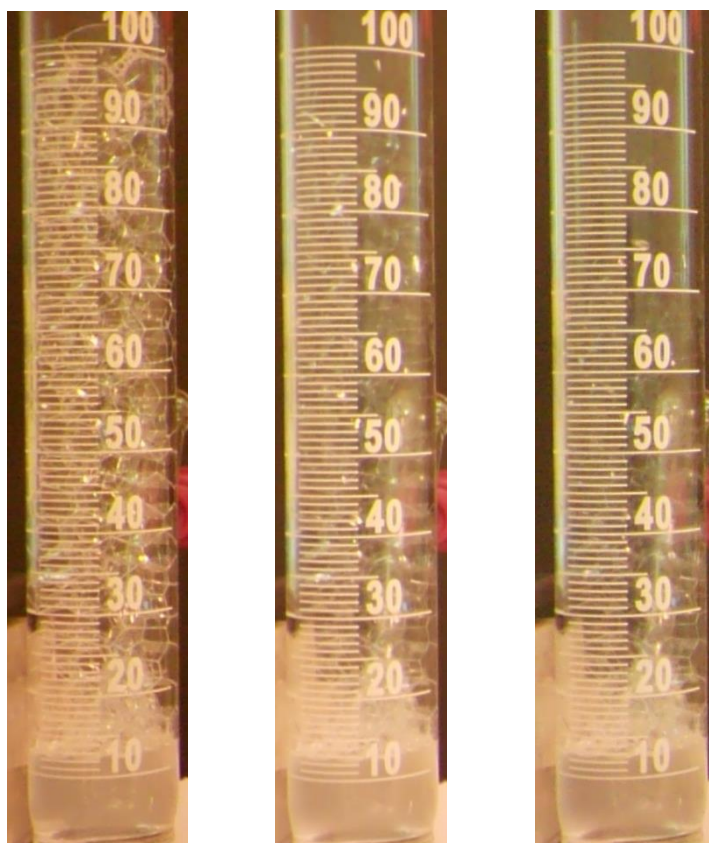

Figure 66- (L-R) Initial, 90 minute and 180 minute foam stability time lapse images of 3% Expandol solution.

7.5.4 - Brookfield viscosity measurements

Viscosity measurements were carried out using a Brookfield DVII+ rotational viscometer temperature controlled to 25°C (±0.3°C). The torque of the viscometer was controlled to fall between 20-80% using spindle 00.

7.5.5 - Evaporation rates

A sample of known volume was placed into a petri dish on a two decimal place balance. This was sited within a sealed Perspex box and the mass of the sample recorded at 30 minute intervals for a duration of 17 hours.

7.5.6 - Hexagonal BN exfoliation

Samples of the formulations detailed were made up to 300 mL volume and placed in a 500 mL vessel before sonication using a Misonix sonicator 3000 equipped with a microtip. Centrifugation was then carried out as detailed before collection of two thirds of the supernatant.

7.5.7 - Neutron poison investigations

A paraffin wax shielded cylindrical vessel of height 47.0 cm and diameter 28.5 cm containing a central hollow cylindrical core of internal diameter 5.0 cm with a depth of 22.0 cm to two AmBe neutron sources of activity 3.7 GBq (ref. date 13/04/1995) was used for neutron experiments.

Samples of 50 g mass in one or more 60 mL lidded glass jars (50 mm sample depth) were lowered into the 22.0 cm deep inlet tube and two pieces (used individually) of 50 mm x 50 mm x 0.5 mm Indium foil of masses 9.122 g and 8.954 g were placed over the aperture.

7.5.8 - Gadolinium nanoparticle synthesis

In accordance with a literature procedure[18] solutions of NaOH (0.48 g, 12 mmol) in DEG (20 mL) and $Gd(NO_3)_3 \cdot 6H_2O$ (1.8 g, 4 mmol) in DEG (20 mL) were combined and heated to approximately 210 °C for 30 minutes with stirring. To this solution was added oleic acid (0.9 g, 3.2 mmol) in DEG (10 mL) and the solution allowed to

stir for 30 minutes. The resultant solution was diluted with equal volumes of methanol and centrifuged at 2500 rpm for 20 minutes. The supernatant was removed and a second wash of methanol (25 mL) before repeating the centrifugation and vacuum filtration through a fine polymer membrane yielded a slightly off-white powder of Gd_2O_3 capped with oleic acid (1.47 g). IR 3400, 2920, 2850, 1556, 1413, 1096, 1053, 920 cm^{-1}.

7.6 - References

1. Smulders, E. *Laundry detergents.* (Weinheim ; Cambridge : Wiley-VCH, 2002).

2. Angus Fire. Expandol LT SDS. (2017). at http://angusfire.co.uk/wp-content/uploads/Expandol.pdf

3. Stacey, W. M. *Nuclear Reactor Physics.* (Wiley-VCH Verlag GmbH and Co. KGaA, 2007).

4. Blasdale, W. C. and Slansky, C. M. The solubility curves of boric acid and the borates of sodium. *J. Am. Chem. Soc.* **61,** 917–920 (1939).

5. International., B. E. *Modern power station practice. incorporating modern power system practiceVolume J, Nuclear power generation. Nuclear power generation* ([Oxofrd] : Pergamon, 1992).

6. Lin, Y., Williams, T., Xu, T., Cao, W., Elsayed-Ali, H., Connell, J. Aqueous dispersions of few-layered and monolayered hexagonal boron nitride nanosheets from sonication-assisted hydrolysis: Critical role of water. *J. Phys. Chem. C* **115,** 2679–2685 (2011).

7. Zhu, J., Kang, J., Kang, J., Jariwala, D., Wood, J., Seo, J., Chen, K., Marks, T., Hersam, M. Solution-Processed Dielectrics Based on Thickness-Sorted Two-Dimensional Hexagonal Boron Nitride Nanosheets. *Nano Lett.* **15,** 7029–7036 (2015).

8. Yang, H., Withers, F., Gebremedhn, E. and Lewis, E. Dielectric nanosheets made by liquid-phase exfoliation in water and their use in graphene-based electronics. *2D Mater.* **1,** 11012 (2014).

9. Secor, E. B. and Hersam, M. C. Emerging carbon and post-carbon nanomaterial inks for printed electronics. *J. Phys. Chem. Lett.* **6,** 620–626 (2015).

10. Cassabois, G., Valvin, P. and Gil, B. Hexagonal boron nitride is an indirect bandgap semiconductor. *Nat. Photonics* **10,** 262–267 (2016).

11. Reim, J. O. G., Gmbh, E. S. K. C., Kg, C. and Company, A. C. in *Ullman's Encyclopedia of Industrial Chemistry* 219–234 (2012).

12. Motojima, S., Tamura, Y. and Sugiyama, K. Low temperature deposition of hexagonal BN films by chemical vapour deposition. *Thin Solid Films* **88,** 269–274 (1982).

13. Cofer, C. G. and Economy, J. Oxidative and hydrolytic stability of boron nitride — A new approach to improving the oxidation resistance of carbonaceous structures. *Carbon N. Y.* **33,** 389–395 (1995).

14. Saito, T. and Honda, F. Chemical contribution to friction behavior of sintered hexagonal boron nitride in water. *Wear* **237,** 253–260 (2000).

15. Streletskii, A., Permenov, D., Bokhonov, B., Kolbanev, I., Leonov, A., Berestetskaya, I., Streletzky, K. Destruction, amorphization and reactivity of nano-BN under ball milling. *J. Alloys Compd.* **483,** 313–316 (2009).

16. Wilde, E., Goli, M., Berry, C., Santo Domingo, J., Martin, H. Removal of Gadolinium Nitrate From Heavy Water. *WSRC-TR--99-00096*, Westinghouse Savannah River Company, (2000).

17. Chao, J. H. and Chiang, A. C. Activation detection using indium foils for simultaneous monitoring neutron and photon intensities in a reactor core. *Radiat. Meas.* **45,** 1024–1033 (2010).

18. Söderlind, F., Pedersen, H., Petoral, R. M., Käll, P. O. and Uvdal, K. Synthesis and characterisation of Gd_2O_3 nanocrystals functionalised by organic acids. *J. Colloid Interface Sci.* **288,** 140–148 (2005).

Blank page

Conclusions

To conclude, this thesis has investigated and developed a novel hydrogel-based decontamination technique with improved DFs when compared with literature sources. A wide range of formulations has been synthesised and characterised; with the effectiveness on surface and subsurface contamination investigated.

The concept of neutron poisoning foams for scenarios requiring contingency has also been investigated; with limitations to deployment and operation documented.

Further work

The investigations into the decontamination effectiveness of hydrogel loaded with water or agents such as 2% nitric acid has shown high levels of success on stainless steel substrates, this would appear to have excellent potential for further investigation. The effectiveness on other non-porous substrates such as aluminium, glass and painted surfaces would be expected to provide similar levels of effectiveness. The ability of these gels to decontaminate other radionuclides commonly produced during nuclear plant operations such as ^{60}Co, ^{234}U, ^{237}Np, ^{238}Pu and ^{241}Am is also worthy of investigation, this would determine the range of potential uses and degree of versatility.

Loading of hydrogels with a range of liquid decontamination technologies could allow the specific tailoring of appropriate technique to a range of scenarios with variations such as substrate and contamination; potentially even leading to the development of a pre-packaged gel decontamination treatment for commonly encountered scenarios. Non-aqueous solvent loadings would also merit investigation, although formulation adjustments may be necessary.

Investigations into the effectiveness of these gels ought to also be performed upon porous substrates commonly encountered in the nuclear industry; such as concrete

and cement. In order to achieve this it may be necessary to reformulate the gels to carry a reduced liquid volume and higher levels of liquid retention to prevent further increasing radionuclide penetration into these substrates.

An additional challenge would be to investigate the effectiveness of these gels upon different surfaces, in addition to substrates. For example vertical, uneven (e.g. ridged) or rough surfaces would be more typical of the surfaces found in reality should such gels be used for site treatment in the event of a chemical, biological or radionuclide attack.

Study into the effectiveness of these gels in solution decontamination would also be expected to show promise; the addition of a gel to contaminated solution may be able to scavenge radionuclides/metal ions etc. from solution.

The relatively short storage after use of these gels has exhibited no visually detectable degradation due to the radiation to which they are exposed but it would be of great interest to investigate the effects of various levels of α, β and γ radiation upon the gel structures.

Whilst these gels are designed to reduce liquid waste and encapsulate waste into a solid form there is the potential to extract the radionuclides to allow re-use of the gels, this would merit investigation, at least in principle. This would be particularly useful if any storage of gels prior to full disposal is considered; leaching potential of dried gels if exposed to water would be known.

Further refinements of the hydrogel formulation would also be worthy of investigation; namely the uses of thermoresponsive pNIPAM which was only briefly investigated in this project. The addition to the polymer gels of chelating groups with a high affinity for metal ions, such as crown ethers, could also aid uptake and radionuclide retention.

With regards to the foams portion of this project any further work is recommended to be carried out in the medium of computer modelling to investigate the volume of foams (with various neutron poisoning loadings) required to provide a reduction in neutron levels. This would allow evaluation of whether this concept is feasible under different conditions to those achievable in a university laboratory setting.

This would overcome the obstacles encountered during the course of this project such as personal radiation exposure limits, neutron source availability, neutron energy distributions, costs of neutron poisons, measurable distances, detector sensitivity and availability.

Don't adventures ever have an end? I suppose not. Someone else always has to carry on the story
Tolkien, J. R. R. (John R. R. The Lord of the Rings. Part 1, The fellowship of the ring. (Allen & Unwin, 1966).